A MÖSSBAUER STUDY OF SOME INDUSTRIAL APPLICATIONS OF ORGANOTIN COMPOUNDS

by

Richard William Clarkson

A thesis submitted to the Council for National Academic Awards in partial fulfilment of the requirements for the degree of Doctor of Philosophy

Collaborating Establishment :

International Tin Research Institute

Department of Applied Physics

Sheffield City Polytechnic

Sheffield S1 1WB

August 1982

Abstract

A Mössbauer study of some industrial applications of organotin compounds

by

Richard William Clarkson

The technique of high dilution Mössbauer spectroscopy using the isotope ^{119}Sn has been employed to study the nuclear environment of several organotin compounds having important industrial applications. For each compound studied structural and co-ordination information has been obtained relating to the mode of action of the organotin compound in it's application.

Chapters one and two of this thesis describe the theory of the Mössbauer Effect and the instrumentation and computational methods of recording and processing the Mössbauer data.

Chapter three provides the main area of study in the thesis and is concerned with the role of organotin compounds in the stabilisation of PVC. Two types of organotin compound, dialkyltin thioglycollates and dialkyltin maleates, have been investigated for their effectiveness in preventing thermal and photochemical degradation of PVC. The resulting changes in the Mössbauer parameters following degradation have led to the identification of the organotin degradation products from which a degradation/stabilisation mechanism has been suggested.

In chapter four the observation of a room temperature Mössbauer resonance is used to indicate that dimethylchlorotin acetate has an associated structure. A subsequent X-ray crystallographic determination supports the implications from the Mössbauer data and reveals dimethylchlorotin acetate to be 6 co-ordinate with a polymeric structure.

In chapter five Mössbauer data have been obtained for a series of trialkyltin derivatives of L-cysteine and L-homocysteine. The trialkyltin moiety has been reported to be a biologically active species and the Mössbauer data have revealed the sulphur atom in the cysteine and homocysteine groups to be a specific site for binding to the trialkyltin moiety.

Finally, in chapter six a simple Debye model of the solid has been applied to variable temperature Mössbauer data to suggest possible structures for two bis(trialkyltin)compounds containing two electronically different tin sites.

CONTENTS

Introduction

The work described in this Thesis is a study of organotin compounds and of the chemical changes undergone by them in some industrial applications, using Mössbauer spectroscopy. Although the first organotin compound was prepared by Frankland in 1849, large scale industrial applications have only become apparent in the last 10 - 20 years, and at present some 30,000 tons of tin are consumed each year. The recent growth in the use of organotin compounds can be attributed to their intrinsically lower toxicity in comparison to organolead and organomercury counterparts, and to the recently appreciated versatility of organotin compounds in their possible applications. 66% of the current total usage of organotin compounds is used for non-biological types of application (R_2SnX_2 and $RSnX_3$ derivatives), and the remaining 7,000 - 10,000 tons are reported as being used as biocides (R_3SnX derivatives) (1).

With reference to the non-biological applications of organotin compounds the largest single application is the stabilisation of PVC, with some 20,000 tons of chemicals currently being used. PVC is degraded by both heat (to which it is subjected during processing at 185°C) and by long term exposure to sunlight producing severe discolouration and embrittlement in the polymer. Dialkyltin compounds are among the most effective stabilisers available for PVC and additions of the stabilisers at 1 - 2% by weight will maintain the clarity of the PVC and significantly retard degradation. In general, the dialkyltinbis(isooctylthioglycollates) are used in applications that require good heat stability, whereas the dialkyltinbis(isooctylmaleates) are used for providing long term stability to light. Di-n-octyltinbis-(isooctylthioglycollate) and maleate have a low mammalian toxicity and are used in many countries as stabilisers for PVC food packaging and drink containers; dimethyltinbis(isooctylthioglycollate) is also used in some European countries for stabilising food-contact PVC packaging.

Di-n-butyl- and di-(2-butoxycarbonylethyl)- tin stabilisers are currently used in non-food-contact PVC. In most applications up to 60% of the corresponding monoalkyltin compound, $RSnX_3$, is added to the dialkyltin stabiliser, R_2SnX_2, as it has been found that this combination gives a synergistic improvement in the stabilising activity.

A number of dialkyltin compounds have also been found to be effective curing agents for room-temperature-vulcanising (RTV) silicones. The three most commonly used derivatives are dibutyltin diethanoate, dibutyltin di-(2 - ethylhexanoate) and dibutyltin dilaurate. If the organotin catalyst is added to the liquid silicone at room temperature, the reactive carboxylate groups are able to bring about cross- linking of the silicone and produce a flexible elastomeric solid. The same dibutyltin compounds catalyse the addition of alcohols to isocyanates, producing polyurethanes, and are used commercially for this purpose.

The biological applications of organotin compounds are numerous and are concerned mainly with trialkyltin derivatives for which the level of toxicity is dependent upon the length of the alkyl chain attached to the tin atom.

Triphenyltin compounds are highly toxic fungicides. The first commercially used fungicide was triphenyltin acetate which was used to control potato-blight fungus and sugar-beet fungus. The other most widely used organotin chemical is triphenyltin hydroxide which shows similar fungicidal behaviour. Present day consumption of these two chemicals in Europe and Japan alone is estimated at 1,000 tons per year.

Tributyltin derivatives have shown a high antibacterial activity particularly against Gram- positive bacteria which has led to their use as disinfectants.

Bis(tri-n-butyltin)oxide has emerged as the most effective organotin derivative for the protection of such cellulosic materials as cotton textiles; wood, and other cellulose - based materials which are susceptible to fungal attack.

Finally, the other major application of organotin compounds is to the closely related area of marine anti-fouling paints. Tributyl- and triphenyltin derivatives incorporated in a polymeric network such as poly(tributyltin methacrylate) have found successful use as additives in paints for the elimination of marine boring creatures and barnacles from the hulls of ships. The triorganotin compound is gradually leached from the paint into the sea water where it acts as a toxicant towards marine growth.

Since the Mössbauer technique using ^{119}Sn provides information on the s - electron density at the tin nucleus it is therefore a direct method for determining the number of ligands associated with the tin nucleus. Consequently structural, co-ordination and mechanistic information about the behaviour of the organotin compounds can be obtained using the Mössbauer Effect. Examples of this are given in chapters 3, 4,5 and 6 of this Thesis.

In chapter 1 the theory of the Mössbauer Effect and of hyperfine interactions is outlined, and in chapter 2 the instrumentation and computational methods of recording and processing the Mössbauer data are discussed.

The changes undergone by organotin stabilisers of the type R_2SnX_2 (where R = butyl or octyl, and X = isooctylthioglycollate or isooctylmaleate) during thermal and photochemical degradation of PVC are discussed in chapter 3. Mössbauer parameters have been obtained for the compounds incorporated in PVC by conventional hot milling techniques and also for the compounds after degradation. The organotin products of the degradation have been conclusively identified and a reaction scheme has been proposed for the stabilisation and degradation processes on the basis of these results and in consultation with the literature. In addition the Mössbauer data have been used to deduce information about the co-ordination chemistry of tin in these compounds.

Chapters 4, 5 and 6 are similarly concerned with the use of the

Mössbauer effect to determine the structure of organotin compounds and the co-ordination number of the tin atom present. In chapter 4 the observation of a room temperature Mössbauer resonance is used to indicate that dimethylchlorotin acetate has a polymeric six co-ordinate structure. The implications from the Mössbauer data are supported by an X - ray crystallographic study of this compound.

In chapter 5 the use of Mössbauer data to provide co-ordination information on a series of trialkyltin compounds of type R_3SnX (where R = butyl, phenyl, cyclohexyl, neophyl, and X = cysteine, homocysteine) is discussed.

Finally, in chapter 6 variable temperature Mössbauer spectra for compounds of the type $R_3SnSCH_2CH_2COOSnR_3$ (where R = butyl or phenyl) are discussed. The two tin atoms in the compounds were found to have different temperature dependent recoilless fractions which were subsequently used in calculations involving the Effective Vibrating Mass model to investigate the co-ordination of the tin atoms.

CHAPTER 1. THE MÖSSBAUER EFFECT AND HYPERFINE INTERATIONS

Contents: Introduction

1.1. The Mössbauer Effect.

The Mössbauer effect is the basis for high resolution nuclear spectroscopy and arises from resonant absorption of nuclear γ- rays in the energy range 10 - 100 KeV. The lifetimes of the excited nuclear states which give rise to such γ - rays are typically of the order of 10^{-8}s. As a result of the high energies of the γ-rays, natural line widths of the order of 10^{-12} are observed resulting in a high intrinsic resolution. In early studies (2), two effects limited the application of the Mössbauer effect to a number of isotopes as well as limiting the degree of resolution. Firstly, thermal Doppler broadening greatly increased the effective line width thereby reducing the resolution, and secondly the recoil of the emitting nucleus displaces the emission line from the absorption line so that little overlap occurs and resonance absorption is not observed.

It was Mössbauer's discovery (3) that securing the emitting nucleus in an inert matrix at low temperatures gave a finite probability that the recoil momentum of the γ- ray would be transferred to the crystal as a whole and not to the single emitting nucleus. This will occur when the recoil energy of the nucleus E_R ($= E_\gamma/mc^2$) is less than the energy required to excite the vibrational energy levels in the lattice. Under these conditions the recoil energy and Doppler broadening associated with the transition are characterised by the mass and random velocity of the whole crystal, and are therefore made negligible so that the emitted line has essentially the energy and width defined by the transition i.e. the emission will be recoilless. This effect therefore makes it possible to obtain the full intrinsic resolution associated with the emitted high energy γ - rays.

1.1.1. Nuclear Resonance Absorption.

Consider the process of resonance absorption in the tin nucleus. The isotope ^{119}Sn is produced from the radioactive decay process in the metastable precursor ^{119m}Sn prepared by neutron capture in isotopically

Figure 1.1. The process of Recoilless Nuclear Resonance Absorption in ^{119}Sn

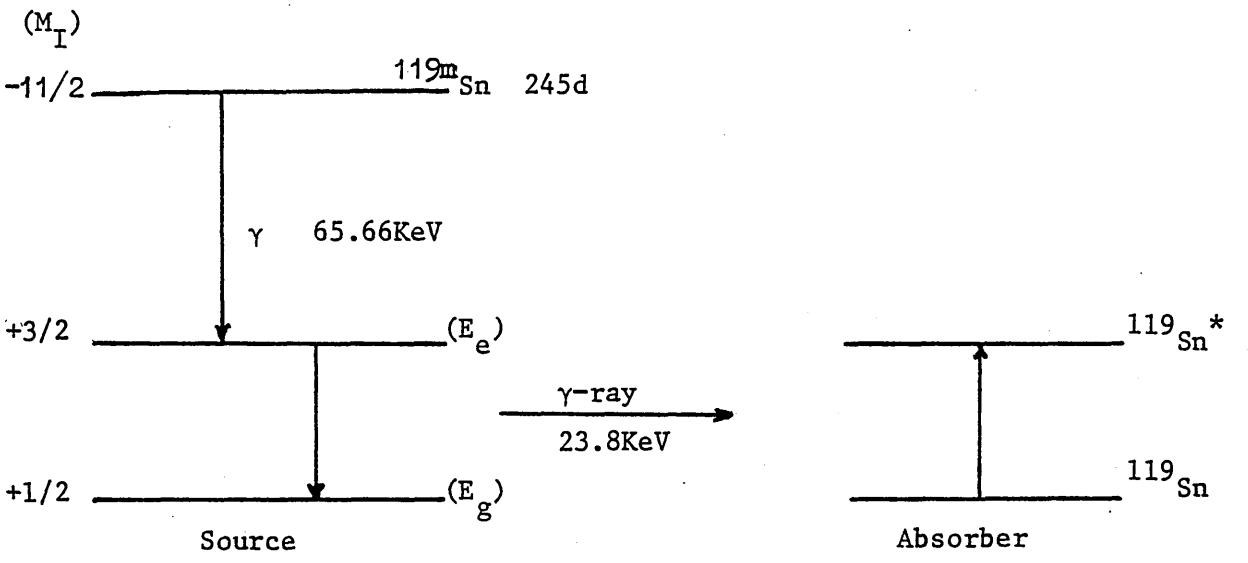

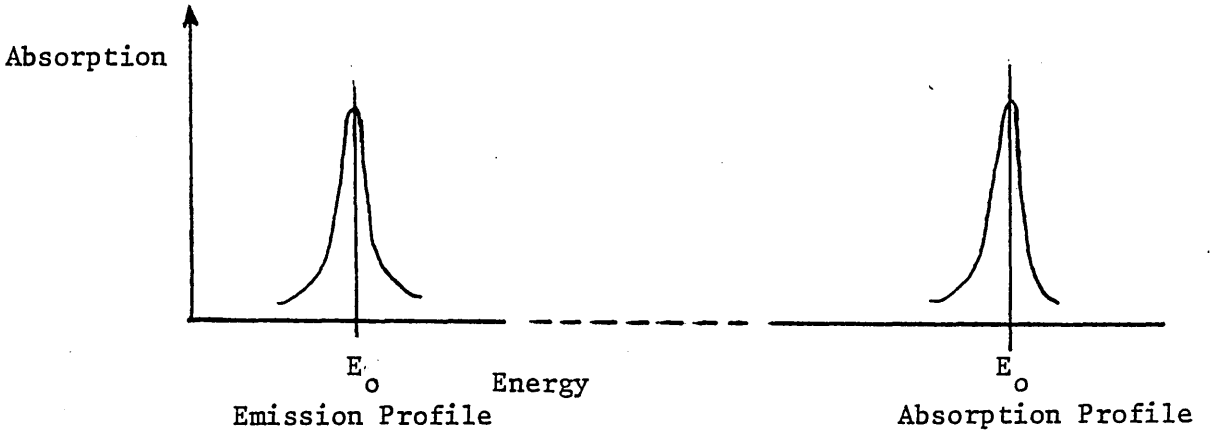

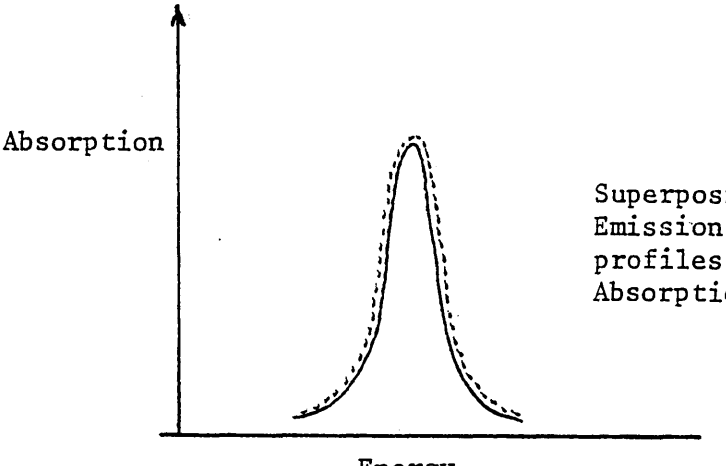

Superpositioning of the Emission and Absorption profiles gives Resonant Absorption.

Resonant Absorption

enriched ^{119}Sn. A simplified energy level diagram is shown in figure 1.1 where, following the normal radioactive decay process, the metastable ^{119m}Sn nucleus is seen to produce ^{119}Sn in an excited state, ^{119}Sn*. The excited nucleus then very rapidly decays to the ground state ^{119}Sn resulting in the emission of a γ - ray of energy 23.8KeV.

A second tin nucleus, initially in the ground state, placed in the path of the emitted photon will, under certain conditions, absorb the energy of the photon to become an excited tin nucleus. This ground state nucleus is referred to as the ABSORBER and the original excited nucleus as the SOURCE. The process of absorption is RESONANT ABSORPTION in which both the emission and absorption energy profiles are seen to completely overlap.

1.1.2 Line Width of γ-ray Emission

The emitted γ-rays are not monoenergetic but have an energy spread about a mean energy E_o (figure 1.2). The distribution has a certain natural line width (Γ) and has a Lorentzian line shape which is defined by the Breit - Wigner equation (4):-

$$I(E) = \frac{fs.\Gamma}{2\pi} \cdot \frac{1}{(E - E_o)^2 + (\Gamma/2)^2} \qquad (1.1)$$

where : $I(E)$ = intensity of the distribution at energy E
fs = probability of emission from the source
Γ = natural line width
E_o = transition energy.

The natural line width (Γ) is determined from the Heisenberg Uncertainty Principle:

$$\Gamma = \frac{\hbar}{\tau} \qquad (1.2)$$

where τ = mean lifetime of the excited state (= $t_{\frac{1}{2}}/0.693$)

The ground state nuclear level has an infinite lifetime and hence a zero uncertainty in energy whereas the energy of the excited state of the source cannot be measured sharply. Hence, the natural line width is proportional to the probability of a transition occurring from an excited energy level to a ground state energy level.

Typical values for τ are of the order of 10^{-6} - 10^{-10}s.

Figure 1.2 Diagram showing the Lorentzian distribution of emitted γ-rays

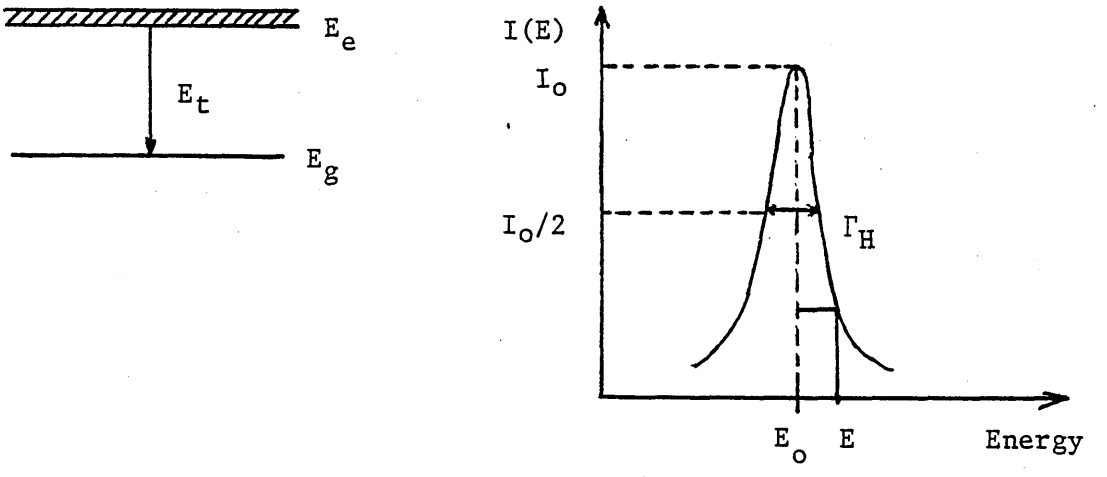

In practical resonance spectroscopy the minimum full width at half height (Γ_H) is used which represents the distribution of γ-ray energies of width Γ_H at half height. (Γ_H is defined as twice the natural line width (= 2Γ)).

The full width at half height also determines the resolution of the technique. For example, for a mean life of $\tau = 2.56 \times 10^{-8}$s then $\Gamma_H = 2.55 \times 10^{-8}$ eV.

If the transition energy is 23.8 keV then:

$$\frac{\Delta E}{E} = \frac{\Gamma_H}{E} = \frac{2.55 \times 10^{-8}}{23.8 \times 10^{3}} = 10^{-12}$$

i.e. a resolution of 1 part in 10^{12} is theoretically possible.

1.1.3 Recoil Energy Loss and Doppler Broadening

In the discussion of Nuclear Resonance Absorption, it was assumed that as a result of the transition from the excited nuclear energy levels to the ground state energy level, the emitted photon has an energy E_γ equal to the transition energy E_t. However, by the emission of a photon momentum conservation demands that the momentum $\underline{p}$ of the photon and the momentum $\underline{P}$ of the recoiling system be equal and opposite. The recoiling system hence receives an energy E_R given by

$$E_R = \frac{P^2}{2M} = \frac{p^2}{2M} = \frac{E_\gamma^{\,2}}{2Mc^2} \qquad (1.3)$$

Therefore, by the conservation of Energy:

$$E_t = E_\gamma + E_R \,. \qquad (1.4)$$

Since E_R is small compared to E_γ , (1.3) becomes

$$E_R = \frac{E_t^{\,2}}{2\,Mc^2} \qquad (1.5)$$

Consequently emission of the γ- ray from the source results in a shift in energy of the emission energy profile of the order $Et - E_R$. For resonance absorption to occur in another atom, a γ- ray of energy $E'_\gamma = E_t + E_R$ is required. The affect of E_R on the emission and absorption energy distributions is shown in figure 1.3. Since there is an energy difference of 2 E_R the probability of resonant absorption being observed depends on the magnitude of E_R . For transition energies of the order 10^4 eV, E_R is significant and overlap of the energy profiles is poor.

In addition, the emission and absorption energy profiles experience 'Doppler Broadening', E_D, which arises from the random thermal velocities of the source and absorber nuclei.

Figure 1.3 The affect of Thermal Doppler broadening and Recoil on the energy profiles of the emitting and absorbing atoms.

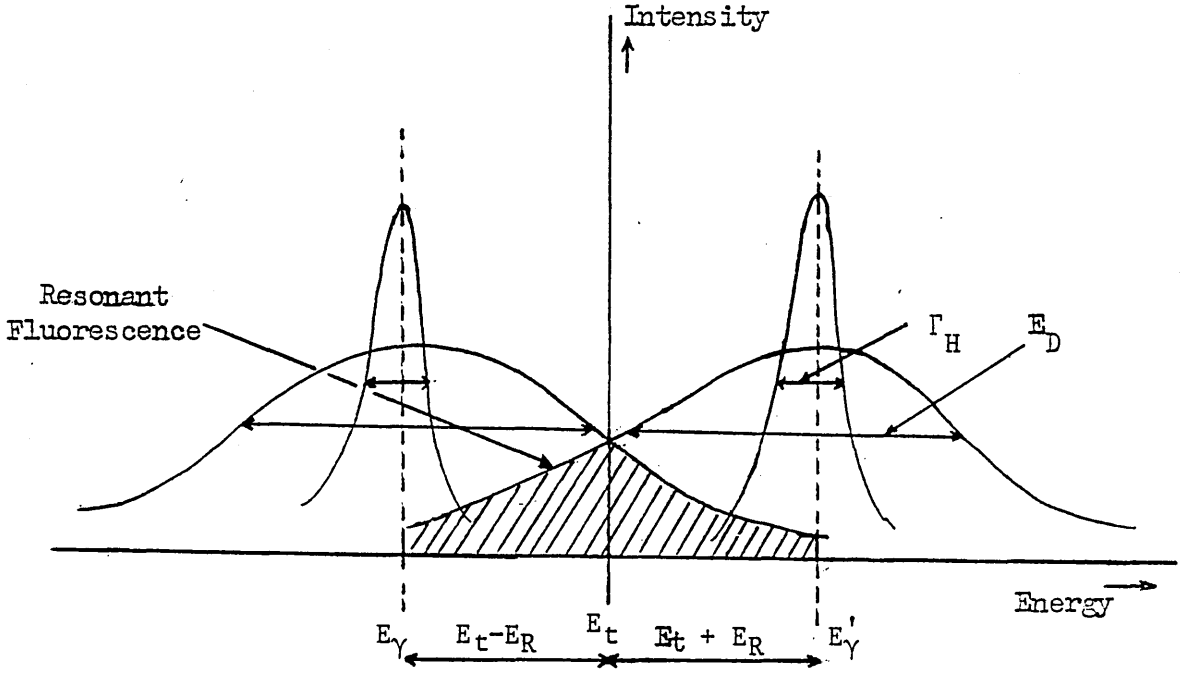

The emisson of a γ - ray of energy E_γ from an excited nuclear state of a nucleus having a velocity Vx, is represented by:-

$$E_e + \tfrac{1}{2} M\, Vx^2 = E_g + E_\gamma + \tfrac{1}{2} M(Vx + v)^2 \qquad (1.6)$$

(where v is the velocity of the γ -ray)

Since $E_t = (E_e - E_g)$:

$$E_t - E_\gamma = \tfrac{1}{2} M\, Vx^2 + Mv\, Vx \qquad (1.7)$$

$$= E_R + E_D \qquad (1.7(a))$$

The kinetic energy of a nucleus in a direction x from recoil is given by:-

$$E_k = \tfrac{1}{2} M\, Vx^2 \approx K\, T \qquad (1.8)$$

$$\text{and } (Vx^2)^{\frac{1}{2}} = \sqrt{\frac{2\, E_k}{M}} \qquad (1.9)$$

Substituting for $(Vx^2)^{\frac{1}{2}}$ in 1.7 gives:

$$E_D = 2\sqrt{E_R \cdot K\, T} \qquad (1.10)$$

Thus the γ-ray distribution is shifted by the magnitude of E_R and broadened by twice the mean of the recoil energy and the average thermal energy. Figure 1.3 shows the effect of E_R and E_D on the emission and absorption spectra. The degree of overlap between the two energy profiles as a result of Doppler broadening is seen to be small. In order to observe resonance absorption it is necessary therefore to eliminate the effects of recoil and Doppler broadening.

1.1.4 Energy transfer to the Lattice and Recoilless Emission

R.L. Mössbauer in 1958 observed that the recoil energy loss could be significantly reduced by making the effective recoiling mass equal to the mass of the lattice rather than the mass of the nucleus, and by cooling the absorber and / or the source to low temperatures whereupon E_R and E_D become negligible and line widths approach the natural width of the nuclear transition (Γ). For practical tin Mössbauer studies the source is placed in an inert solid lattice or matrix (usually barium or calcium stannate) and the absorber is cooled to liquid nitrogen temperatures.

In the Einstein model of the lattice the solid is considered as a quantum mechanical system in which its energy is quantised and transitions within the system occur through Phonon interactions. The Einstein Energy E_e is the minimum energy required to excite the lattice and corresponds to a single phonon transition. The vibrational energy of the lattice as a whole can only change by discrete amounts 0, $\pm\hbar\omega$, $\pm 2\hbar\omega$,etc... ($\hbar\omega$ = E_e the Einstein energy) and, depending on its magnitude, the recoil energy E_R of a single nucleus can be taken up either by the whole crystal or it can be transferred to the lattice through phonon interactions thereby increasing the vibrational energy of the crystal. If the recoil energy is less than E_e then a zero phonon interaction occurs and no energy is transferred to the lattice and the recoil is taken up by the whole crystal. If the recoil energy is greater than E_e then many phonon interactions may be invloved and the energy is transferred to the vibrational energy of the lattice. Consequently the emitted γ- ray suffers energy recoil and is Doppler broadened.

For many low energy transitions ($E_t < 10^5$ eV) in solids at low temperatures there is a finite probability of emission of γ-rays without recoil energy loss. This probability is termed the recoilless fraction 'f' and is expressed as:-

$$f = \exp\left[\frac{-4\pi^2 \langle x^2 \rangle}{\lambda^2}\right] \qquad (1.11)$$

where $\langle x^2 \rangle$ is the mean square vibrational amplitude of the emitting (or absorbing) nucleus in the solid

λ is the wavelength of the photon.

(This expression is obtained by reducing the Hamiltonian operator for the atom to one term which represents the transition from the initial vibrational state L_i to the final vibrational state L_f (5)

$$\text{i.e. } f = \text{constant.} \left| \langle L_f \right| e^{ik.x} \left| L_i \rangle \right|^2 \qquad (1.12)$$

where k is the wave vector for the emitted γ- photon (the number of units of momentum it carries = $E_\gamma / \hbar c$)

x is the co-ordinate vector of the centre of mass of the decaying nucleus).

displacement must be kept to a minimum to observe the Mössbauer Effect (since f increases as $\langle \chi^2 \rangle$ decreases). In the Debye model, the solid is assumed to be composed of a continuum of oscillator frequencies so that equation 1.11 becomes:-

$$f = \exp\left[-\frac{6\,E_R}{K\,\theta_D}\left\{\frac{1}{4} + \left(\frac{T}{\theta_D}\right)^2 \int_0^{\theta_D/T} \frac{x.\,dx}{e^x - 1}\right\}\right] \qquad (1.13)$$

The integral can only be solved under certain conditions i.e. at absolute zero and at high temperatures when the expression reduces to:- (5)

(1) At Absolute zero:

$$f = \exp\left[-\frac{3}{2}\frac{E_R}{\theta_D}\right] \qquad (1.14)$$

(2) At the high temperature limit (where $T > \theta_D$)

$$f = \exp\left[-\frac{6\,E_R\,.\,T}{K\,\theta_D^{\,2}}\right] \qquad (1.15)$$

The relationship between the recoilless fraction 'f' and the temperature has been the subject if numerous investigations and applications, following early investigations by Boyle et al (6) and Hohenemser (7) on standard tin sources.

1.1.5 Observation of the Mössbauer Effect

To observe a conventional Mössbauer spectrum the source is mounted on a moving platform and the energy of the emmitted γ - ray is shifted by the Doppler Effect. Having minimised the recoil energy loss and Doppler broadening the emission and absorption profiles are still,in general, not coincident in terms of energy due to the difference between the source and absorber and only when the two profiles completely overlap will resonance occur. To observe resonance the energy of the emitted γ -ray is modified by imparting a range of velocities to the source such that:-

$$E = E_t + \frac{E_t \cdot v}{c} \qquad (1.16)$$

If the Doppler velocity is applied to the source with respect to

the absorber then a shift in the source spectral line will be observed. i.e. the effective E_γ is now the line position with the new energy according to the above relationship. If a range of velocities is scanned then when the effective emission and absorption profiles are exactly coincident resonance absorption will be at a maximum. At higher or lower velocities the resonance will decrease until it is effectively zero and the two energy profiles are a maximum distance apart. This sequence of events comprises the Mössbauer spectrum - a plot of absorption against a series of Doppler velocities between the source and absorber (figure 1.4)

Figure 1.4 The resultant Mössbauer spectrum .

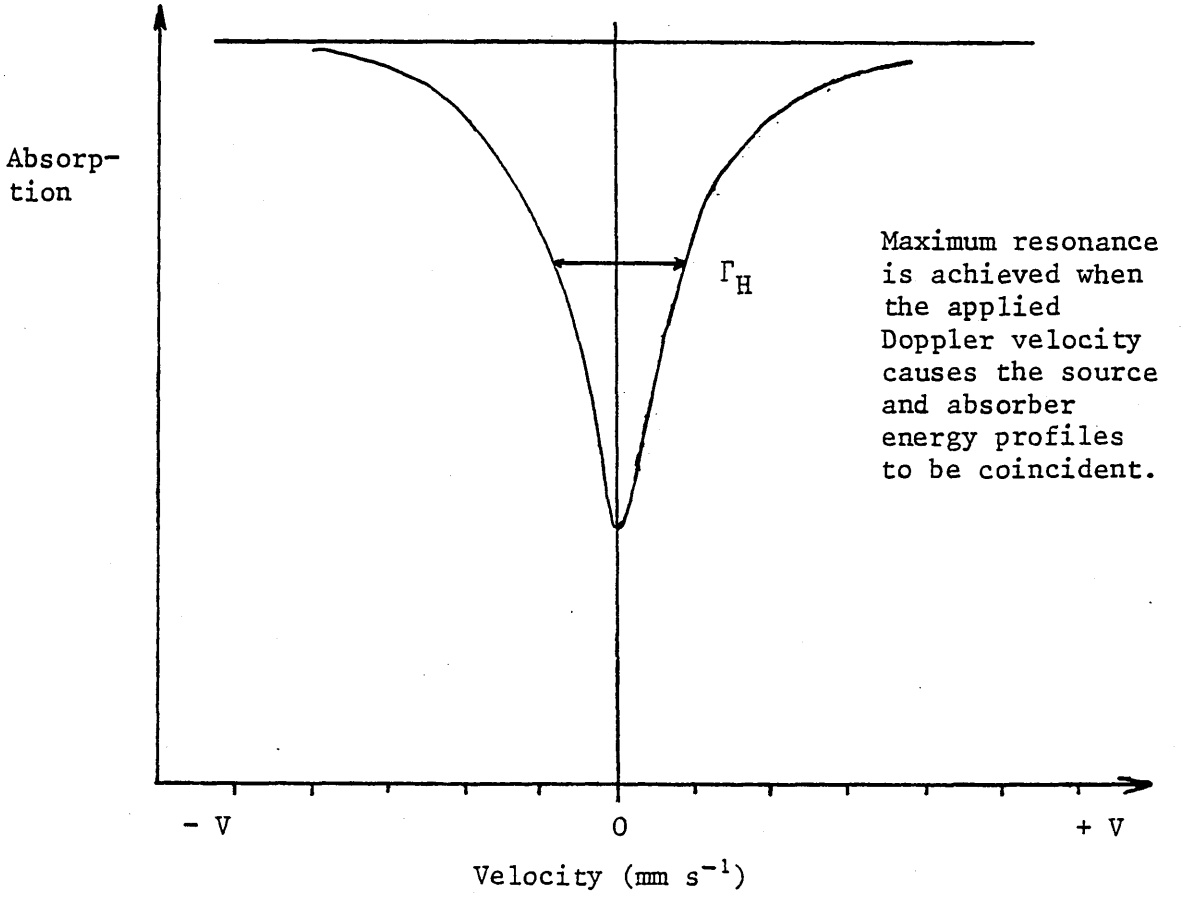

Having established that nuclear resonance absorption occurs when the emission and absorption energy profiles are exactly coincident it follows that a single absorption peak will be observed in the spectrum at zero velocity when the source and absorber nuclear energy levels are identical. Different absorbers will not have the same distribution of nuclear energy levels and therefore require different Doppler velocities to achieve resonance absorption. That different absorbers give rise to different spectra reflects the sensitivity of the Mössbauer technique to changes in the distribution of the nuclear energy levels as a result of changes in the extranuclear environment. These changes arise from Hyperfine Interactions between the nuclear charge distribution and the extra-electric and magnetic fields and give rise to the Isomer Shift (δ), Quadrupole Splitting (ΔE_Q), and magnetic zeeman splitting observed in the Mössbauer spectrum.

1.2.1 The Isomer Shift

The isomer shift arises from the electrostatic interaction between the charge distribution of the nucleus and those electrons which have a finite probability of existing in the nuclear volume i.e. the '<u>s</u>' electrons. The <u>s</u> - electron density of a given absorber, in general, differs from that of the source so that the interaction energies will differ and a shift in the energy levels, with respect to those of the source, is observed. Consequently a Doppler velocity is applied to the source to achieve resonance absorption (figure 1.5).

The interaction energies, and thus the shift in nuclear energy levels, can be estimated from the difference in the electrostatic interaction of a hypothetical point nucleus and a spherical nucleus with a uniform charge distribution (5,8,9). The potential due to the spherical nuclear charge distribution at a radial distance r from the origin is:

$$V_r = \frac{-Ze^2}{R}\left[\frac{3}{2} + \frac{r^2}{2R^2}\right] \qquad \text{for } r < R$$

(R is the radius of the nuclear volume)

Figure 1.5 The effect of the electrostatic interaction on the distribution between the absorber energy levels with respect to those of the source.

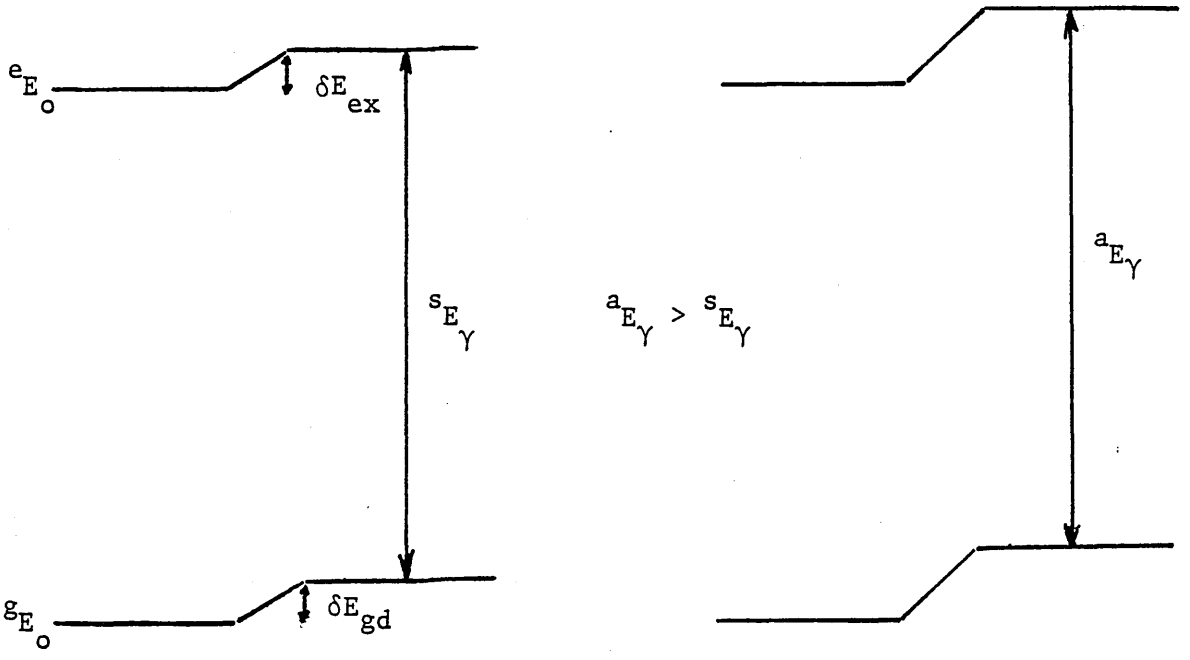

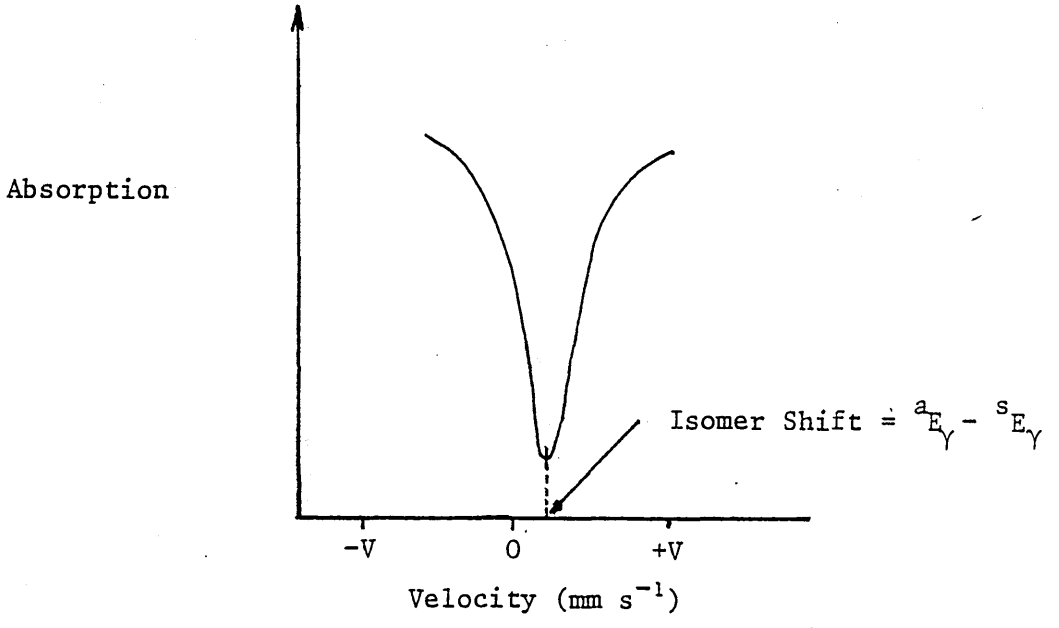

$$V_{pt} = -\frac{Z\,e^2}{r} \qquad \text{for } r > R$$

The difference between the electrostatic interaction of a nucleus of finite volume with s-electron density $\left[\psi(o)_s\right]^2$, and the interaction of a point nucleus of equal charge density is therefore:

$$\delta E = \int_{r<R}^{r>R} \left[\psi(o)_s\right]^2 \cdot (V_r - V_{pt}) \cdot 4\pi r^2 \cdot dr \qquad (1.17)$$

(where $4\pi r^2 \cdot dr$ is the change in nuclear volume).

Evaluating the term $(V_r - V_{pt})$ under the limits set reduces the equation to:

$$\delta E = \frac{2\pi}{5}\, Z\, e^2 \cdot \left[\psi(o)_s\right]^2 \cdot R^2 \qquad (1.18)$$

Since the nuclear excited and ground states do not have the same radii of equivalent charge distribution the s-electrons will therefore have a different interaction with the nuclear charge.

i.e. $R_{ex} \neq R_{gd}$

Therefore:

$$\delta E_{ex} - \delta E_{gd} = \frac{2\pi}{5}\, Z\, e^2 \cdot \left[\psi(o)_s\right]^2 (R_{ex}^2 - R_{gd}^2) \qquad (1.19)$$

The term $(\delta E_{ex} - \delta E_{gd})$ can only be evaluated with respect to a given source - absorber pair since $(\delta E_{ex} - \delta E_{gd})$ for the absorber will differ from the corresponding term for the source.

The term $(R_{ex}^2 - R_{gd}^2)$ will be constant in both source and absorber for a given isotope and thus the only remaining influence on the isomer shift is the term involving the s-electron density which will be different in the source and absorber.

From figure 1.5

$$E_{source} = E_o + \frac{2\pi}{5}\, Z\, e^2 \left[\psi(o)_s\right]^2_s \left[R_{ex}^2 - R_{gd}^2\right] \qquad (1.20)$$

$$E_{absorber} = E_o + \frac{2\pi}{5}\, Z\, e^2 \left[\psi(o)_s\right]^2_a \left[R_{ex}^2 - R_{gd}^2\right] \qquad (1.21)$$

Since the Isomer Shift = $\delta = E_a - E_s$

then: $$\delta = \frac{2\pi}{5}\, Z\, e^2 \left(\left[\psi(o)_s\right]^2_a - \left[\psi(o)_s\right]^2_s \right) (R_{ex}^2 - R_{gd}^2) \qquad (1.22)$$

Equation 1.22 shows the isomer shift to be dependent upon the s-

electron density at the nucleus. Although the electrons in the 1s, 2s, 3s... levels will all contribute to $[\psi(o)_s]^2$, for tin these inner shells are not markedly affected by the chemical bonding so that the principal influence on the isomer shift will be by the outermost occupied s - orbital.

In addition, the isomer shift is sensitive to contributions from the non - s electrons. p - electrons in the tin isotope will spend a finite time near to the nucleus thereby changing the s - electron density at the nucleus and resulting in a change in the effective potential acting on the outermost s - electrons. Such shielding effects cause a rearrangement of the spatial distribution of the s - electrons and results in a change to the total electron density at the nucleus.

The term $(R_{ex}^2 - R_{gd}^2)$ represents the difference in nuclear radii between the excited and ground states of the nucleus and may have positive or negative values. Since this term is constant for a given isotope the isomer shift is directly related to the difference in s - electron density between the source and absorber. For example, where $(R_{ex}^2 - R_{gd}^2)$ is positive (as for ^{119}Sn) an increase in the s -electron density results in a more positive isomer shift. Conversely, where the term is negative (as for ^{57}Fe) an increase in the s - electron density at the absorber nucleus results in a more negative isomer shift.

In ^{119}Sn Mössbauer spectroscopy tin compounds having the minimum s - electron density (such as stannic oxide, and barium and calcium stannates) are used as standard sources so that all other tin absorbers give a zero or positive isomer shift relative to the source.

1.2.2 The Quadrupole Splitting

The quadrupole splitting arises from the interaction of the nuclear quadrupole moment with the local electric field gradient. In defining the interaction that gave rise to the isomer shift the nucleus was considered to be spherical with a uniform charge density i.e. the spin angular momentum (I) = 0 or $\frac{1}{2}$ resulting in a zero quadrupole moment.

For nuclei with a spin angular momentum greater than $\frac{1}{2}$ the charge density is no longer uniform and the nucleus assumes either a prolate or an oblate shape resulting in a discrete quadrupole moment. The expression describing the interaction of the quadrupole moment (M_I) with the local electric field gradient is given by (5):-

$$E_Q = \frac{e^2 q Q}{4I(2I-1)} \left[3M_I^2 - I(I+1) \right] \left[1 + \frac{\eta^2}{3} \right]^{\frac{1}{2}} \qquad (1.23)$$

where Q = nuclear quadrupole moment

η = asymmetry parameter

(M_I^2 removes the degeneracy from the nuclear energy levels which have different values for the magnetic quantum number. The levels for which M_I changes in sign only remain degenerate). For ^{57}Fe and ^{119}Sn, $I_e = 3/2$ and $I_g = 1/2$. The I = 3/2 level is split into two levels ($M_I = \pm 3/2, \pm 1/2$) while the I = 1/2 level remains degenerate as shown in figure 1.6. Both transitions shown in the diagram are allowed and a characteristic two line spectrum is observed. The separation of the two peaks is the quadrupole splitting $\left[\Delta E_Q \ (=e^2qQ/2) \right]$ and the centre of the splitting gives the isomer shift.

In each case where the degeneracy is removed the magnitude of the splitting is determined by the interaction of the quadrupole moment with the Z component of the electric field gradient (E.F.G).

The E.F.G. arises as a result of the non-spherical charge distribution around the nucleus and, by determination of its origin, allows the basis for determining the co-ordination about the nucleus to be derived. It is defined by a 3 x 3 matrix which contains the resultant combinations of the cartesian axes from the centre of the nucleus, and which represents the negative gradient of the electric field from a point charge situated at any point around the nucleus within the limits set by the resultant cartesian co-ordinates i.e.

$$\text{E.F.G.} = \nabla E = \begin{bmatrix} V_{xx} & V_{xy} & V_{xz} \\ V_{yx} & V_{yy} & V_{yz} \\ V_{zx} & V_{zy} & V_{zz} \end{bmatrix} \qquad \text{where } V_{ij} = \frac{\partial^2 V}{\partial i \partial j}$$

Figure 2.6: Interaction of the nuclear quadrupole moment with the Electric Field Gradient for $I_e=3/2$ and $I_g=1/2$.

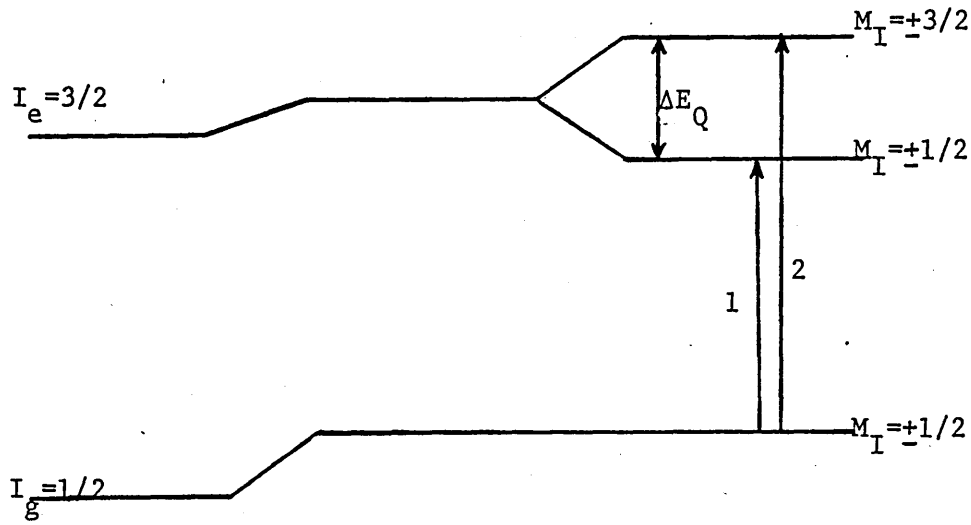

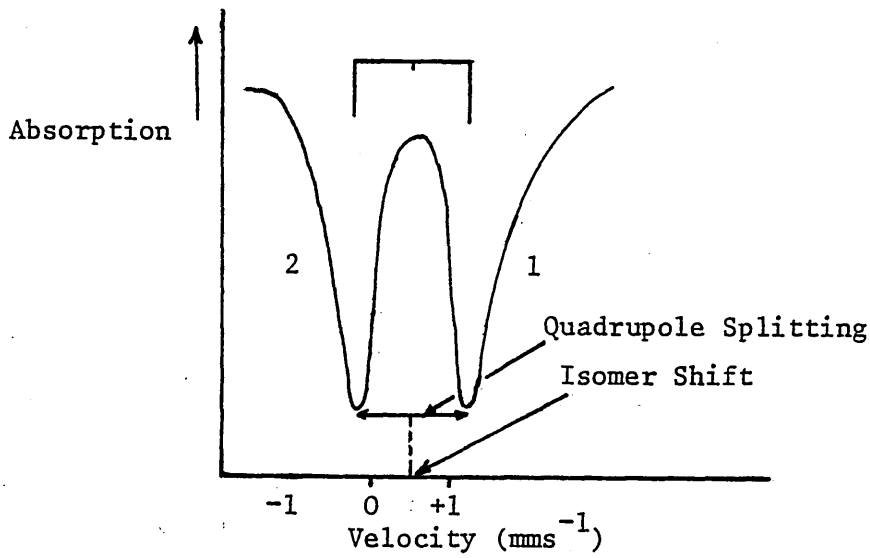

The above matrix is reduced by choosing a principal set of axes so that the off-diagonal terms are reduced to zero and the tensor has only three components: V_{xx}, V_{yy}, V_{zz}. Under such conditions these three components are not independent and are related by the Laplace equation:

$$V_{xx} + V_{yy} + V_{zz} = 0$$

By convention the Z co-ordinate of the E.F.G. is chosen to coincide with the highest symmetry axis of the molecule or crystal. The remaining two co-ordinates are evaluated using an asymmetry term, η,

which normalises the difference in potential between V_{xx} and V_{yy} with respect to V_{zz} i.e.

$$\eta = \frac{V_{xx} - V_{yy}}{V_{zz}}$$

Thus V_{zz} and η are the only two independent components in equation 1.23. The principal axes are usually chosen such that the non-diagonal components are zero and that $V_{zz} \geq V_{yy} \geq V_{xx}$, thereby making $0 \leq \eta \leq 1$. For an axially symmetric field gradient $V_{xx} = V_{yy}$ and so $\eta = 0$, and for cubic or spherical symmetry each of the $V_{ii} = 0$ and the quadrupole interaction is zero.

It is evident that the position of the point charges in the vicinity of the nucleus, with respect to the three components of the E.F.G. tensor, dictates the magnitude of the quadrupole splitting. Consequently any change in the position or any asymmetry introduced into the geometry of the arrangement, will be reflected in the contributions from V_{zz} and η thereby changing the value for the quadrupole splitting. V_{zz} and η , however, cannot be evaluated quantitatively from measurement of the quadrupole splitting alone.

The electric field gradient in general has two contributions. Each electron in the atom makes a contribution to a component of the E.F.G. tensor and, if the orbital population is not spherical, the total value of V_{zz} will be non-zero because of this Valence contribution. Thus if there is an excess of electron density along the Z axis (i.e. electrons in p_z, d_{z^2}, d_{xz}, d_{yz} orbitals) V_{zz} will be negative in sign, whereas if the excess in electron density is in the xy plane(i.e. electrons in p_x, p_y, d_{xy}, $d_{x^2-y^2}$ orbitals) V_{zz} will be positive in sign.

Secondly, there is a contribution from the distant charges (ionic charges) associated with the ligands and is referred to as the Lattice contribution. This term becomes important for an s-state ion where the valence contribution is negligible.

Finally to conclude the discussion of electrostatic interactions the effect of shielding on the quadrupole splitting must be considered.

The effective field gradient at the nucleus arising from either the surrounding ions or the outer unfilled valence shells is significantly modified by the atom's own inner closed shell electrons. Distribution of the closed shells, giving rise to a hyperfine interaction with the nucleus, may occur resulting in shielding or anti-shielding effects on the effective field gradient. Corrections for shielding or anti-shielding can be made by multiplying the uncorrected quadrupole moment by a factor of $1/(1 - R)$ (5,9).

(The factor R is the Sternheimer shielding factor).

1.2.3 Magnetic Hyperfine Interaction

The magnetic hyperfine splittings arise from the interaction of the Nuclear Magnetic Dipole Moment 'μ' with the hyperfine magnetic field 'B' existing at the nucleus. The Hamiltonian representing the interaction is given by:

$$\mathcal{H} = -\mu.B = -g_N\mu_N I.B \qquad (1.24)$$

where g_N = nuclear gyromagnetic ratio
μ_N = nuclear magneton
I = nuclear spin angular momentum

The interaction removes the degeneracy of the nuclear spin I to split each level into (2I + 1) sub-levels (figure 1.7). The shifts in the nuclear energy levels associated with the loss of degeneracy, are given by the relationship:

$$E_{M_I} = -\frac{\mu_N.B.M_I}{I} \qquad (\text{for } M_I = I, I-1, I-2 \ldots\ldots I)$$

$$= -g_N\mu_N B.M_I \qquad (1.25)$$

A practical application of the magnetic interaction is obtained using the ^{57}Fe nucleus. For ^{57}Fe, g_N differs in sign for the ground and excited states and the selection rules concerning the allowed Mössbauer transitions ($\Delta M_I = 0, \pm 1$) apply giving rise to a symmetric six line spectrum (figure 1.7).

occuring in the ^{57}Fe nucleus and the resultant Mössbauer spectrum

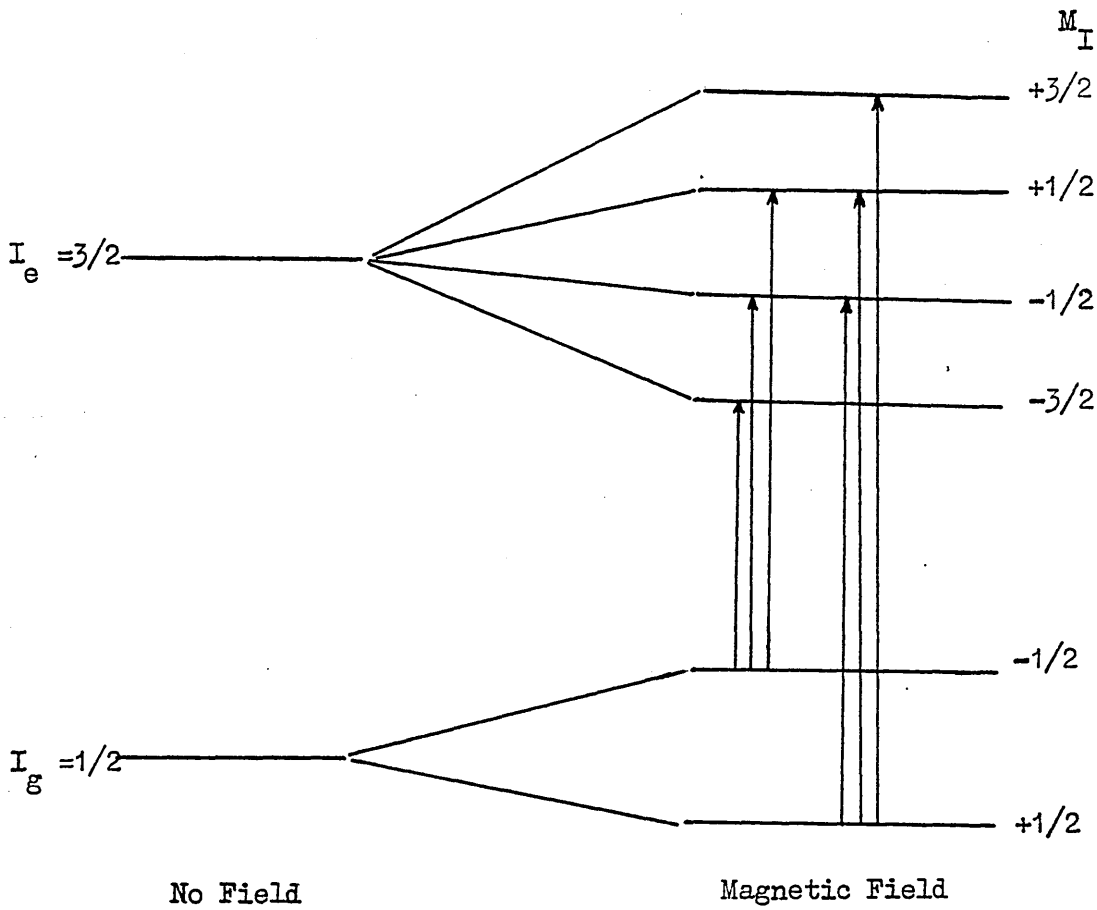

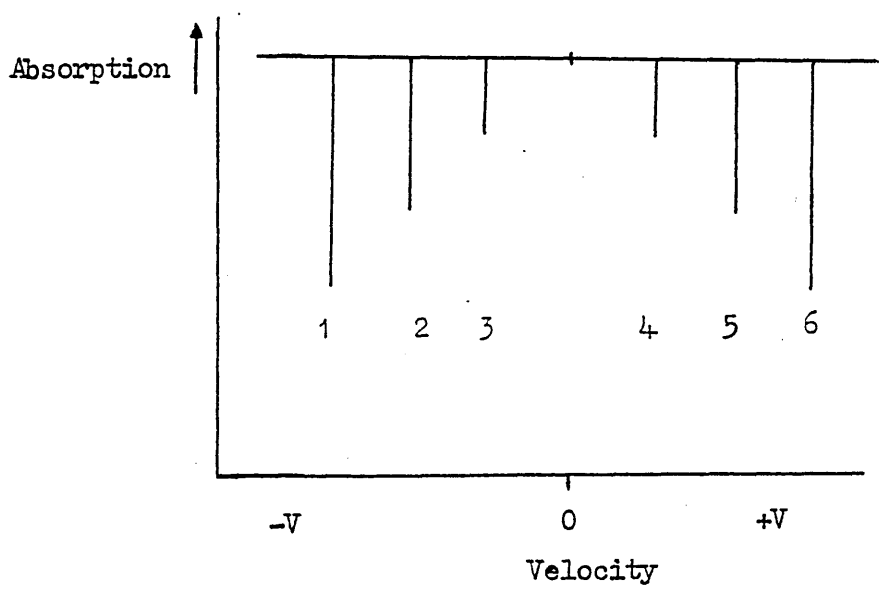

The spacings between the line pairs (1,2), (2,3), (4,5) and (5,6) are equal since for $I = 3/2$ $\quad E = -g_N \cdot \mu_N \cdot B \cdot 3/2$

and for $I = 1/2$ $\quad E = -g_N \cdot \mu_N \cdot B \cdot 1/2$

Hence $\quad M = (I_{3/2} - I_{1/2}) = -g_N \cdot \mu_N \cdot B.$

Consequently the iron spectrum is used for calibration and linearity checks.

Finally, the intensities of the lines are dependent upon the angle θ between the effective magnetic field, B, and the direction of propagation of the radiation. Bancroft (8) has shown that the intensities of the lines are given by the relationships:-

$$\begin{aligned} I_1 &= I_6 = 3 (1 + \cos^2\theta) \\ I_2 &= I_5 = 4 \sin^2\theta \\ I_3 &= I_4 = 1 + \cos^2\theta \end{aligned} \qquad (1.26)$$

For the example shown in figure 1.7 in which the six line spectrum has the magnetic domains randomly orientated, the area ratio of the six lines is 3:2:1:1:2:3, which results from integrating the above expressions over all angles.

Contents:

2.1. Experimental

2.1.1. Important Criteria for a Mössbauer Isotope

The Mössbauer Effect is not observed in many of the nuclei in the Periodic Table. The criteria which determine in which nuclei the Mössbauer Effect is observed are listed as follows:-

(i) The source must emit a suitable low energy γ-ray which gives an unsplit emission line. The magnitude of E_γ is important since the smaller E_γ the greater the recoilless fraction 'f' (equation 1.11).

(ii) The Mössbauer γ-ray must be well separated in energy from other photons in order to reduce background levels in the Mössbauer spectrum.

(iii) The radioactive decay of the source must prove convenient for practical experiments. (For example, the parent nuclei for Nickel Mössbauer Spectroscopy are ^{61}Co and ^{61}Cu, which have half-lives of 17 hours and 3.3 hours respectively and are far too short for routine experiments).

(iv) The magnitude of the Mössbauer Effect is proportional to the area under the absorption curve. In general, for a 'thin' Lorentzian absorption line and using a single-line source the area is given by:-

$$A = \tfrac{1}{2}\pi . f_a . f_s . \sigma_o . n . X \qquad (2.1)$$

where f_a, f_s = recoilless fraction of the absorber and source respectively
σ_o = isotope cross section
n = isotope natural abundance
X = absorber thickness

From the above expression it is apparent that only those isotopes which have a high natural abundance, large cross section and large recoilless fractions will give a significant Mössbauer Effect.

It should be noted that the above expression only applies to thin absorbers and that where X is large, deviations from the Lorentzian shape occur resulting in saturation. The effect of absorber thickness on the area under the absorption curve is discussed in section 2.1.3.

(v) Finally, having chosen an isotope that gives a large Mössbauer

direct and has a long parent half-life, the line positions must be sensitive to the chemical enviroment and any changes in the line positions must be measureable.

2.1.2. The Source

The decay of ^{119}Sn emits a γ -ray of energy 23.8KeV (half-life = 245 d) which has a natural line width of ω_o =0.6467 mms^{-1} (10). The decay scheme for ^{119}Sn is shown in figure 2.1(a). The source used during this investigation was a 15mC ^{119}Sn isotope in a $BaSnO_3$ matrix supplied by New England Enterprises. This has a full width at half-height of 0.8196 mms^{-1}, measured against a 0.0005" tin absorber and an isomer shift of + 2.55mms^{-1} corresponding to the β -tin arrangement in the $BaSnO_3$ lattice.

For the purpose of calibration and linearity checks, the magnetic hyperfine splitting of the ground and first excited state of ^{57}Fe was used. To observe this the 14.4KeV γ -ray transition to the ground state of ^{57}Fe was used, which is emitted during the decay of ^{57}Co (shown in figure 2.1 (b) (half-life = 270 d). The 14.4KeV γ -ray has a natural line width ω_o = 0.1940 mms^{-1}(10). The source used was a ^{57}Co isotope in a Palladium matrix with an estimated activity of 3mC , having a single line with a full width at half-height of 0.22mms^{-1}. Both sources had an acceptable recoilless fraction at room temperature. Nuclear parameters for tin and iron are given in Table 2.1.

2.1.3. The Absorbers

In Chapter 1 the line widths were shown to be related to the half life of the excited nuclear state by the expression:

$$\Gamma_H = \frac{\hbar \cdot 0.6939}{t_{1/2}}$$

In practice, however, the observed line width at half maximum is influenced by the thickness of the absorber. As the thickness of the absorber increases the line shape begins to deviate from the Lorentzian shape and saturation effects are observed. On the other hand the absorber needs to be of finite thickness for resonant absorption to be

Figure 2.1(a). Nuclear Decay Scheme for ^{119}Sn.

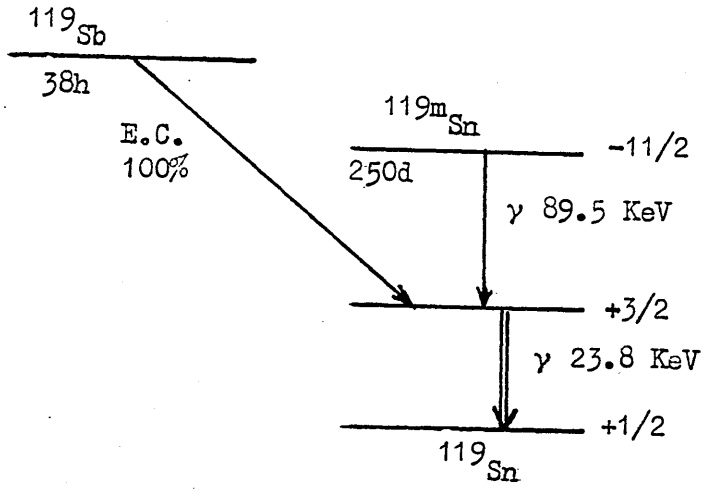

(b) Nuclear Decay Scheme for ^{57}Fe.

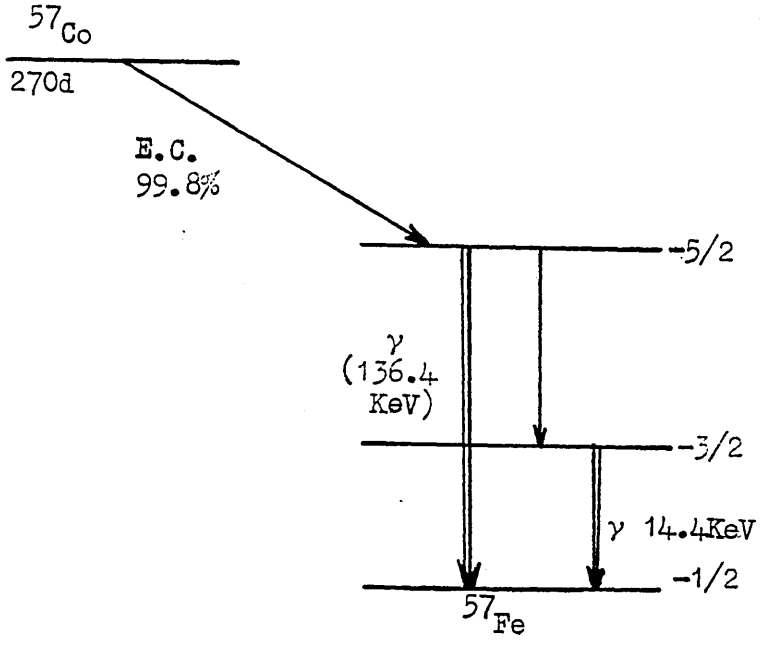

Table 2.1. Mössbauer nuclear parameters and calibration data for ^{119}Sn and ^{57}Fe.

(Data for both nuclei obtained from the Mössbauer Effect Data Index 1975).

^{119}Sn	^{57}Fe
E_γ = 23.8 KeV	E_γ = 14.4 KeV
μ_g = -1.04621(6) nm	μ_g = +0.09024(7) nm
μ_e = +0.682(8) nm	μ_e = -0.15460(16) nm
$R_\mu = \frac{\mu_e}{\mu_g}$ = -0.6519	$R_\mu = \frac{\mu_e}{\mu_g}$ = -1.7132
$\Gamma = 2.570 \times 10^{-8}$ eV	$\Gamma = 4.665(7) \times 10^{-9}$ eV
ω_o = 0.646(4) mms^{-1}	ω_o = 0.1940(3) mms^{-1}
Isotopic Abundance =8.58%	Isotopic Abundance = 2.14%
	Line positions (symmetrical)
	E 1,6 ±5.312(4) mms^{-1}
	E 2,5 ±3.076(2) mms^{-1}
	E 3,4 ±0.840(2) mms^{-1}
$\frac{g_e}{g_g}$ = -0.2173	$\frac{g_e}{g_g}$ = -0.57106

..., and so an optimum thickness must be estimated to give an optimum absorption curve. A quantitative appreciation of the effect of varying the absorber thickness is obtained by considering the area under the absorption curve. Brooks and Williams (11) showed that, in general:

$$A(t) \propto \tfrac{1}{2}t \exp(-\tfrac{1}{2}t).\left[I_o(\tfrac{1}{2}t) + I_1(\tfrac{1}{2}t)\right] \qquad (2.2)$$

where $A(t)$ is the Area under the absorption curve arising from an absorber of thickness 't'
I_o is a Zero order Bessel function
I_1^o is a First order Bessel function.

The above expression can be reduced, to a first approximation, to:-

$$A(t) \propto f_s\, t\,(1 - 0.25t + 0.0625t^2 + ...) \qquad (2.3)$$

for values of $t \ll 5$.

f_s = Lamb - Mössbauer factor for recoilless fraction in the source.

where t is large ($\simeq 10$) equation 2.2 must apply.

The absorber thickness is calculated using the equation:-

$$t = \beta \cdot n \cdot f_a \cdot \sigma_o \cdot X \qquad (2.4)$$

where n = no. of resonant nuclei/cm^3
σ = resonant cross section
f^o = absorber recoilless fraction
X^a = actual absorber thickness
β = relative intensity of the absorption lines.

In practice, evaluation of the optimum absorber thickness using equation 2.4 is limited in that for many compounds f_a is not known. In addition, the absorption curves are susceptible to deviations from the Lorentzian shape due to particle-size effects, crystal orientation effects, the Goldanskii - Karyagin effect , and from additional non-resonant intensities produced by the scattering of higher - energy γ -rays.

The tin compounds investigated were obtained as either powders or liquids or incorporated in a PVC matrix. The physical state of the sample determined the amount of tin in the sample which consequently dictated the length of the run time required to obtain the Mössbauer spectrum. Long run times (of the order of 48 hours) were found necessary for samples of the tin compounds dispersed in the PVC matrix due to the

low concentration (4%w/w of the polymer) of the tin and the absorption of γ - rays by the PVC. For powder and liquid samples such as pure dimethylchlorotin acetate and dibutyltinbis(isooctylthioglycollate) respectively run times of only four hours were required to obtain the Mössbauer spectrum.

Typical t values for the organotin stabilisers dispersed in PVC (at 1.2% w/w) can be calculated using equation 2.4:

$$t = \beta.n.f.\sigma_o$$

where $\beta = 1/2$ for a single quadrupole doublet.

$f = 0.6$ (corresponding to the maximum value where fa = fs - the recoilless fraction of the source).

$\sigma_o = 1.403 \times 10^{-18}\ cm^2$

n = number of resonant atoms/cm^2

(i) To calculate n:

Weight of stabiliser in PVC sample	=	9.96×10^{-3} g
Weight of ^{119}Sn in the stabiliser	=	1.59×10^{-4} g
Weight of $^{119}Sn/cm^2$	=	6.25×10^{-5} g/cm^2
$\therefore$ Number of atoms of $^{119}Sn/cm^2$	=	3.16×10^{17} atoms/cm^2

Substituting the value for n into equation 2.4 gives

$t = 0.133$.

This represents a maximum expected value for a recoilless fraction of 0.6. In general organotin compounds have recoilless fractions in the range (0.06 to 0.4) at 80K (5).

Equation 2.3 relates the area under the absorption peaks to the absorber thickness:

$$A(t) \propto f_s.t\ (1 - 0.25\ t + 0.0625\ t^2 + ...)$$

$$A(t) \propto f_s.t - 0.25\ f_s\ t^2 + ...$$

Substituting for t gives:

$$A(t) \propto f_s.(0.133 - 0.0026)$$

The term $f_s\ t^2$ can be considered negligible and the values calculated show the area under the absorption peaks (A(t)) to be directly proportional to the absorber thickness.

in Chapter 1 the Mössbauer spectrum was defined as a plot of the number of γ-ray photons transmitted through an absorber as a function of the instantaneous relative Doppler velocity of the source with respect to the absorber. Servo and power amplifiers drive the source producing Doppler - shifted γ -rays which interact with the absorbers. The transmitted γ -rays then pass through a suitable detector and into a multichannel analyser where the spectrum is compiled over 512 channels, each channel representing a particular γ -ray energy corresponding to a specific Doppler velocity. Accumulated in the multichannel analyser the spectrum is available for computer processing. Figure 2.2 shows a block diagram of the Mössbauer system used during these investigations.

2.2.1. Mössbauer Drive System and Multichannel Analyser

Throughout this investigation a Northern Scientific ECON series II 1024 multichannel analyser was used. Two modes of operation were available: the TIME mode, in which the analyser operates as a multichannel scaler, and the Pulse Height Analysis (P.H.A.) mode. In the time mode the analyser stores the total count information in each channel through a preset time interval of 50 - 100 μs. At the end of the time interval the address is advanced to the next sequential channel. The only dead time is that incurred during the channel - advance and this has been estimated to 5 - 10% of the total scan time. This operating cycle is repeated over 512 channels and then recycled. When operated in the P.H.A mode random input pulses are sorted and counted according to their peak amplitudes. The height of the pulse is directly proportional to the energy of the γ-ray producing the pulse and the resulting energy spectrum is stored in the 512 channels of the multichannel analyser.

A constant acceleration vibrator was used to scan a range of fixed velocities ($\pm$ 0$\rightarrow$10 mms^{-1})linearily and repetitiously with the counts being stored in the multichannel analyser such that the velocity

Figure 2.2 Block diagram of the Mössbauer system

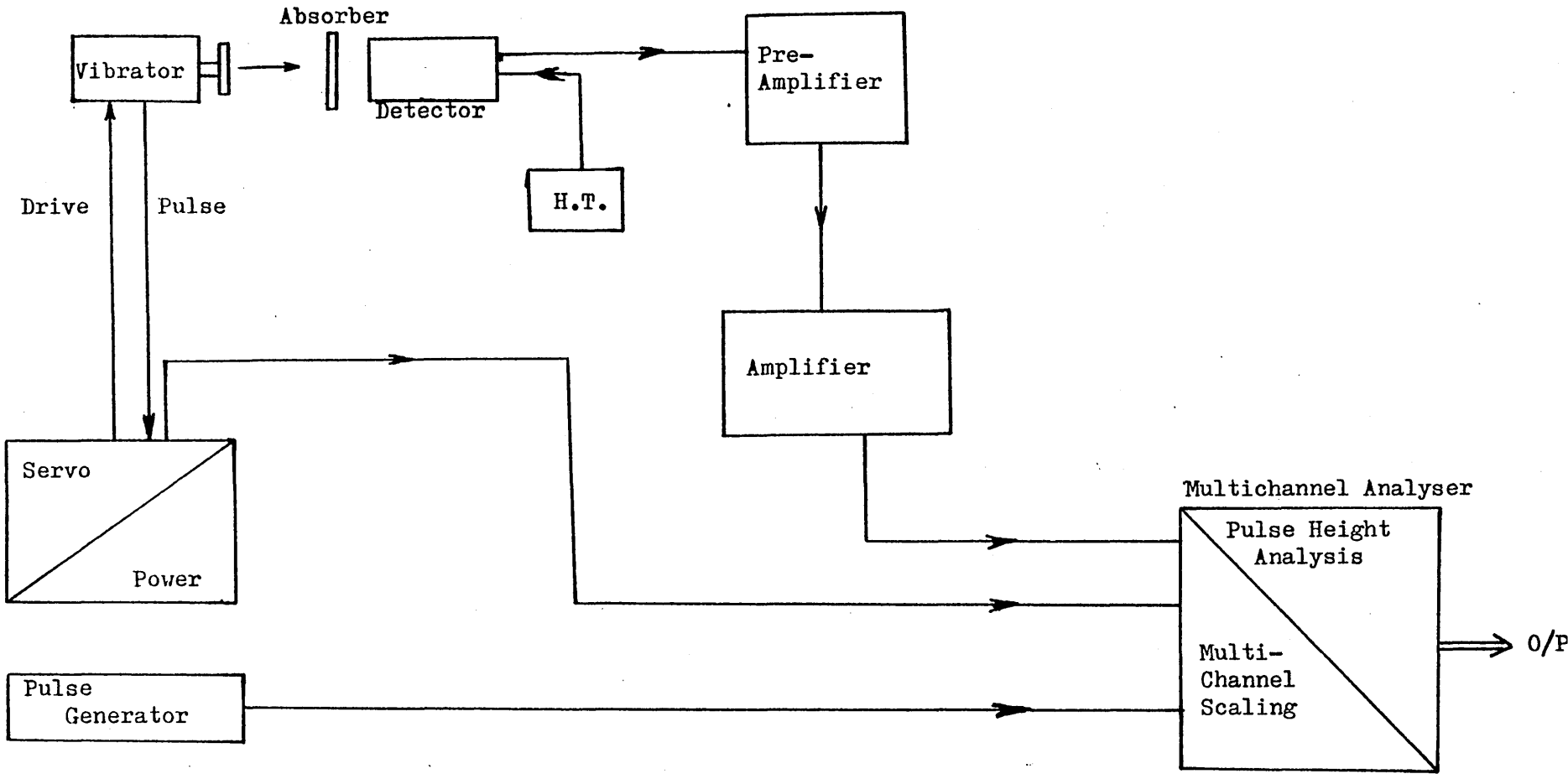

increment per channel was constant. Using 512 channels of the multi-channel analyser a square wave was extracted from the 'Most Significant Bit' (MSB) of the MCA such that its leading edges were 256 and 512. Since the vibrator is driven by a symmetric triangular waveform the square wave is then integrated to give the required reference waveform to drive the vibrator (figure 2.3). The drive or transducer produces a voltage proportional to the velocity of the vibrator's drive shaft. The servo amplifier compares this signal to the reference triangular waveform and applies corrections to the drive coil to minimise any differences. The amplitude of the triangular waveform determines the velocity scan of the vibrator and can be changed using a conventional potentiometer (helipot). While the vibrator is sweeping continuously over a range of velocities, the MCA is sweeping continuously through 512 channels. The two sweeps are automatically synchronised and the γ-rays from a particular velocity are fed to the same channel in the analyser.

Using this symmetric waveform a mirror image of the spectrum is obtained since, by the nature of the waveform, the velocity of the source will change from 'positive to negative' and from''negative to positive' during a single cycle. This serves a useful purpose in that the duplicate spectrum can be 'folded over'-with a mirror centre at channel 256 - and computer averaged (figure 2.6). The process of folding the data also aids the resolution of the spectra and serves as an additional check on d.c. drift.

2.2.2. Detectors

The detection system employed consists of either a proportional counter or a scintillation counter (depending on the energy of the γ -rays involved), a pre-amplifier and a high count - rate amplifier. Since the γ-ray transition giving rise to the Mössbauer Effect in iron compounds occurs at 14.4KeV the proportional counter is prefered as the low energy γ -rays are absorbed totally by the gas filling of the counter. This has better resolution and better signal/noise ratio than

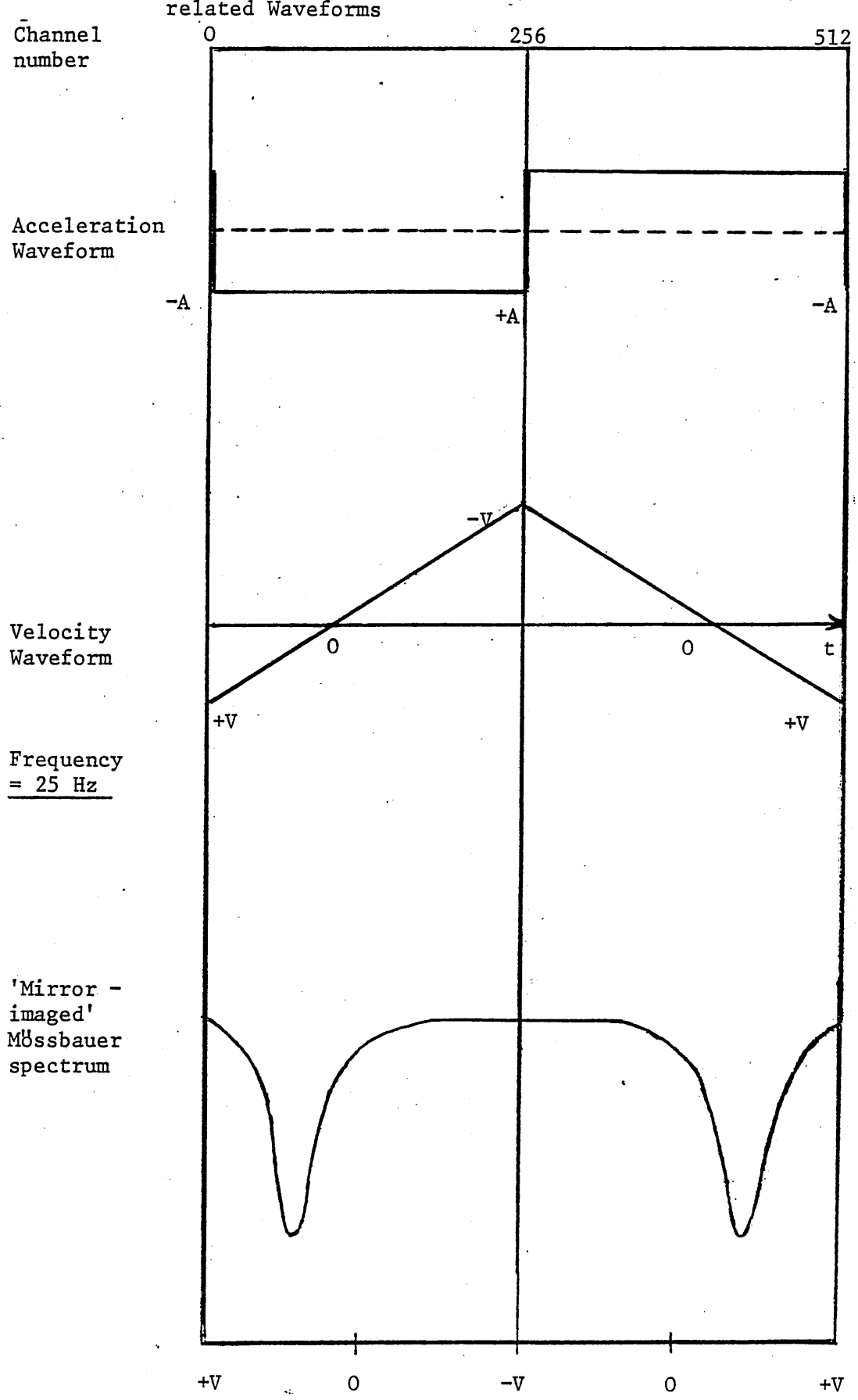

The output is folded about channel 256, each channel corresponding to a fixed velocity.

(Zero velocity is expected at channel 128.5)

the scintillation counter, the efficiency of which deteriorates at low energies on account of the thickness of the NaI(Tl) crystal employed. The proportional counter used for iron studies contains a mixture of 90% Argon and 10% Methane providing optimum conditions for the ionising radiation. The operating voltage is at 2.28 KV .

In studies with tin compounds in which the γ-ray transition energy is 23.8KeV , the sodium iodide - thallium activated NaI(Tl) crystal scintillation counter is used since this shows much greater efficiency than the gas-filled proportional counters at energies greater than 15KeV (12). The main advantage the solid scintillator has over the proportional detector lies in its operation.

Figure 2.4 Typical Resolution Curves of commonly used γ -ray Detectors

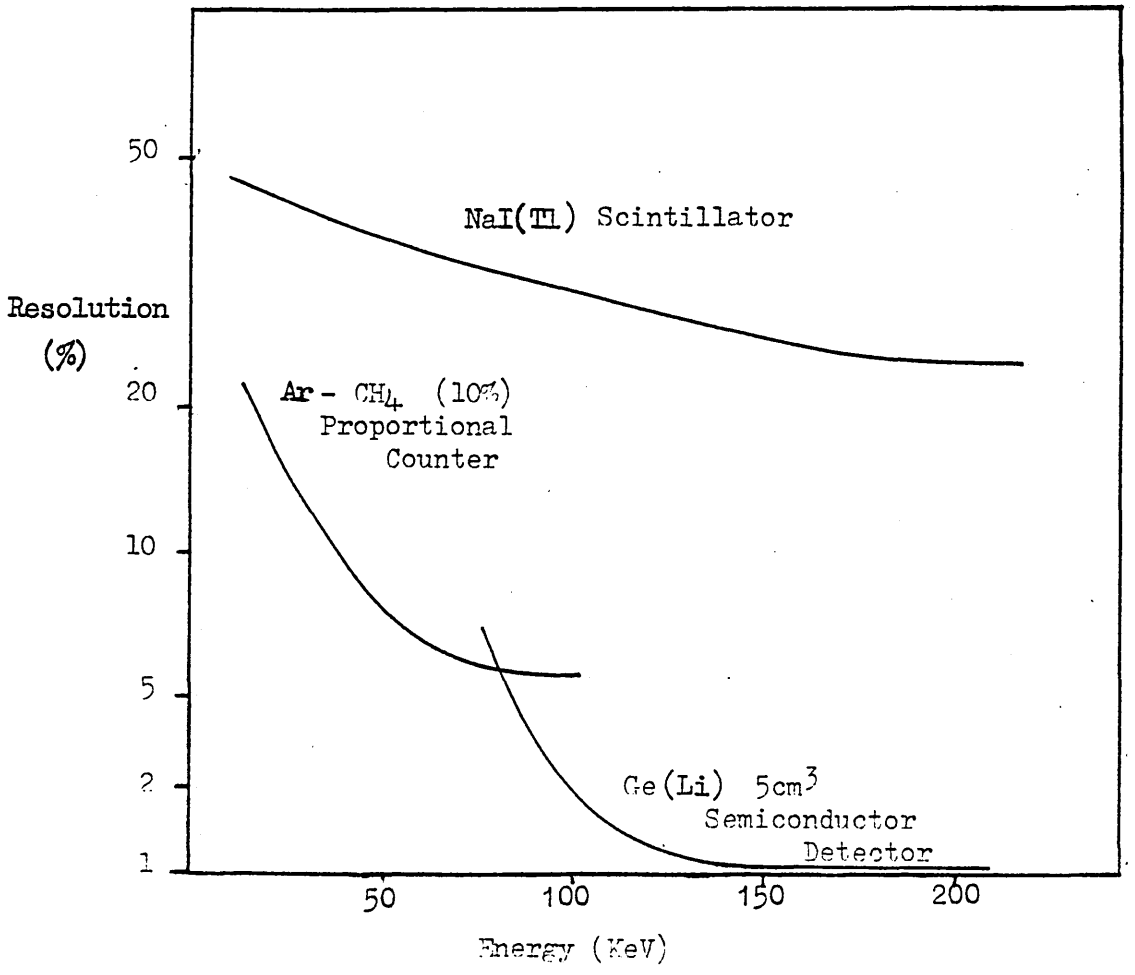

The scintillation counter operates by producing electron-hole pairs as a result of absorption of the high energy γ-ray on the NaI(Tl) crystal. The energy of the photon is rapidly transferred through a large number of

electron-hole interactions to produce a large number of low energy photons which then activate a photomultiplier. The total number of light pulses emitted by the crystal are proportional to the energy of the original γ -ray. The resolution of the detector is further increased by using a NaI(Tl) crystal which has a high light output compared to other crystals.

If a gas-filled proportional counter is used to measure the high energy γ -rays the number of ions produced in the gas becomes very high and the counter loses its proportionality due to space-charge effects in the 'avalanche' electrons and in the limit of high multiplication the output pulse height becomes independent of the primary ionisation. Hence a loss of stability and a loss of resolution occurs for higher energy radiations.

The scintillation detector used containes a 1 mm thick NaI(Tl) crystal mounted behind a very thin ($\simeq$ 0.025 mm) aluminised -mylar window and has an operating voltage of 1KV. Figure 2.4 shows a comparison of the characteristic resolution obtained with a NaI(Tl) detector and an Argon - Methane proportional counter (12).

2.2.3. Cryogenic System

A CF200 continuous flow cryostat was used to maintain the low temperatures (80K) required to record the Mössbauer spectra of the organotin compounds used in these studies. The cryostat (figure 2.5) contains a central chamber at its base in which a gold-plated sample probe (figure 2.5(a)) is located, and which is filled with Helium exchange gas thereby eliminating the problem of cooling inherently poor thermal conductors.

Temperature control and measurement is achieved using a DTC 2 digital temperature controller and a CLTS carbon resistor located on the side of the heat exchanger as a sensor which converts temperature into an electrical signal. This signal is fed to the DTC 2 which indicates the temperature on a four digit display. The measured

Figure 2.5 CF200 Continuous Flow Cryostat

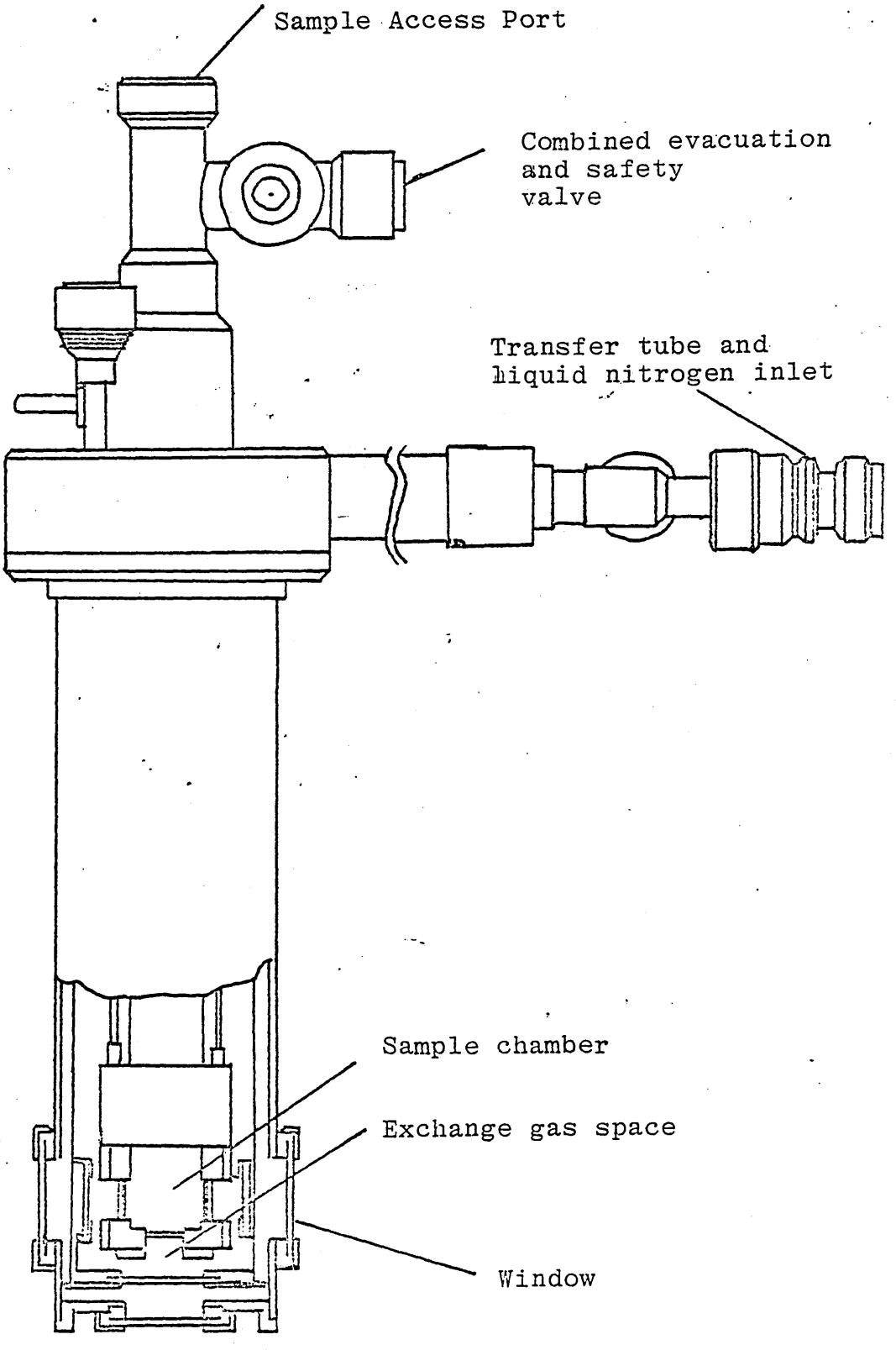

Figure 2.5(a) Sample probe for CF200 Continuous Flow Cryostat

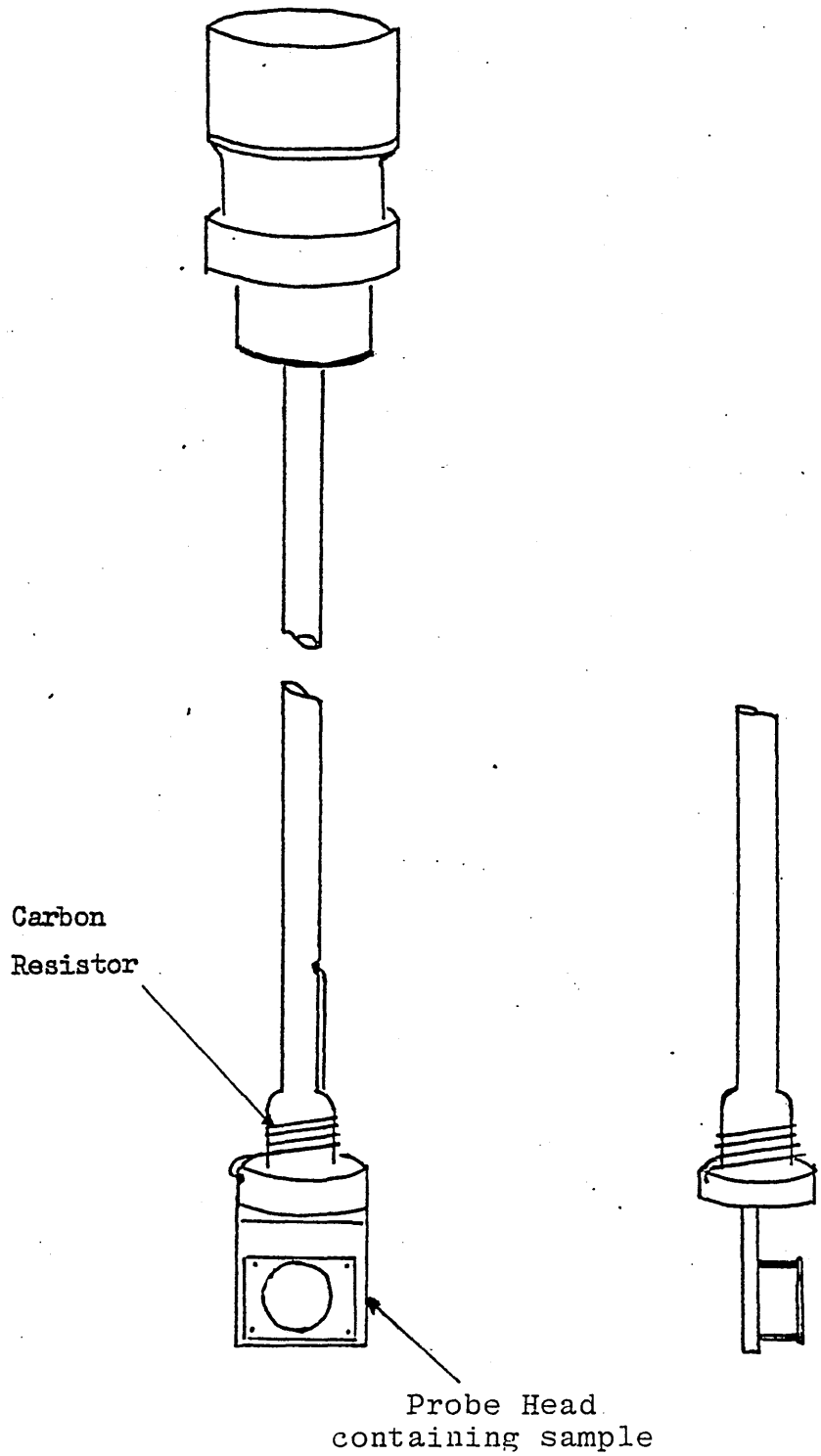

temperature is compared with the desired temperature and an error signal is generated proportional to the temperature difference. The controller then regulates the amount of power fed to a heater depending on the magnitude of the error signal.

An additional temperature monitor is also carried out using a calibrated carbon resistor located at the base of the sample holder. The output, in terms of resistance, is monitored on a digital multimeter and represents the temperature inside the sample chamber.

Liquid nitrogen is used to obtain a temperature of 80K and is drawn from a reservoir through a transfer tube to the outer jacket of the cryostat where it is circulated around a heat exchanger. The sample chamber, also in contact with the heat exchanger, is first evacuated and then filled with Helium exchange gas, thereby allowing for efficient cooling of the sample.

Powder and liquid samples were studied using the same sample probe. In the case of powdered samples the absorber is placed in a small perspex disc which is then sealed and secured to the base of the probe. The liquid absorbers, however, were injected through a small hole drilled into the sealed disc such that no air bubbles were present. The hole was then plugged using perspex wedges and the disc secured to the sample probe.

The discs were secured to the probe by placing them between the base of the probe and a cover plate which is attached to the probe by four brass screws (figure 2.5 (a)). The cover plate has a central hole drilled out slightly smaller in diameter than the perspex disc to allow passage of the γ -rays through to the detector. The probe is positioned in the cryostat in alignment with the aluminised - mylar windows at its base. Sample replacement is achieved by removing the probe from the cryostat, allowing it to reach room - temperature, and then removing the cover plate retaining the sample disc.

2.3. Computer Fitting Process.

The use of computational facilities is essential for the interpretation of Mössbauer spectra in terms of line position, line widths and relative intensities. A program based on the work of Lang and Dale (13) on the computer fitting of Mössbauer spectra was used for the analysis of the Mössbauer data.

As described in section 2.2.1 the constant acceleration vibrator produced a Doppler velocity which varied from + V to 0 to -V and back to +V through one complete cycle of 512 channels. By the nature of the triangular waveform produced by the transducer the two zero velocity positions are at mirror positions and at the extremities of the source displacement. Consequently the spectrum produced contains the mirror image of the data in the first half (0→256 channels) of the multichannel analyser.

2.3.1. Folding Program

The first operation in the fitting process is to fold the data stored in channels 0→256 onto the data in channels 256→512 and to add the counts stored in the corresponding channels. An accurate determination of the zero velocity position (expected at channel 128.5) is ensured in the folding process by scanning 10 half - channels either side of expected folding positions to find the best mirror axis for the absorption peaks so allowing for small fluctuations in the D.C. level of the drive system. The best mirror axis is determined by evaluating the minimum difference between the sum of the squares of the mirrored data points. Figures 2.6 & 2.6.1 (a→c) shows the sequence of events in the folding giving rise to zero positions at (a) an offset of - 10 (channel 123.5) (b) an offset of - 5 (channel 126) and (c) an offset of 0 (channel 128.5).

2.3.2. Fitting Program

A visual inspection of the Mössbauer spectrum determined the type of fit to the data in the folded spectrum (now in 256 channels). The

Figure 2.6 Data comprising two mirror image spectra

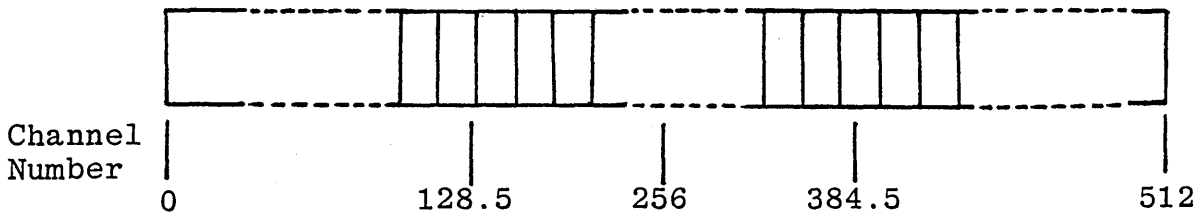

Figure 2.6.1 Folded data showing zero position at:

(a) Offset = -10
(channel 123.5)

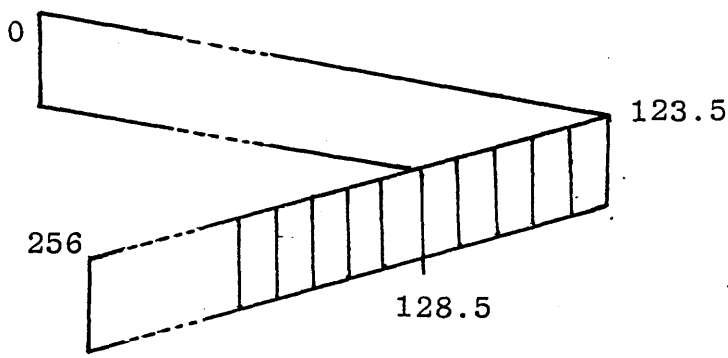

(b) Offset = -5
(channel 126)

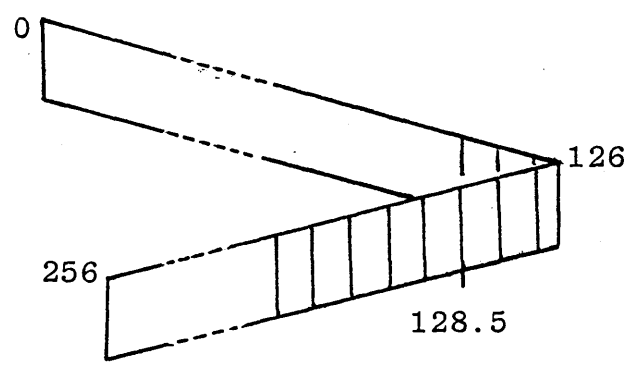

(c) Offset = 0
(channel 128.5)

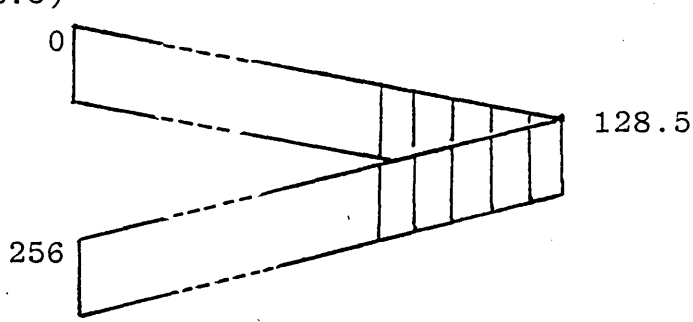

options available describing the different types of fitting conditions are listed as follows:-

Option 1 : the absorption peaks are fitted as individual lines. The computer varies the position, width and depth of each line independently to obtain the best fit.

Option 2 : the absorption peaks are fitted as a number of doublets. The centre, splitting / 2, widths and depths estimated from the folded data are varied until the best fit is obtained. The widths of the component lines of each doublet are made equal.

Option 3 : the absorption peaks are fitted as individual lines having the same widths. The computer varies the positions, widths and depths of the lines under the restriction that each line is given the same width, until the best fit is obtained.

Option 4 : the absorption peaks are fitted as a number of doublets but under the same restriction given in Option 3. The centres, splittings/2, widths , and depths of each doublet are varied until the best fit is obtained.

Using any of these options a non - linear least squares program is used to fit the data to theoretical Lorentzian line shapes relative to a constant background which takes into account small variations from the cosine effect. This program is then used to:-

(i) calculate the line positions, widths and intensities in the spectrum from the folded data.

(ii) calculate a minimum in the difference between the sum of the squares of the experimental data points and the theoretical data points (obtained from a second subroutine in the program). This defines the χ^2 value which has the expression:

$$\chi^2 = \sum_{i=0}^{i=256} \left(x_i^{\text{experimental}} - x_i^{\text{theoretical}} \right)^2$$

(If the difference between the experimental and theoretical data is large or if the amount of background scatter is great, then χ^2 will be

large).

(iii) use the least squares analysis to determine the optimum values of the background counts, baseline curvature and overall intensity of the final spectrum.

2.3.3. Calibration of the Mössbauer Spectrum

The amplitude of the symmetric triangular waveform which drives the vibrator, is determined by the helipot setting on the servo amplifier and is related to the velocity range through which the vibrator is driven. Consequently the 512 channels containing the Mössbauer spectrum must be calibrated using the velocity range set by the helipot relative to the amplitude of the waveform. The calibration constant (defined in terms of channels $mm^{-1} s^{-1}$) for a particular helipot is obtained using the magnetic six-line spectrum of enriched iron as a calibration standard (figure 2.7).

Figure 2.7 Enriched iron spectrum recorded over 512 channels.

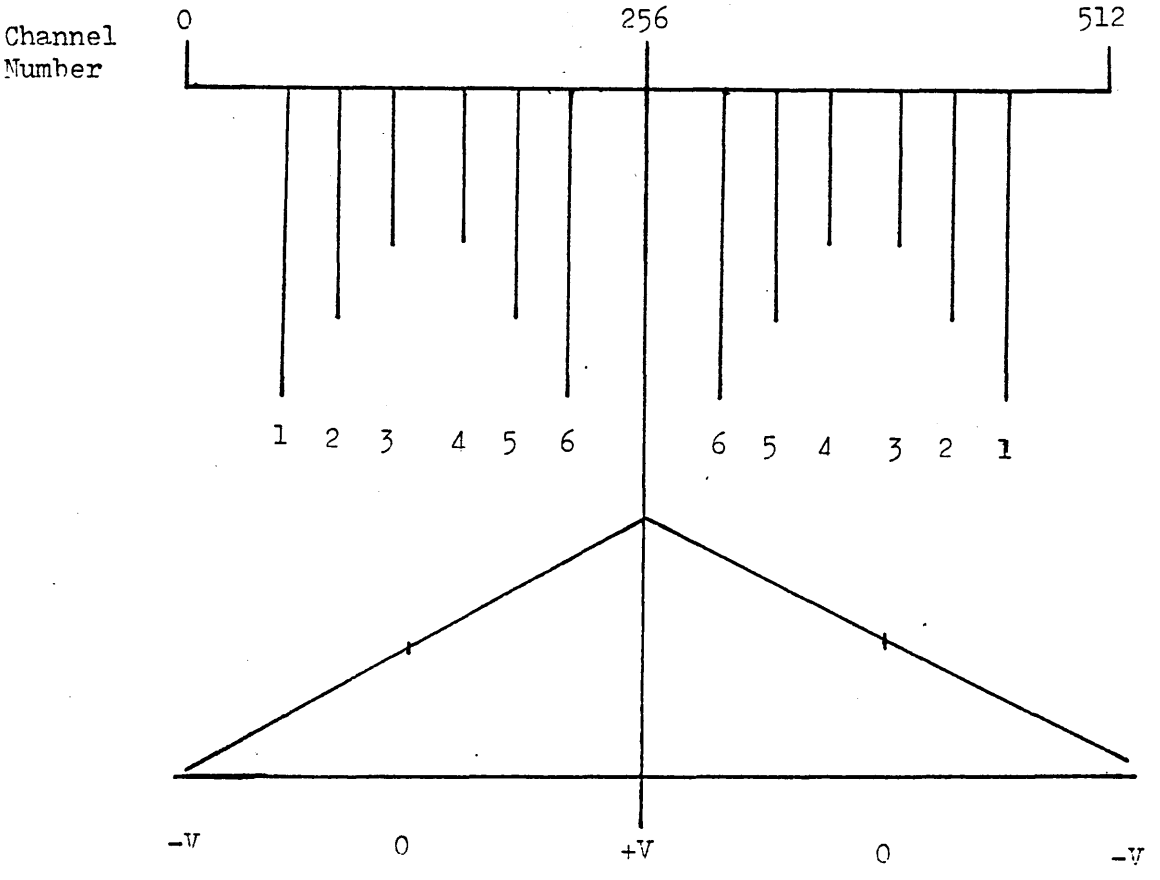

From figure 2.7 it can be seen that the data on the ascending arm of the voltage ramp (0→256 channels) is the mirror image of the data on the descending arm of the voltage ramp. The data is thus folded thereby reducing the amount of data handled and enabling calculation of the zero velocity (to within ±0.5 channels).

Having folded the data the lines are fitted in their pairs i.e. (1,6), (2,5), (3,4) as described in Option 2. Using the known Doppler velocities of the six lines (10) and calculated splitting / 2 parameter for each pair, the calibration constant is determined using the expression:

$$C = \frac{\text{SPLITTING}}{2 \times \text{Doppler Velocity}} \qquad \text{channels mm}^{-1}\text{s}^{-1}$$

The positions of the lines have the Doppler velocities:-

lines (1,6) = ±5.312 mms^{-1}
lines (2,5) = ±3.076 mms^{-1}
lines (3,4) = ±0.84 mms^{-1}

The final value for C is the determined average of the three results using the above expression.

Calculation of the calibration constant for different velocity ranges depended upon the helipot being accurately linear. This only applies if all other features of the velocity drive system remain unaltered. The linear calibration of the helipot was checked by measuring the calibration constant for several helipot settings and the error in linearity was found to be smaller than the error involved in setting the helipot. Further a check on the linearity of the triangular wave is achieved by noting the differences in the positions of the lines (in channels).

i.e. (line 2 - line 1)
(line 3 - line 2)
(line 5 - line 4)
(line 6 - line 5)

The standard deviation of this data gives an indication of the linearity. (The difference between line 3 and line 4 is not used since this represents the difference between the ground and excited energy levels

in the magnetic splitting).

2.3.4. Errors in the Mössbauer System

The major sources of error inherent to the system have previously been quantified (14) for compounds having a high concentration of tin. The sources of the errors and their contributions have been listed as:-

(1)	Fitting error	± 0.09 channels
(2)	Error in determining zero velocity	± 0.25 channels
(3)	Error in linearity	± 0.05 channels
(4)	Error in calibration	± 0.11 channels

The total contribution from the above errors amounts to ± 0.50 channels (equivalent to ± 0.02 mms^{-1}). Although the above sources of error are present in the high dilution studies of this investigation an increased contribution is observed as a function of the run time.

As previously discussed long run times of the order of 48 hours were required for samples of tin compounds dispersed in PVC which added increased contributions from the D.C. drift levels in the instrumentation to the error in the zero velocity and linearity. Comparison of the RMS error $/\sigma$ values for data obtained after long min times with those for data obtained after only a few hours analysis reflect the increase in the D.C. drift.

i.e. R M S $/\sigma$ = 1.508 for T = 24 hours

R M S $/\sigma$ = 2.998 for T = 48 hours

(σ is the standard deviation in the statistics for counting for the respective run times ' T ').

A further estimation of the effect of run times on the error in the line position and linearity was obtained from three individual analysis of dibutyltin dichloride in PVC (at 1.2% w/w) for run times of 24 and 48 hours.

Run Time (Hours)	Line Position (channels)	Quadrupole Splitting (mms^{-1})
24hrs	3.0702 0.0234	3.05
48hrs	3.0899 -0.0061	3.09
48hrs	3.0940 -0.0114	3.10

The above data indicates a maximum increased error of ± 0.05 mms^{-1} in the line positions for extended run times.

STABILISERS IN POLY(VINYL CHLORIDE).

Contents:

3.1 Introduction

Organotin compounds have proved to be efficient stabilisers against thermal and photolytic degradation of PVC. The most damaging process of degradation is dehydrochlorination which proceeds by a ' zipper reaction ' and results in the formation of long chain polyene sequences in the polymer. Such polyene sequences impart severe discolouration and brittleness to the PVC. While dehydrochlorination is common to both thermal and photolytic degradation, two classes of organotin compound have emerged as the most effective stabilisers. Organotin mercaptides of the type R_2SnY_2 (where R = alkyl and Y = alkylthioglycollate) are the most common and most efficient stabilisers against thermal degradation, and organotin carboxylates of the same type (Y = alkylmaleate) are the most efficient stabilisers against photolytic degradation. There is, however, some degree of overlap in the use of either class of stabiliser.

Using Mössbauer spectroscopy it is intended to follow the changes that occur to the organotin stabilisers during thermal and photolytic degradation of PVC with subsequent identification of the degradation products. Goldanskii (15) recently reported a similar application of the technique to various polymer systems.

3.2 Literature Review

The subject of heat and light stabilisation with respect to the mode of action of organotin stabilisers, as well as the processes involved in the degradation of PVC has been discussed in numerous books and reviews (16 - 31). However, the mechanism of stabilisation is still not yet fully understood despite the many papers and detailed investigations into the subject (32 - 40). With respect to thermal stabilisation perhaps one of the most constructive reports to emerge from the initial investigations is that by Frye, Horst and Paliobagis (17). By studying the reactions between PVC and some organotin stabilisers of the general type R_2SnY_2 using radioactive labelling of various functional groups it was shown that neither of the R groups nor the tin atom were permanently

attached to the polymer, but there was evidence that the chlorine atoms on the polymer were co-ordinated to the tin atom of the stabiliser to give it an octahedral geometry. A mechanism for stabilisation was suggested in which the Y groups were exchanged for the chlorine atoms to form the dialkylchlorotin ester R_2SnClY or dialkyltin dichloride (reactions 1 and 2)

$$\text{i.e.} \quad R'Cl + R_2SnY_2 \longrightarrow R'Y + R_2SnClY \qquad (1)$$

$$2R'Cl + R_2SnY_2 \longrightarrow 2R'Y + R_2SnCl_2 \qquad (2)$$

Klemchuk (41) working in part to confirm the stabilisation theory of Frye et al studied the reactions of allylic and tertiary alkylchloride model compounds with dibutyltin dilaurate and dibutyltinbis(dodecylmercaptide). It was concluded that the presence of allylic chlorine atoms in the PVC may well be an influencing factor in the degradation process of the polymer. This work also confirmed the formation of the dibutylchlorotin derivative as a product from reactions with the model compounds.

Ayrey et al (42) confirmed that reactions (1) and (2) readily occured with model compounds at 180°C, and in a later paper (20) studied the reactions of the model compounds t-butylchloride and 3-chlorobutene, containing tertiary and allylic chlorine atoms respectively with various organotin mercaptides, thioglycollates and carboxylates to confirm Klemchuk's conclusions on the nature of the process leading to degradation of the polymer.

Many workers, however, have concluded that the organotin stabiliser reacts with the liberated hydrogenchloride to form dialkyltin dichloride. Stapfer and Grannick (43) studied the process of degradation in PVC containing anti-oxidant stabilisers. It was recognised that dibutyltinbis(isooctylthioglycollate) functioned as a potent anti-oxidant which, when present at 2% by weight of the polymer, imparted the best long-term stability to the unplasticised PVC, and it was concluded that after dehydrochlorination the stabiliser formed dibutyltin dichloride prior to degradation of the polymer.

Poller (44) studied the interactions between PVC and an isotopically labelled stabiliser, $Bu_2Sn(^{35}SBu)_2$, during degradation and concluded that the dominant reaction in the stabilisation process was the absorption of hydrogen chloride to form dibutyltin dichloride.

In a later review (45) Poller suggested that the stabiliser performed two roles:-

(i) during an induction period, the stabiliser functions in a preventative way by exchanging allylic chlorine atoms present in the polymer with the thioglycollate groups, and

(ii) during the main degradation process it serves to remove the liberated hydrogen chloride, forming dibutyltin dichloride and a thiol which then adds to the double bonds in the polymer.

Wirth and Andreas (26) in an extensive review of the process of stabilisation also concluded that the main factor in both thermal and light degradation is the presence of labile allylic chlorine atoms which act as initial sites for the dehydrochlorination process.

Finally, Ayrey and his co-workers (46) suggested that chlorine atom initiators are generated in the induction period preceding decomposition. The organotin stabilisers delay the decomposition of the PVC by exchange of X groups (in R_2SnX_2 where X = OCOR , SR) for allylic chlorine atoms, and generation of HX compounds which add to the double bonds formed. The scavenging role of the stabiliser for chlorine atoms was considered and a mechanism suggested involving chlorine atoms absorbed by the stabiliser resulting in the formation of dibutyltin dichloride.

3.3 Objectives

The main aims of this study were to follow the reactions undergone by two types of commercial organotin stabilisers during thermal and U.V. degradation of PVC using Mössbauer spectroscopy, to identify the degradation products, and to propose a reaction mechanism to account for the observed

changes. In addition, it was hoped to use the Mössbauer parameters to suggest structures for the stabilisers and their degradation products and to account for any changes in structure or co-ordination arising from the degradation process. Finally an attempt was to be made to use the information from the above study to prepare and investigate some novel organotin compounds as potential thermal stabilisers and similarly follow their reactions during degradation and to identify the degradation products.

3.4 Thermal Stabilisers

3.4.1. Results and Discussion

(a) PVC Stabilisation

PVC sheets containing the organotin stabilisers to be studied were prepared using conventional hot milling techniques at Lankro Chemicals Ltd. An intimate mix of PVC powder and stabiliser (at the required concentration) was continually passed between two rollers heated at 185°C to produce uniform and clear sheets. The contact time between the PVC mix and the rollers was kept as small as possible to reduce the possibility of thermal and mechanical degradation occuring to the PVC (32,33).

To determine whether degradation had occured during the rolling Mössbauer parameters of the stabiliser in solvent cast sheets of PVC were compared with the parameters obtained for the stabiliser in the rolled sheets.

The solvent cast sheets of PVC and stabiliser were prepared by slow evaporation of the solvent from a dispersion of the PVC and stabiliser in either dichloromethane or tetrahydrofuran.

In initial studies Mössbauer parameters were obtained for dibutyltinbis(isooctylthioglycollate)[1] , dioctyltinbis(isooctylthioglycollate) [2] , and dibutyltinbis(isooctylmaleate) [3] , present at 4% by weight of the polymer. Mössbauer parameters were also obtained for the above compounds in PVC after heating the polymer in an oven in an air atmosphere for one hour at 185°C. The results are given in Tables 3.1 and 3.2. For comparison

Table 3.1 ^{119}Sn Mössbauer parameters for dialkyltinbis(isooctylthioglycollates) in PVC (at 4% w/w) at 80K. (Alkyl = Bu or Oct).

Sample	Isomer Shift* (mms^{-1})($\pm$0.05)	Quadrupole Splitting (mms^{-1})($\pm$0.05)	Full Width at half height (mms^{-1})
Dibutyltinbis(isooctylthioglycollate) in PVC (milled, unaged)	1.43	2.26	1.07
Dibutyltinbis(isooctylthioglycollate) in PVC (solvent cast from dichloromethane)	1.48	2.32	0.90
Dibutyltinbis(isooctylthioglycollate) in PVC (thermally aged for 1 hour at 185°c)	1.45	2.83	0.95
Dioctyltinbis(isooctylthioglycollate) in PVC (milled, unaged)	1.50	2.27	0.99
Dioctyltinbis(isooctylthioglycollate) in PVC (thermally aged for 1 hour at 185°c)	1.46	2.70	0.94

* Relative to $CaSnO_3$

Table 3.2 ^{119}Sn Mössbauer parameters for dibutyltinbis(isooctylmaleate) in PVC (at 4% w/w) at 80K.

Sample	Isomer Shift (mms-1)(±0.05)	Quadrupole Splitting (mms-1)(±0.05)	Full Width at half height (mms^{-1})
Dibutyltinbis(isooctylmaleate) in PVC (milled, unaged)	1.39	3.34	1.05
Dibutyltinbis(isooctylmaleate) in PVC (solvent cast from tetrahydrofuran)	1.36	3.34	0.98
Dibutyltinbis(isooctylmaleate) in PVC (thermally aged for 1 hour at 185°C)	1.39	3.18	0.98

Table 3.3 ^{119}Sn Mössbauer parameters for compounds of general formula R_2SnY_2 and R_2SnClY, (R = Bu, Oct; Y = isooctylthioglycollate, isooctylmaleate) in the pure state or dispersed in PVC (at 4% w/w) at 80K.

Sample	Isomer Shift (mms^{-1})(±0.02)	Quadrupole Splitting (mms^{-1})(±0.02)	Full Width at half height (mms^{-1})
Dibutyltinbis(isooctylthioglycollate). Pure	1.39	2.20	0.88
Dioctyltinbis(isooctylthioglycollate). Pure	1.49	2.36	0.96
Dibutylchlorotinisooctylthioglycollate. Pure	1.44	2.88	1.14
Dibutylchlorotinisooctylthioglycollate in PVC	1.43 ±0.05	2.85 ±0.05	0.95
Dioctylchlorotinisooctylthioglycollate. Pure	1.47	2.94	1.04
Dibutyltinbis(isooctylmaleate). Pure	1.44	3.62	1.14
Dibutylchlorotinisooctymaleate. Pure	1.49	3.54	1.16
Dibutychlorotinisooctylmaleate in PVC	1.40 ±0.05	3.16 ±0.05	0.97
Dibutyltin dichloride. Pure	1.64	3.47	0.97
Dibutyltin dichloride. Pure. Ref (10).	1.62	3.45	
Dibutyltin dichloride in PVC (solvent cast from dichloromethane)	1.54±0.05	3.09±0.05	1.00
Dioctyltin dichloride. Pure	1.75	3.73	1.03

Table 3.4 ^{119}Sn Mössbauer parameters for dibutyltinbis(isooctylthioglycollate) and dibutyltinbis (isooctylmaleate) in PVC (at 1.2% and 2% w/w respectively) at 80K.

Sample	Isomer Shift (mms^{-1})($\pm$0.05)	Quadrupole Splitting (mms^{-1})($\pm$0.05)	Full Width at half height (mms^{-1})
Dibutyltinbis(isooctylthioglycollate) in PVC (milled, unaged)	1.45	2.29	1.07
Dibutyltinbis(isooctylthioglycollate) in PVC (solvent cast from dichloromethane)	1.48	2.32	0.90
Dibutyltinbis(isooctylthioglycollate) in PVC (thermally aged for 1 hour at 185°C)	1.47	2.86	1.08
Dibutyltinbis(isooctylmaleate) in PVC (milled, unaged)	1.42	3.36	0.94
Dibutyltinbis(isooctylmaleate) in PVC (solvent cast from tetrahydrofuran)	1.36	3.34	0.98
Dibutyltinbis(isooctylmaleate) in PVC (thermally aged for 1 hour at 185°C)	1.39	3.18	0.98

Table 3.3 gives the Mössbauer parameters obtained for the corresponding compounds in the pure state, and for the model compounds dibutylchlorotin-isooctylthioglycollate [4], dibutylchlorotinisooctylmaleate [5], and dibutyltin dichloride [6], (in the pure state and dispersed in PVC) considered to be the thermal degradation products in PVC in the literature.

The results indicate that for both types of stabiliser the main degradation product is the dialkylchlorotinthioglycollate / maleate and not dialkyltin dichloride as suggested by other workers. On the basis of these results a more detailed investigation was carried out on the PVC containing either dibutyltinbis(isooctylthioglycollate) [1], or dibutyltinbis(isooctylmaleate) [3], at the commercially used levels of 1.2% and 2% by weight of the polymer respectively. These results are given in Table 3.4 and can be seen to be indistinguishable from the results obtained on the thermal degradation of PVC containing the stabilisers at 4% by weight of the polymer.

Comparison of the Mössbauer data for the freshly milled sample of PVC containing stabiliser [1], (ΔE_Q = 2.29mms^{-1}) with that for the pure stabiliser (ΔE_Q = 2.20mms^{-1}) shows a small change in the quadrupole splitting which is probably due to a small degree of degradation during the initial hot milling process as concluded by Harrison et al (47).

The quadrupole splitting for the solvent cast sample of PVC containing stabiliser [1], (ΔE_Q= 2.32mms^{-1}) is significantly higher than that of the pure stabiliser indicating possible co-ordination of the dichloromethane to the tin. This result cannot therefore be used to support the above suggestion of minor degradation in the PVC.

The similarity between the data for the pure stabiliser and that of the stabiliser in the milled sample clearly indicates that there is no significant structural change in the stabiliser which might have arisen as a result of co-ordination between chlorine atoms on the polymer and the tin atoms of the stabiliser, as suggested by other workers (17).

Prolonged degradation of the PVC sheet containing stabiliser [1]

Table 3.5 ^{119}Sn Mössbauer parameters for dibutyltinbis(isooctylthioglycollate) in PVC at 80K at various aging times.

Sample / time	Isomer Shift (mms^{-1})($\pm$0.05)	Quadrupole Splitting (mms^{-1})($\pm$0.05)	Full Width at half height (mms^{-1})
Dibutyltinbis(isooctylthioglycollate) in PVC (at 1.2% w/w). Thermally aged for:-			
5Mins	1.48	2.38	1.13
10 "	1.45	2.42	1.14
15 "	1.46	2.41	1.11
30 "	1.47	2.56	1.27
50 "	1.48	2.90	1.00
70 "	1.47	2.84	0.99
85 "	1.47	2.86	1.08

(at 1.2% by weight) carried out in an oven in an air atmosphere at 185°C resulted in extensive discolouration of the polymer. The Mössbauer parameters for the degraded polymer and stabiliser compare exactly with those recorded for a sample of PVC containing dibutylchlorotinisooctylthioglycollate [4] indicating the degradation product in the PVC to be the dibutylchlorotin-isooctylthioglycollate as concluded in the initial studies.

Further studies of the progressive aging for short periods in the range 5 - 85 minutes indicate a gradual increase in the apparent quadrupole splitting from that of the unaged stabiliser [1] to that of the dibutylchlorotinisooctylthioglycollate [4]. The change in the apparent quadrupole splitting is also accompanied by a line broadening effect (Table 3.5). It is apparent that during the course of thermal degradation both the unchanged stabiliser [1] and the dibutylchlorotin ester [4] are present in the Mössbauer spectra and hence the increase in the apparent quadrupole splitting and the line broadening can be attributed to unresolved Mössbauer quadrupole doublets. Fitting the data at 10, 15 and 30 minutes using two doublets with parameters corresponding to the two components gave the following results:-

Component 1	Isomer Shift	= $1.45 mms^{-1}$
	Quadrupole Splitting	= $2.26 mms^{-1}$
	Full Width at half height	= $1.07 mms^{-1}$
Component 2	Isomer Shift	= $1.47 mms^{-1}$
	Quadrupole Splitting	= $2.88 mms^{-1}$
	Full Width at half height	= $1.08 mms^{-1}$

The parameters obtained for the two components compare exactly with those recorded for dibutyltinbis(isooctylthioglycollate) and dibutylchlorotinisooctylthioglycollate and therefore confirm the prescence of the two components in the spectra. Figure 3.1 shows the Mössbauer spectrum of thermally degraded PVC containing dibutyltinbis-(isooctylthioglycollate) at 1.2% by weight after heating at 185°C for 30 minutes. The two components of the computer fit are shown corresponding to (A) dibutylchlorotinisooctylthioglycollate [4] and (B) dibutyltinbis-(isooctylthioglycollate) [1]

FIG 3.1

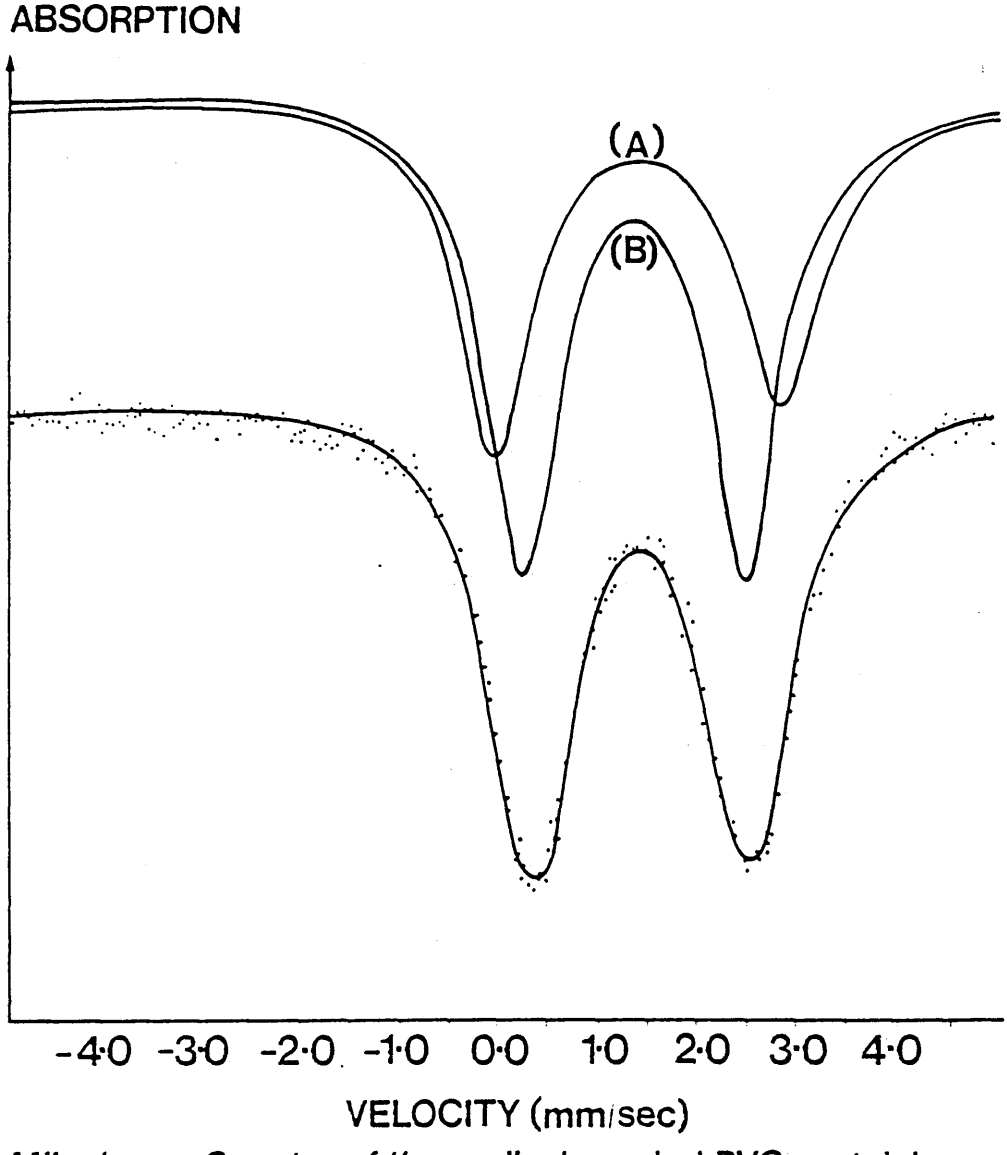

Mössbauer Spectra of thermally degraded PVC containing $Bu_2Sn(IOTG)_2$ stabiliser at 1·2% after heating at 185°C for 30 minutes. The two components of the computer fit are shown corresponding to (A) $Bu_2SnCl(IOTG)$ and (B) $Bu_2Sn(IOTG)_2$

The trend shown in Figure 3.2 shows the gradual increase in the apparent quadrupole splitting with thermal aging time and corresponds to the change to the dibutylchlorotinisooctylthioglycollate as degradation occurs. There is no indication that further degradation occurs at 185°C to form dibutyltin dichloride [6]. By fitting the data in Table 3.5 as two quadrupole doublets corresponding to dibutyltinbis-(isooctylthioglycollate) and dibutylchlorotinisooctylthioglycollate the relative areas due to the two components under the absorption peaks could be determined.

i.e. $$\text{Area} = \frac{\text{Full Widths at half height } (\Gamma_H) \times \text{Depth}}{\text{Background counts}}$$

and since: Total Area = (Area (1) + Area (2))

where Area (1) = Area due to dibutyltinbis(isooctylthioglycollate)
Area (2) = Area due to dibutylchlorotinisooctylthioglycollate

it is possible to estimate the percentage content of dibutylchlorotinisooctylthioglycollate [4] in the PVC during its degradation. Figure3.3 shows the change in percentage content of [4] in the PVC with thermal degradation time. However, from these results the rate of conversion to dibutylchlorotinisooctylthioglycollate cannot be accurately determined as the technique is relatively insensitive to small contributions in unresolved spectra. From Table 3.5 it is evident that complete conversion to the chlorotin ester [4] has taken place after 50 minutes of aging by which time a rapid discolouring of the PVC is observed. The optical density of PVC samples stabilised with dibutyltinbis(isooctylthioglycollate) [1] was measured using a N.E.L. Radiological Densitometer and the change in optical density (arbitrary units) with thermal aging time is shown in Figure 3.4. The rapid increase observed after 50 minutes is coincident with complete conversion of the stabiliser [1] to the dibutylchlorotinisooctylthioglycollate.

From these results it is evident that the final product is dibutylchlorotinisooctylthioglycollate and not dibutyltin dichloride as concluded by other workers (43-47).Further, in support of these results Mellor(48)

Figure 3.2 Apparent Quadrupole Splitting of thermally aged dibutyltinbis(isooctyl-thioglycollate) as a function of Thermal Degradation Time

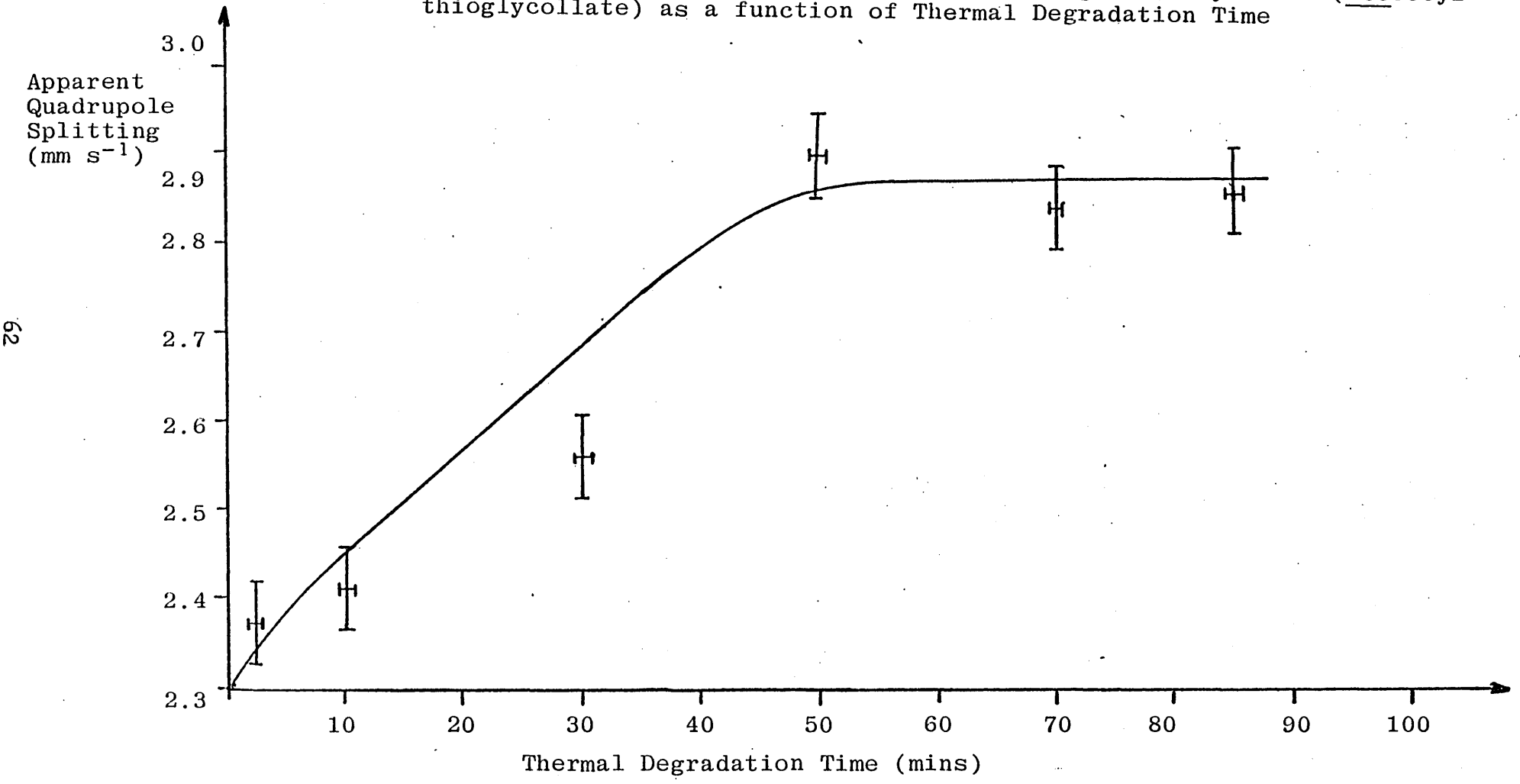

Figure 3.3 Percentage of dibutylchlorotinisooctylthioglycollate as a function of thermal degradation time

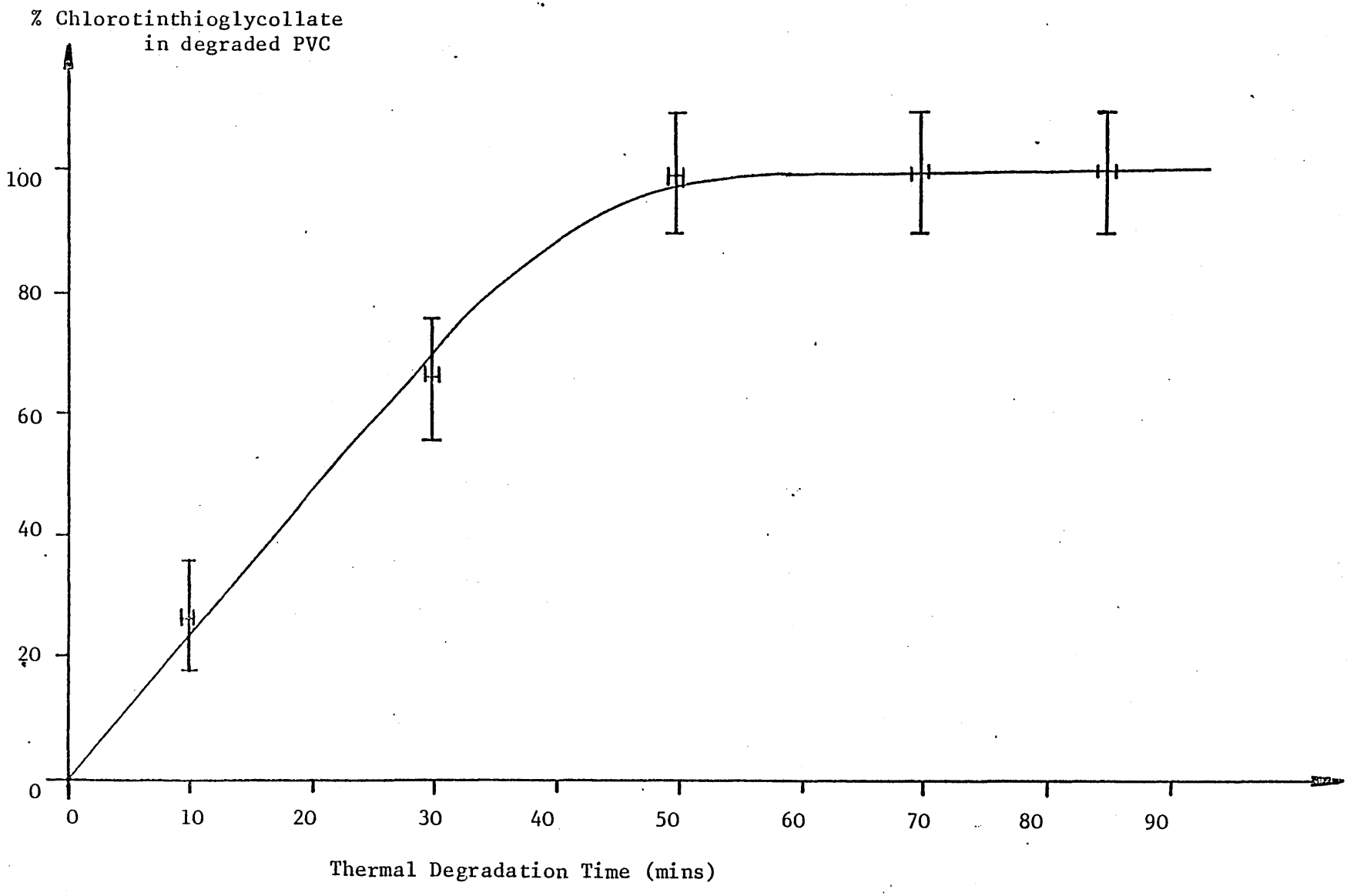

Figure 3.4 Optical Density of PVC as a function of thermal degradation time

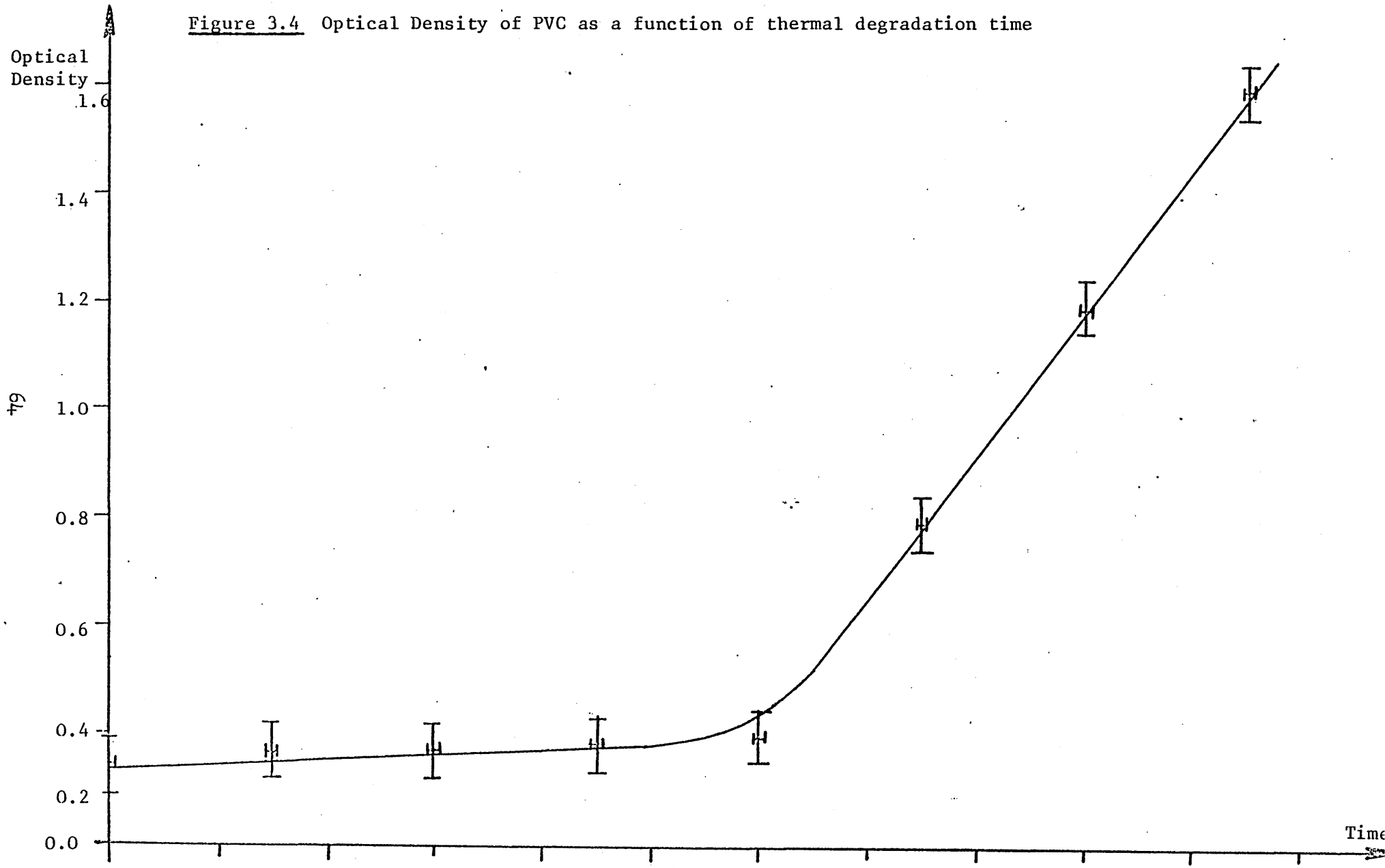

degraded PVC subsequent analysis identified it as dibutylchlorotiniso-octylthioglycollate.

The Mössbauer results on the thermal degradation of PVC stabilised with dioctyltinbis(isooctylthioglycollate) [2] (Table 3.1) and dibutyltinbis(isooctylmaleate) [3] (Table 3.4) show clearly that in both cases the degradation product is also the dialkylchlorotin ester. Figure 3.5 shows comparative Mössbauer spectra of dibutyltinbis(isooctylmaleate) [3] in (A) its pure state, (B) in the PVC after milling, and (C) of the thermal degradation product [5] in the PVC after aging for one hour at 185°C.

After extensive degradation of each sample it was not possible to detect any dibutyltin dichloride in the polymer matrix. This result supports the recent work of Parker and Carman (49) who have shown that dialkyltin mercaptides in solution undergo a ligand-exchange reaction with dialkyltin dichlorides to form the mixed halo mercapto derivatives $R_2SnCl(SR')$. This reaction also serves to remove any dialkyltin dichloride which may also act as a Lewis acid catalyst for the degradation of the PVC.

In a study of the effectiveness of various organotin stabilisers Troitskii et al (50) concluded that in the absence of stabilisers the thermal degradation of PVC proceeds by a molecular-ionic mechanism in which the hydrogen chloride released has an autocatalytic effect on the degradation process. Conversely if the hydrogen chloride is removed upon formation degradation proceeds mainly by a molecular mechanism complicated by radical reactions. Further, considering the reviews by Poller (45) and Ayrey (20) which suggest that initiation of degradation takes place at allylic chlorine sites then clearly the process of degradation/stabilisation is very much more complex than initial investigations into the mechanism indicated.

Figure 3.5 (A): ^{119}Sn Mössbauer Spectrum of Pure Dibutyltinbis(isooctylmaleate) at 80K

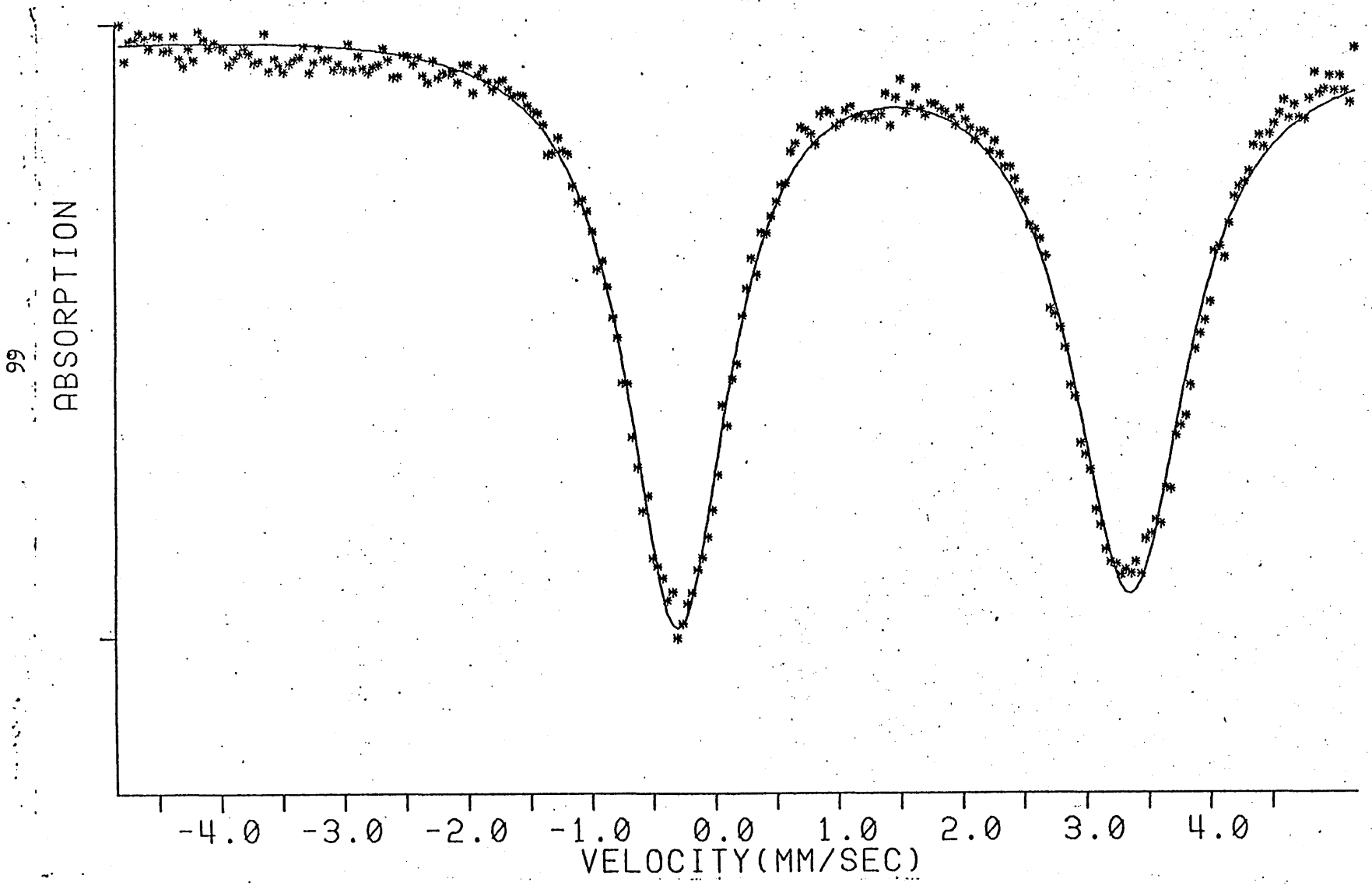

Figure 3.5 (B): ^{119}Sn Mössbauer Spectrum of Dibutyltinbis(isooctylmaleate) in PVC (milled) recorded at 80K

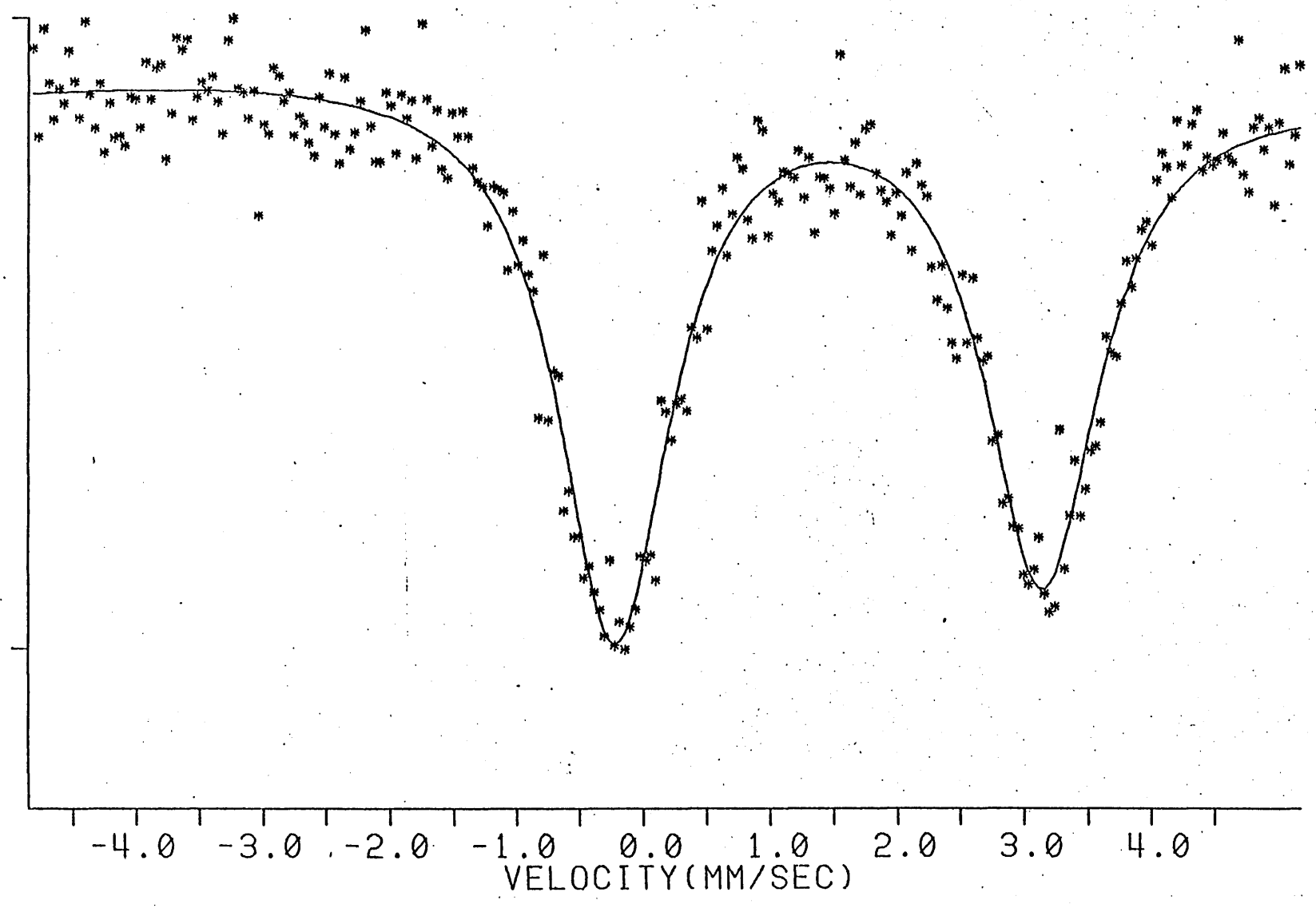

Figure 3.5 (C): ^{119}Sn Mössbauer Spectrum of Dibutyltinbis(isooctylmaleate) in PVC aged for 1 hour at 185°C recorded at 80K

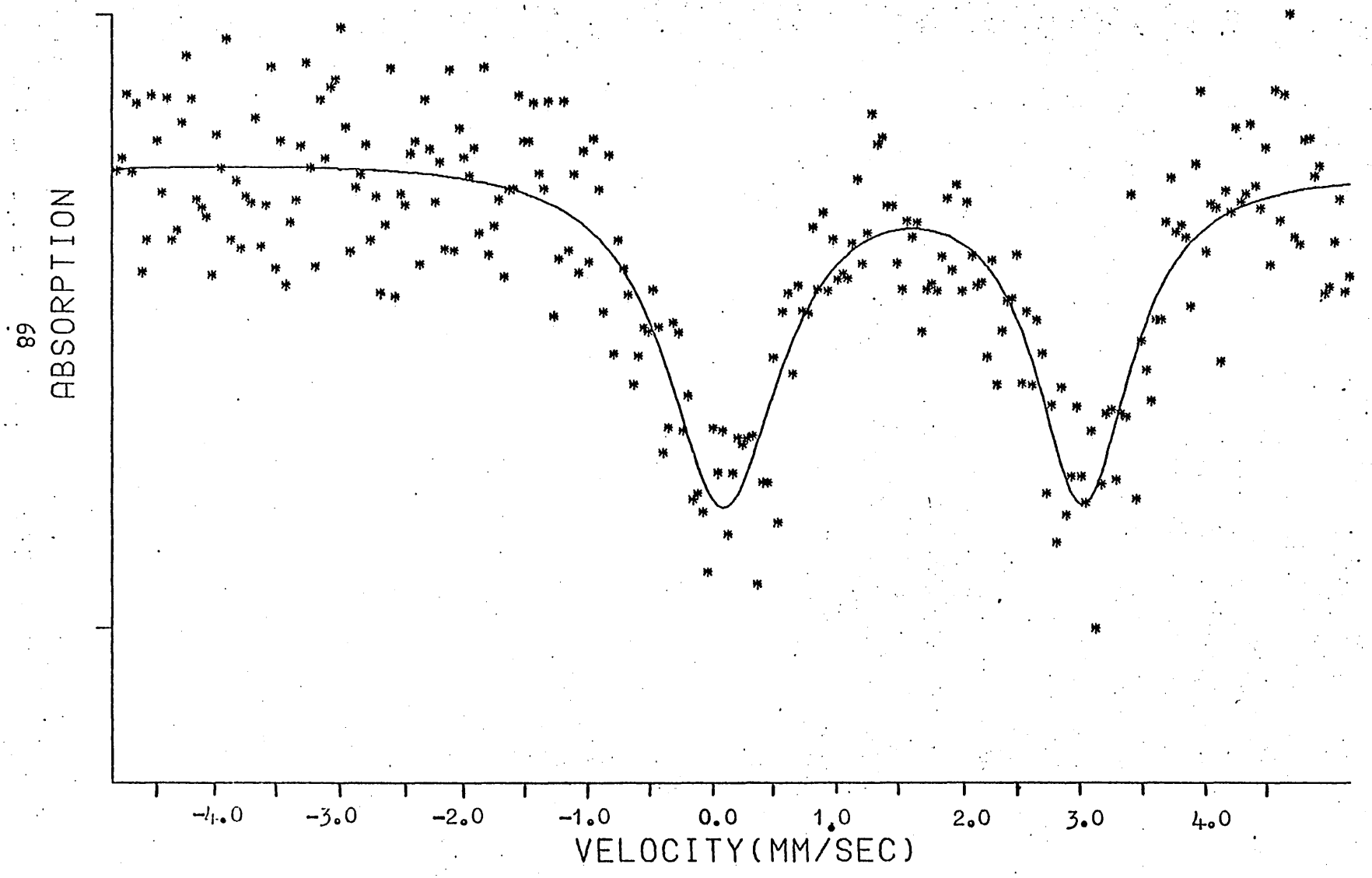

On the basis of the above results and the work reviewed a reaction scheme is proposed for the stabilisation and degradation of the PVC. Degradation is initiated at allylic chlorine sites during the milling process, as indicated by our results, by release of proportionate amounts of hydrogen chloride. Replacement of the thioglycollate or maleate groups on the stabilisers by chlorine atoms from the hydrogen chloride occurs with resultant formation of the thiol or maleic acid. Further degradation of the PVC during the milling is prevented by addition of the thiol or maleic acid across the double bond:

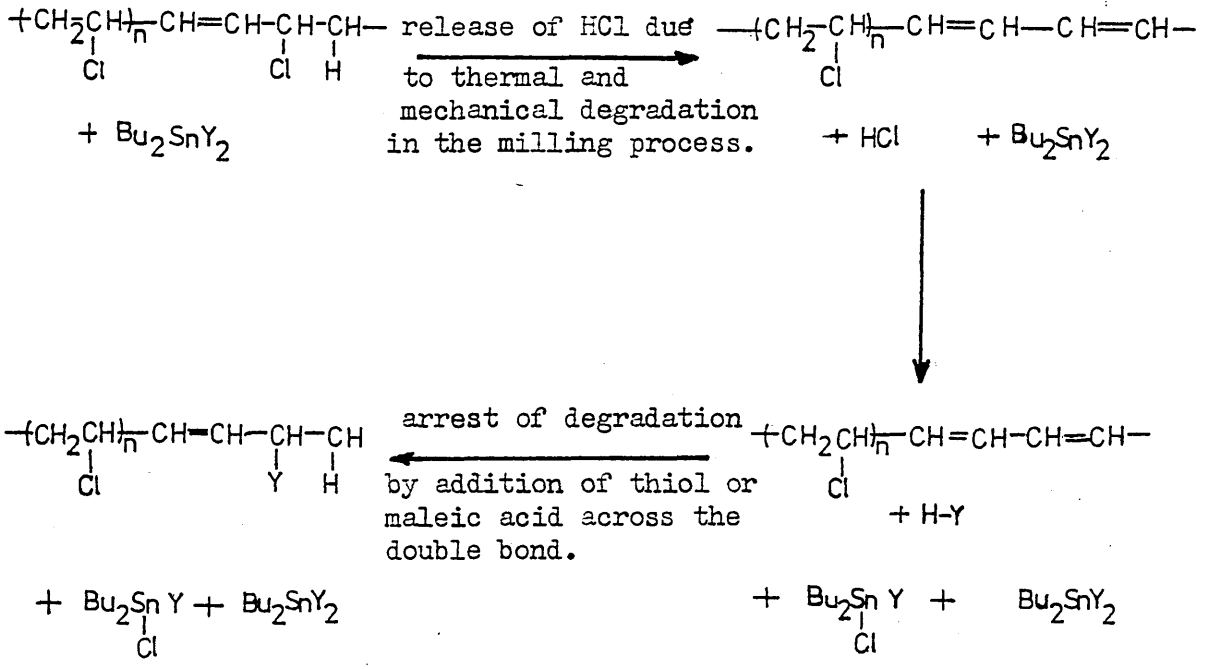

(where Y = isooctylthioglycollate, isooctylmaleate).

Since there are reported to be relatively few allylic chlorine atoms on the polymer (41,45)only small amounts of hydrogen chloride are released during initial degradation. Consequently reaction with the hydrogen chloride results in only small depletion of the stabiliser.

On thermally aging the polymer further degradation occurs involving rapid depletion of the stabiliser and subsequent formation of the dibutylchlorotin ester. Rasuvaev et al (51) suggest that the degradation proceeds by a molecular mechanism complicated by radical reactions:

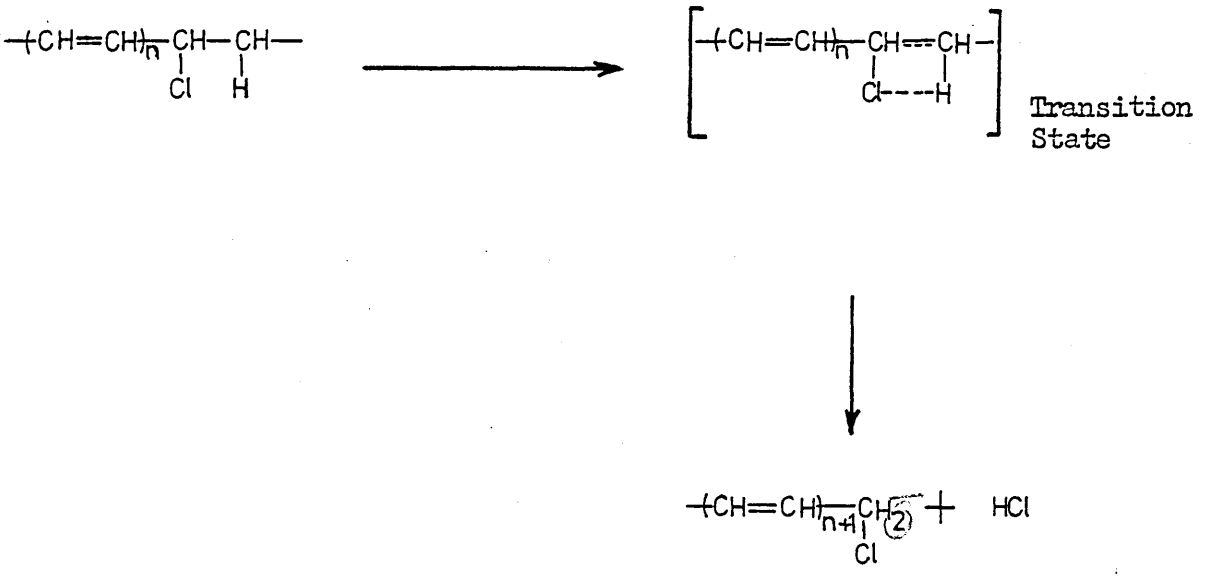

Production of HCl results in rapid stabiliser depletion and subsequent formation of the dibutylchlorotin ester:

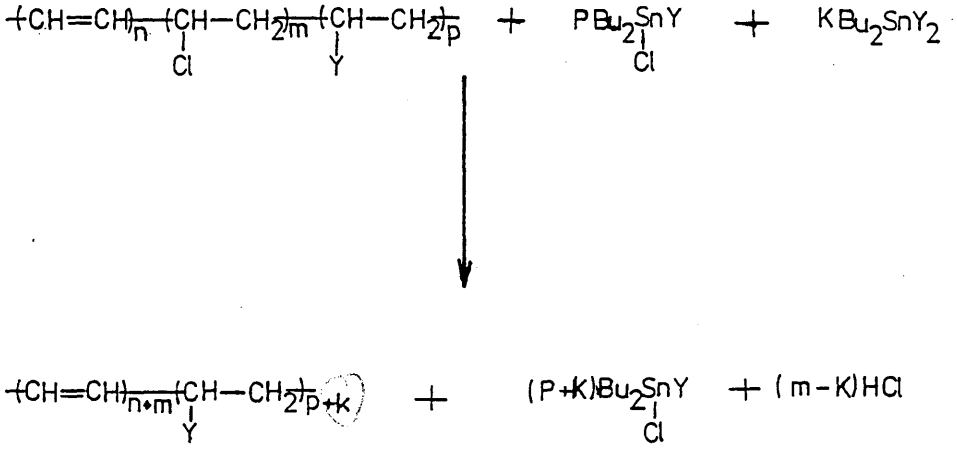

After thermally aging the polymer for 50 minutes all the stabiliser has been converted to the dibutylchlorotin ester. Further dehydrochlorination results in extensive degradation and discolouration of the polymer due to the formation of long chain polyene sequences. The hydrogen chloride is reported to have an autocatalytic effect on the degradation process causing further dehydrochlorination of the polymer (51). Troitskii et al (50) suggest the degradation to proceed by both a molecular and an ionic mechanism:

(i) Molecular:

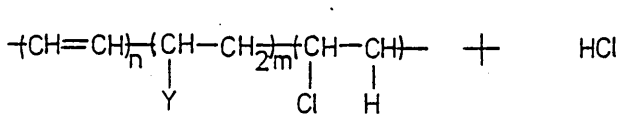

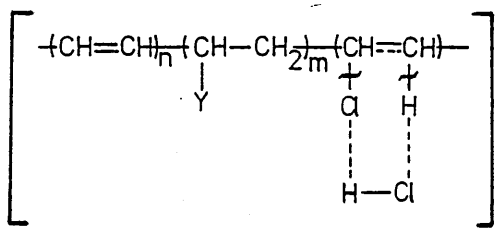

Transition State

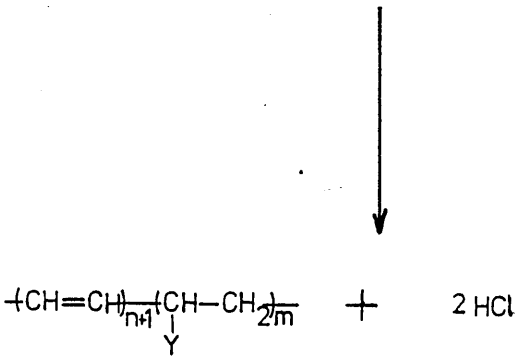

(ii) Ionic:

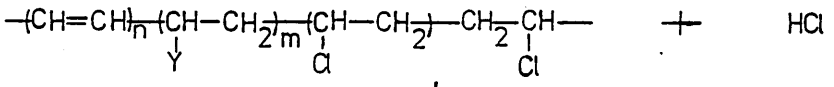

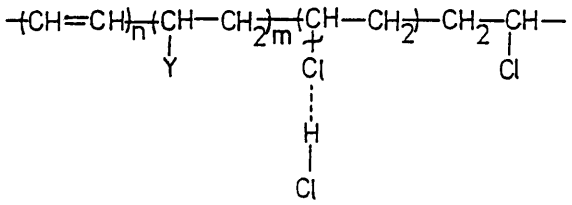

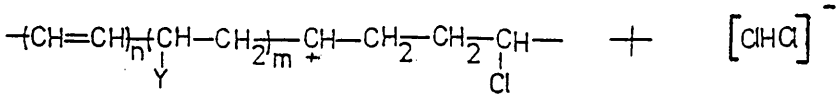

The formation of the ion pair in the step above is suggested by Troitskii to stabilise the carbonium ion and provides an intermediate stage in the formation of more hydrogen chloride. The reaction is said to proceed further by deprotonation by the $[ClHCl]^-$ ion with the subsequent formation of 2 moles of hydrogen chloride and a carbanion:

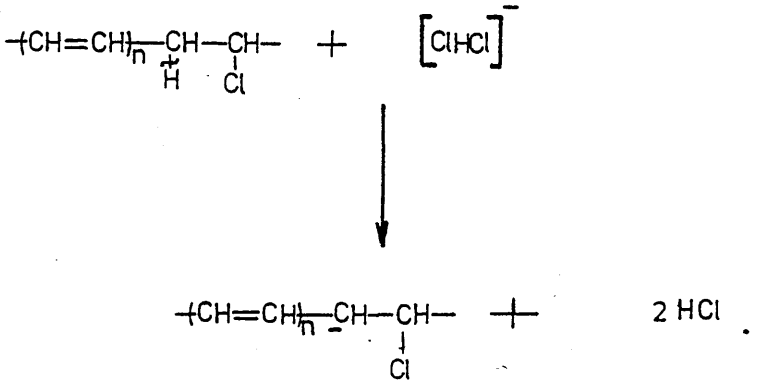

(b) Co-ordination Chemistry

The Mössbauer data in Tables 3.1 - 3.5 have given conclusive evidence for the nature of the thermal degradation products. In addition the changes in the quadrupole splitting during degradation of the PVC indicate significant changes in co-ordination around the tin atom.

The structures of the thioglycollate stabilisers have been little studied although Stapfer and Herber (52) have recorded Mössbauer and infrared data for these compounds. It was concluded that dibutyltin-bis(isooctylthioglycollate) [1] adopts either a cis - or a trans - trigonal bipyramidal configuration depending upon the method of preparation i.e.

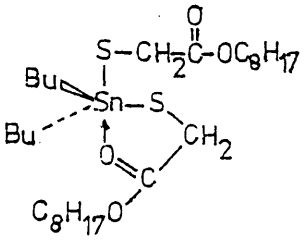

cis-

[1]

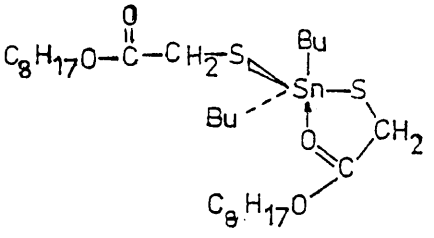

trans-

monodentate.

Hutton and Burley (53) have also prepared and recorded the infrared spectrum of dibutyltinbis(isooctylthioglycollate) [1] and concluded that the reaction between dibutyltin dichloride and isooctylthioglycollate under anhydrous conditions gives almost entirely dibutylchlorotinisooctylthioglycollate [4] and not as suggested by Stapfer and Herber, the trans - isomer of dibutyltin bis(isooctylthioglycollate). This becomes significant on comparison of the Mössbauer data for the dibutyltinbis(isooctylthioglycollate) prepared under different conditions by Stapfer and Herber and could explain the difference in the observed quadrupole splittings.

The Mössbauer data (Tables 3.1, 3.2 and 3.3) for dibutyl- and dioctyltinbis(isooctylthioglycollates) [1], [2] (ΔE_Q = 2.20mms^{-1} and 2.27 - 2.37mms^{-1} respectively) are indicative of four- co-ordinate structures:

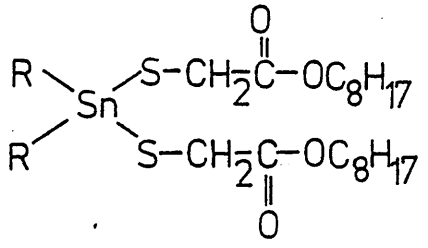

for R = Bu [1]
= Oct [2]

($\nu_{c=o}$ = 1740 cm^{-1})

Infrared data also supports this suggestion since the carbonyl stretching frequency at 1740cm^{-1} is typical of an unco-ordinated carbonyl group. No evidence is found in the infrared spectrum for a co-ordinated carbonyl group.

The higher quadrupole splitting (ΔE_Q = 2.88mms^{-1}) observed for dibutylchlorotinisooctylthioglycollate [4] is indicative of the tin being five - co-ordinate with a trigonal bipyramidal structure:

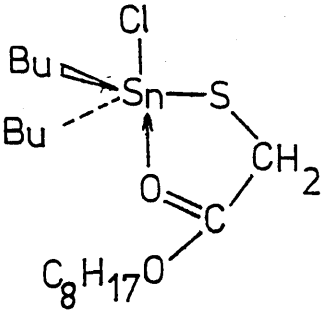

[4]

($\nu_{c=o}$ = 1700cm^{-1})

Infrared data again supports this structure showing a co-ordinated carbonyl stretching frequency at 1700cm^{-1}.

For the maleate stabiliser [3] the quadrupole splitting of pure dibutyltinbis(isooctylmaleate) [3] (ΔE_Q = 3.62mms^{-1}) is indicative of six co-ordinated tin sites associated intermolecularly through the carbonyl groups:

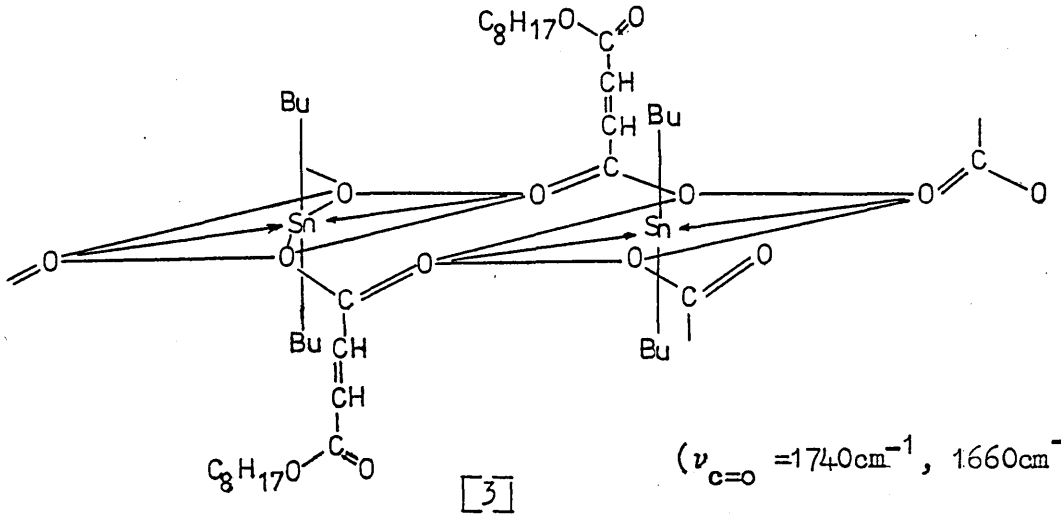

[3]

($\nu_{c=o}$ =1740cm^{-1}, 1660cm^{-1})

Infrared data shows both unco-ordinated ($\nu_{c=o}$ = 1740cm^{-1}) and co-ordinated ($\nu_{c=o}$ = 1660cm^{-1}) bands present. Studies of dialkyltin acetylacetonates and oxinates show similar values for the quadrupole splitting and these have similarily been assigned trans - octahedral structures(54,55).

A significant difference is observed in the quadrupole splitting for the pure dibutyltinbis(isooctylmaleate) [3] (ΔE_Q = 3.62mms^{-1}) and for the maleate in PVC after milling (ΔE_Q = 3.36mms^{-1}). The para-

meters for the maleate in PVC from a solvent cast sample (ΔE_Q = $3.34 mms^{-1}$) are in close agreement with those of the milled sample and suggests that the difference is not due to degradation but rather that dispersion in the PVC affects the steric arrangement of the ligands around the tin atom. Indeed, the change in quadrupole splitting on incorporation into the polymer suggests a change in the O - Sn - O bond angle which would occur on going from the inter-molecular associated unit to an intra-molecular un-associated complex:

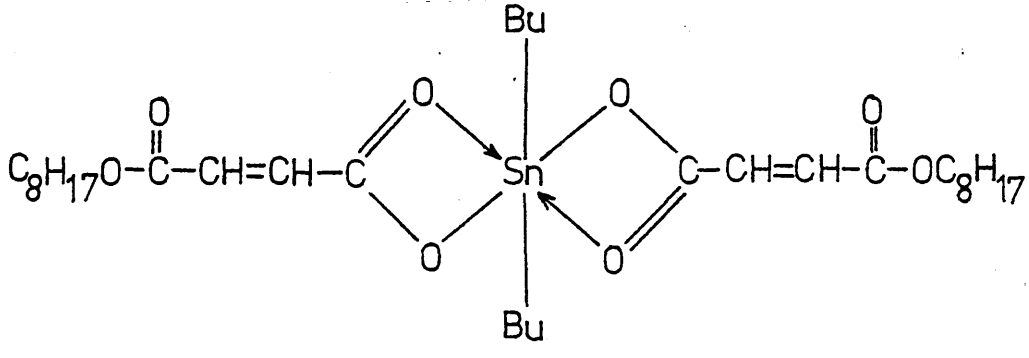

[3]

It is also noteworthy that for dibutylchlorotinisooctylmaleate [5] a significant change in the quadrupole splitting is observed between that of the pure compound and when dispersed in PVC suggesting a structural change. Honnick and Zuckerman (56) have recently discussed the structures of the diorganotin halide carboxylates and suggested that the origin of certain changes in infrared spectroscopic properties in passing from a pure compound to a solution in an inert solvent might be a change from a polymeric penta - co-ordinated structure (A) to a monomeric penta - co-ordinated structure(B):

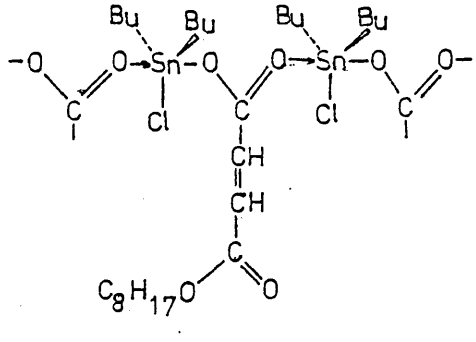

[5A]

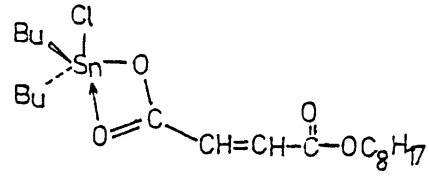

[5B]

7.4.4 Conclusions

The Mössbauer parameters for both types of stabiliser in the PVC give no evidence of any co-ordinative interactions between the chlorine atoms on the polymer and the tin atoms of the type suggested by Frye et al (17). For dibutyl - and dioctyltinbis(isooctylthioglycollate) [1,2] the magnitudes of the quadrupole splittings suggest the tin atoms on both stabilisers in the PVC to be four- co-ordinate. The parameters for dibutyltinbis(isooctymaleate) [3], however, show the tin atom to be six co-ordinate in both the pure state and when dispersed in PVC; a structural change is apparent on incorporation into the polymer.

The main degradation product from each stabiliser was identified as the mixed chloride-ester. The formation of the dialkylchlorotiniso octylthioglycollate supports, in part, the ligand-exchange theory of Parker and Carman (49) and similarily the formation of the dibutylchlorotinisooctylmaleate supports the work of Cohen and Dillard (57) on the ligand-exchange reactions of organotin carboxylates.

Degradation of the PVC is suggested to occur at 'defect' allylic chlorine sites and is clearly a complex process involving radical, and ionic-molecular mechanisims. The presence of hydrogen chloride in the polymer appears to contribute to two processes:-

(i) a non - autocatalytic effect in which the hydrogen chloride brings about slight degradation of the polymer by a molecular/radical process initiated at the allylic chlorine sites. The stabiliser reacts with the liberated hydrogen chloride to form the dialkylchlorotin ester.

(ii) an autocatalytic process in which the hydrogen chloride which is released brings about extensive degradation of the polymer by a molecular - ionic process. At this stage all the stabiliser appears to have been converted to the chlorotin ester.

The formation of the dialkylchlorotin ester is seen to occur as early as 15 minutes into the degradation process.

Finally, comparison of the Mössbauer parameters for the hot - milled

and solvent cast samples containing the dialkyltinbis(isooctylthioglycollates) or dibutyltinbis(isooctylmaleate) indicates only slight degradation occuring during the initial hot - milling process.

3.5 Photochemical Stabilisers

3.5.1 Introduction

Following studies of the reactions occuring in the PVC matrix by organotin stabilisers during thermal degradation of the polymer, a similar study was undertaken of the reactions undergone by the stabilisers dibutyltinbis(isooctylthioglycollate) [1] and dibutyltinbis(isooctylmaleate) [3] during U.V. - induced degradation of the stabilised polymer in air at 25°C. Of the two classes of stabiliser used, the maleate is reported to be an excellent light stabiliser whereas the thioglycollate stabiliser is of limited efficiency (16,26,28,46,58-62).

3.5.2 Results and Discussion

Samples of PVC sheet containing the stabilisers [1] or [3] (present at 1.2% w/w or 2% w/w of the polymer, respectively) were subjected to irradiation with ultra - violet light (> 290 nm) in a commercial "Xenotest" apparatus, in which the samples are rotated about a central discharge lamp at the axis of the apparatus, in an atmosphere of air at approximately 25°C for various intervals of time. The derived Mössbauer parameters for the samples and for other reference organotin compounds are given in Tables 3.6, 3.7, 3.8 and 3.9.

The results for the thioglycollate stabiliser (Table 3.6) show that after 400 hours exposure it is converted into two degradation products, as indicated by the asymmetry and broad line widths in the Mössbauer spectrum (fig 3.6). Fitting the data under Option 4 (see section 2.3) gave the final parameters of the two components to be:-

Component 1:	Isomer Shift	= 1.43mms^{-1}
	Quadrupole Splitting	= 2.88mms^{-1}
	Full Width at half-height	= 1.30mms^{-1}

Table 3.6 ^{119}Sn Mössbauer parameters for Dibutyltinbis(isooctylthioglycollate) in PVC (at 1.2% w/w) at 80K against Exposure Time in the Xenotest apparatus.

Exposure Time (hours)	Isomer Shift (mms^{-1})($\pm$0.05)	Quadrupole Splitting (mms^{-1})($\pm$0.05)	Full Width at half height (mms^{-1})	Relative % Stannic oxychloride ($\pm$ 5%)
0	1.43	2.26	1.07	0
400	(i) 1.43	2.88	1.30	21
	(ii) 0.42	0.93	1.30	
1000	(i) 1.46	2.89	1.20	24
	(ii) 0.31	0.64	1.20	
3288	(i) 1.35	2.77	1.38	48
	(ii) 0.39	0.79	1.38	
4320	(i) 1.49	2.78	1.23	55
	(ii) 0.40	0.69	1.23	

(i) Corresponds to dibutylchlorotinisooctylthioglycollate.

(ii) Corresponds to stannic oxychloride.

Table 3.7 ^{119}Sn Mössbauer parameters for dibutyltinbis(isooctylthioglycollate) in PVC (at 1.2%) after 404 hours exposure in the Xenotest apparatus and showing the effect of artificially increasing the starting parameters for the stannic oxychloride component by 5%

Sample	Isomer Shift (mms^{-1})(±0.05)	Quadrupole Splitting (mms^{-1})(±0.05)	Full Width at half height (mms^{-1})	χ^2 value	% Area (±5%) $\left(= \frac{\Gamma_H \times \text{Depth}}{\text{Background counts}}\right)$	
					stannic oxychloride	chlorotin ester
(A) Control run (typical parameters fitted as two doublets containing 21% stannic oxychloride and 79% chlorotin ester)	(1) 0.42 (2) 1.43	0.93 2.88	1.30 1.33	2985	21%	79%
(B) Run containing artificially increased starting parameters of 26% stannic oxychloride and 74% chlorotin ester	(1) 0.44 (2) 1.43	0.94 2.89	1.37 1.31	2981	22%	78%

(1) corresponds to the stannic oxychloride component
(2) corresponds to the dibutylchlorotin*iso*octylthioglycollate component

Xenotest apparatus.

Exposure Time (hours)	Isomer Shift (mms^{-1})($\pm$0.05)	Quadrupole Splitting (mms^{-1})($\pm$0.05)	Full Width at half height (mms^{-1})
0	1.38	3.35	1.04
404	1.45	3.35	1.02
1000	1.44	3.35	0.99

Table 3.9 ^{119}Sn Mössbauer parameters of some reference organotin compounds.

Sample		Isomer Shift (mms^{-1})($\pm$0.05)	Quadrupole Splitting (mms^{-1})($\pm$0.05)	Full Width at Half-Height (mms^{-1})
Dibutyltinbis(isooctylthioglycollate) in PVC (at 1.2%w/w) (milled, unaged)		1.45	2.29	1.07
Dibutylchlorotinisooctylthioglycollate in PVC		1.43	2.85	0.95
Dibutyltinbis(isooctylmaleate) in PVC (at 2%w/w) (milled, unaged)		1.42	3.36	0.94
Dibutylchorotinisooctylmaleate in PVC		1.40	3.16	0.97
Pure Stannic Oxide		-0.01$\pm$0.02	Unresolved	1.30
Dibutylchlorotinisooctylthioglycollate + stannic oxide solvent cast in PVC	(i)	1.50	2.96	0.88
	(ii)	0.05	0.53	0.88
Pure Stannic Oxychloride Ref (10)		0.25	0.73	1.12

(i) Corresponds to dibutylchlorotinisooctylthioglycollate.

(ii) Corresponds to stannic oxide.

Component 2:	Isomer Shift	= 0.42mms
	Quadrupole Splitting	= $0.93mms^{-1}$
	Full Width at half-height	= $1.30mms^{-1}$

Component 1 was conclusively identified as dibutylchlorotin*iso*-octylthioglycollate [4], and component 2 was considered at first to be stannic oxide although a small isomer shift ($0.44mms^{-1}$) had been measured. To ensure that this was not a computer-fitting artifact a simulation experiment was carried out using a 1:1 mixture of pure stannic oxide and dibutylchlorotin*iso*octylthioglycollate [4] in PVC (at a total of 2% w/w), solvent cast from dichloromethane and showed the stannic oxide to have a zero isomer shift and a small quadrupole splitting (ΔE_Q = $0.53mms^{-1}$). These parameters are typical for stannic oxide (10) and do not compare with those observed for the second component. Component 2 was finally identified as being stannic oxychloride, $SnOCl_2$, [7] on comparison of the Mössbauer data with those previously recorded for this compound (66). Figure 3.6 shows the Mössbauer spectra for dibutyltinbis(*iso*-octylthioglycollate) (1), in PVC after 4320 hours exposure. The two components of the computer fit are shown and correspond to (A) dibutyl-chlorotin*iso*octylthioglycollate [4] and (B) stannic oxychloride. [7] The proportion of the latter component is seen to increase with increasing exposure time up to 4320 hours after which the PVC is seen to be considerably discoloured and brittle and found to contain approximately 55% stannic oxychloride. Owing to the poor quality of data and the long run times involved large error limits of the order ± 5% must be assigned to the percentage concentration values for stannic oxychloride. These error limits were estimated by determining the effect of artificially increasing the area under the absorption peak due to the stannic oxychloride component, and simultaneously reducing the area due to the chlorotin ester for the starting parameters, and refitting the experimental data. In most cases the χ^2 values were not significantly altered, but the fitting routine converged on parameters which approached the initial completed fits.

i.e Since Area = $\frac{\Gamma_H \cdot \text{Depth}}{\text{Background Counts}}$

Figure 3.6

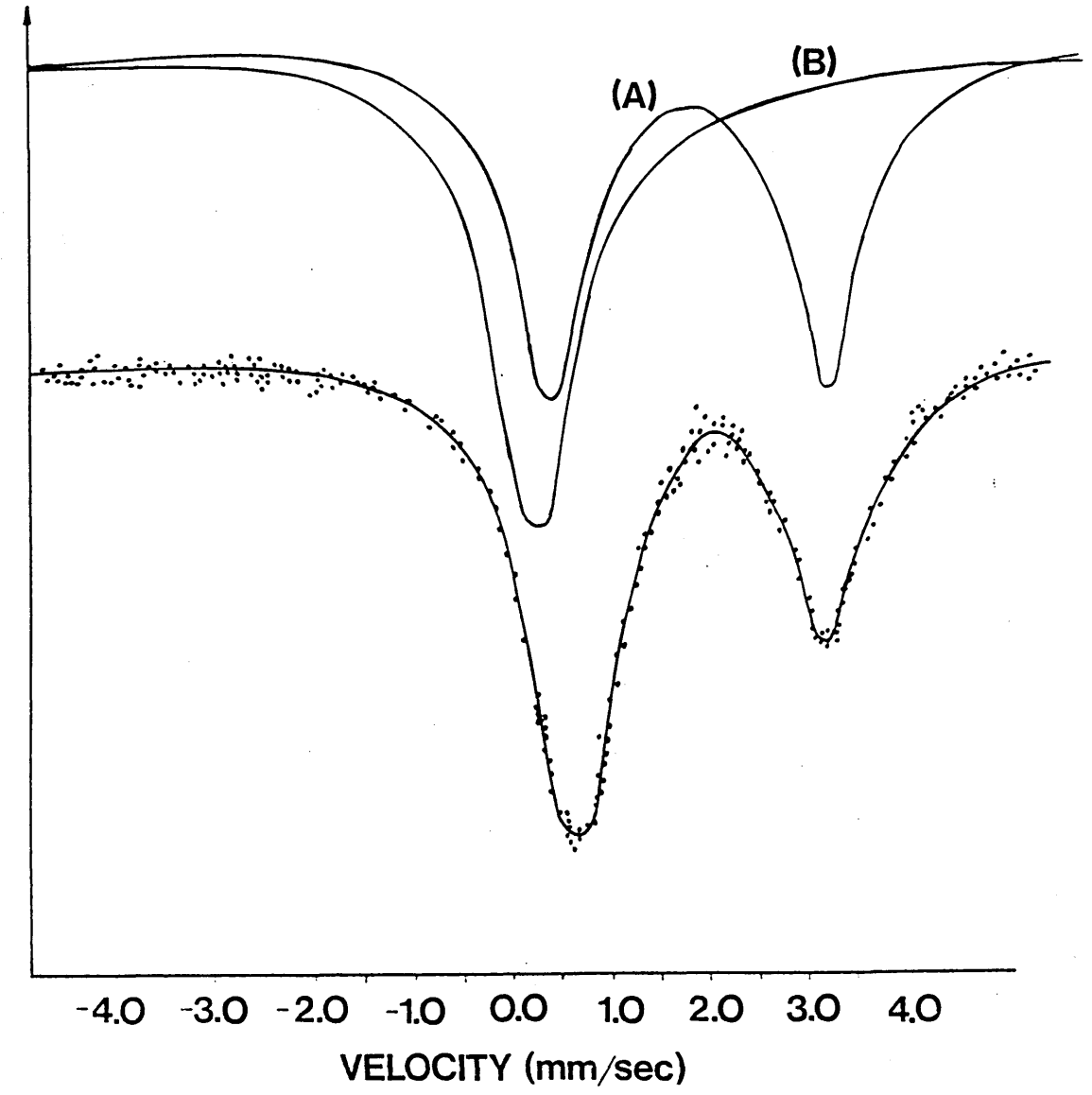

Mössbauer Spectra of U.V. degraded PVC containing $Bu_2Sn(IOTG)_2$ stabiliser at 1.2% after 4320 hours exposure. The two components of the computer fit are shown corresponding to (A) $Bu_2SnCl(IOTG)$ and (B) $SnOCl_2$

then artificially increasing Γ_H. Depth/for stannic oxychloride and reducing(Γ_H. Depth)for dibutylchlorotinisooctylthioglycollate by equal amounts produces the required increase / reduction in areas.

The results are shown in Table 3.7 and confirm that for an increase / reduction in Area of 5% for stannic oxychloride and dibutylchlorotiniso-octylthioglycollate respectively in the starting parameters no change occurs to the final values for the isomer shift, quadrupole splitting, and full width at half height parameters on comparison with the original data.

The results for the maleate stabiliser [3] given in Table 3.8 confirm that this stabiliser is more effective in preventing photochemical degradation of the polymer . No degradation appears to have occured after 1000 hours exposure and, furthermore, the Mössbauer parameters for the maleate stabiliser present in the exposed polymer are indistinguishable from those of the maleate in the unexposed sample.

The difference in the behaviour of the two compounds must lie in the nature of the processes involved in the photochemically - induced degradation of the polymer. The mechanism of photochemical degradation is clearly very complex and is still not yet fully understood. Several workers(58,59,60) have proposed that degradation is initiated by the action of peroxides and free - radicals produced from U.V. absorption. Stabilisation is considered to involve prevention of the formation of such peroxides and free-radicals by the use of "quenching" agents capable of taking part in an energy transfer process with the polymer after absorption of U.V. light (63-65).Absorption of U.V. light promotes excited triplet energy levels in both the polymer and stabiliser across which energy transfer is possible only if the excited energy levels of the stabiliser are of lower energy than those of the polymer (fig. 3.7). After energy transfer the polymer returns to the ground state energy level leaving the excited stabiliser to return to the ground state by normal fluorescence/phosphorescence processes. At this stage, no bond cleavage

has taken place and the stabiliser is acting as a quenching agent. Similar energy transfer processes have been suggested between other polymer systems and organic quenching agents (59,64,65).

Figure 3.7 Energy level diagram showing process of U.V.-stabilisation of PVC containing either the thioglycollate or maleate stabilisers.

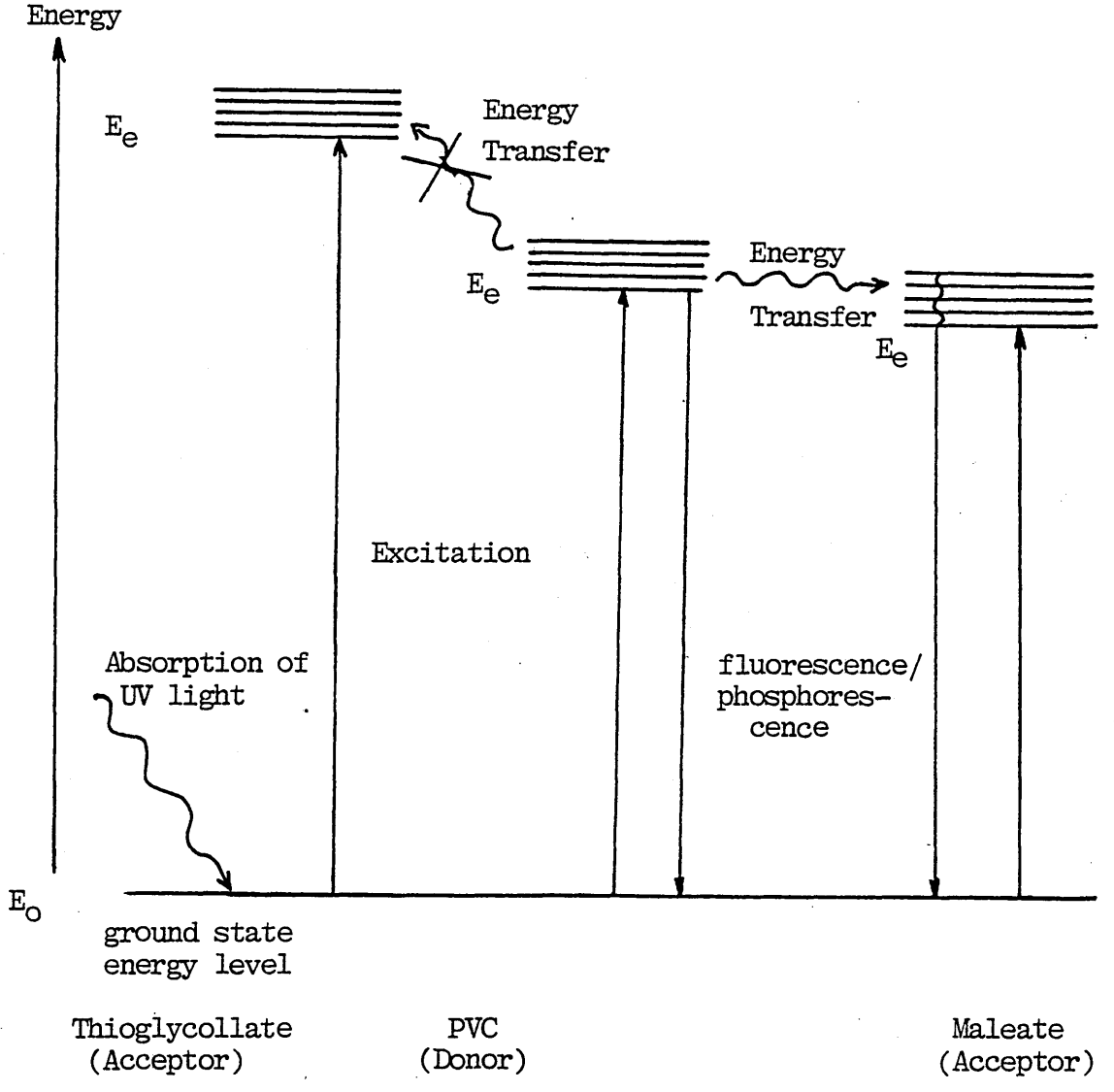

Since efficient stabilisation is not achieved with the thioglycollate [1] stabiliser this suggests that the excited energy levels of the stabiliser are higher in energy than those of the polymer. Consequently energy transfer does not occur and the stabiliser itself undergoes degradation to form stannic oxychloride and dibutylchlorotin-isooctylthioglycollate. The formation of these products indicates at least two complimentary processes occurring as a result of U.V. degrad-

ation of both the stabiliser and the polymer:

(1) the formation of dibutylchlorotinisooctylthioglycollate in relatively higher concentrations at early exposure times suggests that dehydrochlorination of the polymer is the first stage in the degradation process and is complemented by:

(2) elimination / oxidation of the alkyl groups to form stannic oxychloride arising from peroxide oxidation.

The two processes are probably further enhanced by the prescence of chlorine atoms, and molecular oxygen in the polymer providing complementary mechanisms for the formation of the two products.

3.5.3 Conclusions

The Mössbauer results show dibutyltinbis(isooctylmaleate) to be a more effective stabiliser against U.V. degradation than dibutyltinbis-(isooctylthioglycollate). The mechanism by which stabilisation occurs is reported to involve energy transfer from the excited energy levels of the polymer (donor) to the excited energy levels of the stabiliser (acceptor), followed by de-activation to the ground state energy levels. A necessary requirement for stabilisation is that the excited energy levels of the acceptor be of lower energy than those of the donor.

Dibutyltinbis(isooctylthioglycollate) in PVC degrades rapidly during U.V. exposure to form dibutylchlorotinisooctylthioglycollate and stannic oxychloride. The proportion of the latter component is seen to increase with increased exposure time to approximately 55% after 4320 hours in the Xenotest apparatus. Stannic oxychloride is probably formed as a result of reaction of hydrogen chloride, chlorine atoms and peroxides released in the polymer with dibutylchlorotinisooctylthioglycollate.

3.6 Dilution Studies

3.6.1 Introduction

In section 3.4.1 the significant change in the quadrupole splitting on passing from pure dibutyltinbis(isooctylmaleate) to a dilute dispersion of the stabiliser in PVC was attributed to a change in the co-ord-

lination and steric arrangement of the maleate groups around the tin atom. A similar change in the quadrupole splitting of dibutyltin dichloride is observed on dispersion in PVC at 1.2% by weight as shown in Table 3.3.

On the basis of the reported distorted octahedral, associated structures of dimethyl- and diethyltin dichloride (67,68) and of the similarity between the Mössbauer parameters for dibutyltin dichloride and the above two compounds (5) it is suggested that pure dibutyltin dichloride similarly has the associated six-co-ordinate structure shown in figure 3.8(a). The magnitude of the quadrupole splitting for dibutyltin dichloride on dispersion in PVC by solvent casting is typical of five-co-ordinate tin (figure 3.8(b)) suggesting a change in structure and co-ordination occurs.

Figure 3.8. Suggested structures for Dibutyltin dichloride:

(a) Pure (ΔE_Q= 3.45 mms^{-1})

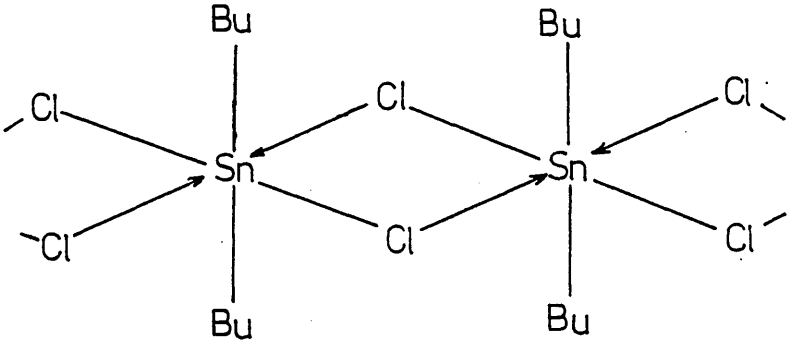

(b) Dispersed in PVC at 1.2% w/w.

(ΔE_Q= 3.09 mms^{-1}; p.q.s. ΔE_Q= 3.07 mms^{-1})

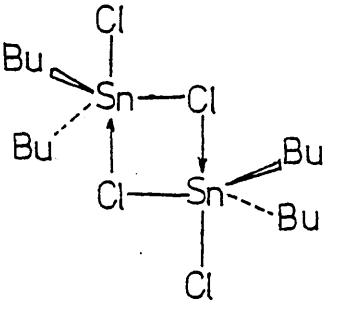

3.6.2 Results and Discussion

To confirm the proposed change in structure from octahedral to a penta-co-ordinate state (figure 3.8(b)) on dispersion in PVC it was decided to attempt to calculate the theoretical partial quadrupole splitting values for the possible structures (figure 3.8(a) and 3.8(b)). Using the additive model proposed by Bancroft et al (69) for the five-co-ordinate structure shown in figure 3.8 (b) gives:-

$$\Delta E_Q \text{ (calc)} = \frac{-7\,(\text{alkyl})^{tbe} + 8\,(\text{Cl})^{tba} + (\text{Cl})^{tbe}}{\sqrt{7}}$$

where $(\text{alkyl})^{tbe} = -1.13 \text{mms}^{-1}$

$(\text{Cl})^{tba} = +0.00 \text{mms}^{-1}$

$(\text{Cl})^{tbe} = +0.20 \text{mms}^{-1}$

gives $\Delta E_Q \text{ (calc)} = 3.07 \text{mms}^{-1}$

The isomer having the above partial quadrupole splitting can be distinguished from the other possible stuctures / isomers shown in figure 3.9 (70).

Further, by extrapolating from this model using a series of partial quadrupole splittings of five-co-ordinate tin compounds, Bancroft showed that it is possible to calculate the partial quadrupole splitting for the octahedral polymeric structure R_2SnL_4. Applying the model to the six-co-ordinate form of dibutyltin dichloride gives a partial quadrupole splitting of 3.36mms^{-1}. This value while being significantly different from the calculated value for the 5-co-ordinate dimer, is also different to the observed splitting for the polymeric dibutyltin dichloride showing the limitations to the extrapolation.

Table 3.10 gives the Mössbauer data for dibutyltin dichloride at various concentrations in the PVC. At a concentration of 1.2% it is suggested that the dibutyltin dichloride is present as a five-co-ordinate dimer. Pure dibutyltin dichloride, on the other hand, has an associated octahedral structure. On increasing the concentration of dibutyltin dichloride in the polymer six-co-ordinate tin species are formed, the

Figure 3.9. Other structures/isomers for Dibutyltin dichloride and their calculated partial quadrupole splittings.

(a) Tetrahedral

p.q.s.= 2.74 mms^{-1}

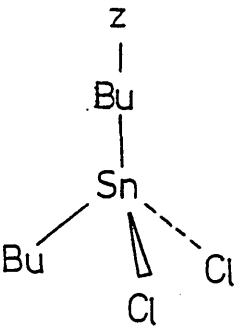

(b) Trigonal bipyramidal

(i) p.q.s. = 2.53 mms^{-1}

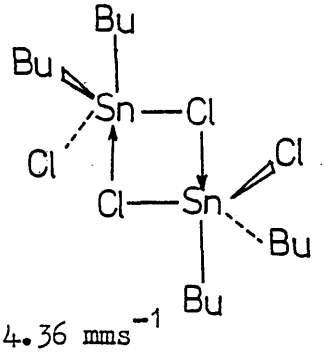

(ii) p.q.s. = 4.36 mms^{-1}

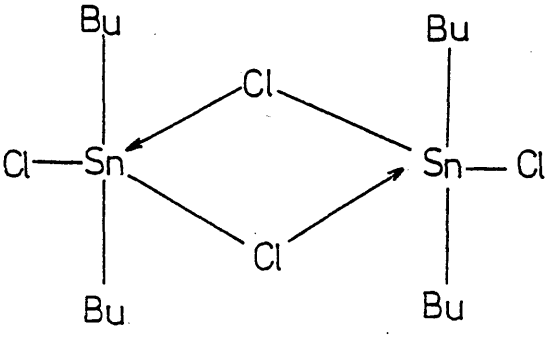

Table 3.10 ^{119}Sn Mössbauer parameters for dibutyltin dichloride in PVC at various concentrations at 80K.

Concentration in PVC	Isomer Shift (mms^{-1})($\pm$0.05)	Quadrupole Splitting (mms^{-1})($\pm$0.05)	Full Width at Half-height (mms^{-1})	Relative % Concentration of Dimeric units
1.2 %	1.54	3.09	1.00	100
10 %	1.54	3.09	1.04	100
15 %	1.55	3.07	1.02	65
20 %	1.55	3.21	1.05	50
30 %	1.57	3.25	1.02	49
50 %	1.60	3.28	1.12	44
75 %	1.59	3.28	1.12	38
Pure dibutyltin dichloride	1.62$\pm$0.02	3.45$\pm$0.02	0.99	-
Dibutyltin dichloride in Polystyrene (at 1.2 %w / w)	1.53	3.00	1.04	-

Fig 3.10 Variation of Isomer Shift and Quadrupole Splitting with concentration

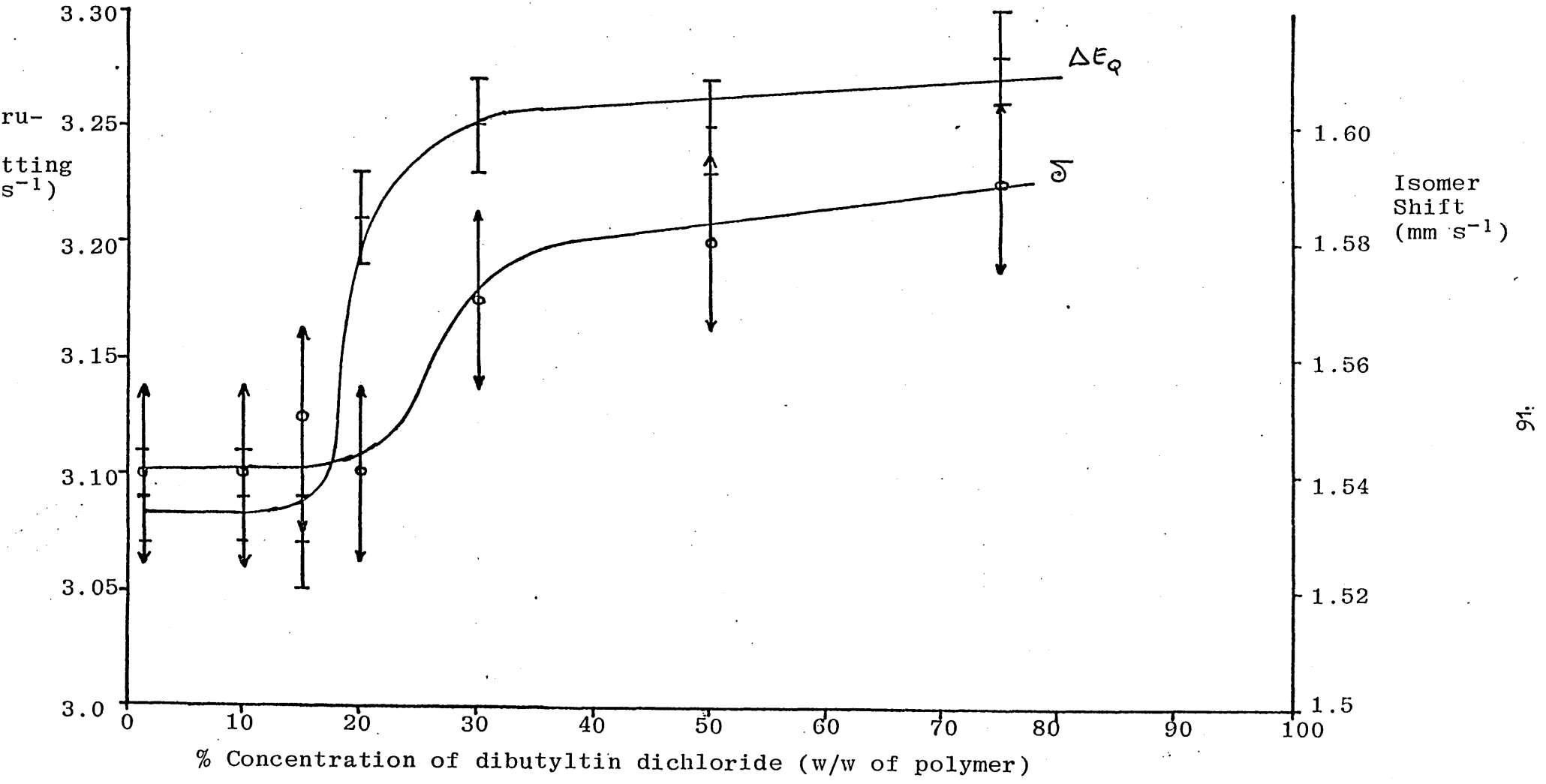

concentration of which is seen to increase relative to the concentration of the five-co-ordinate species as shown in figure 3.10. The graph shows that at a concentration of dibutyltin dichloride of 20% $w/_w$ the concentration of the six-co-ordinate species is significant to cause an appreciable change to the quadrupole splitting. The values for the quadrupole splittings above the 20% concentration represent an averaged value arising from the splittings of both five - and six - co-ordinate forms of dibutyltin dichloride in the polymer.

In an attempt to estimate the relative concentration of the dimeric units at the respective concentrations the data were fitted as two doublets with parameters for both the five-co-ordinate and six-co-ordinate species. The results are shown in Table 3.9. In each case the validity of the fit was ensured by comparing the χ^2 value of the 4-line fit with that of the 2-line fit.

In addition, to eliminate the possibility that co-ordination from the chlorine groups on the polymer is responsible for the change in co-ordination a dispersion of dibutyltin dichloride (at 1.2% by weight) in an "inert" polymer matrix (polystyrene) was prepared and the Mössbauer parameters recorded. The results are given in Table 3.10 and clearly agree with those observed for dibutyltin dichloride in PVC.

Finally, it should be noted that a similar 'dilution effect' is observed for dioctyltin dichloride on dispersion in PVC at 2% by weight as shown in Table 3.4.

3.6.3 Conclusions

The magnitude of the quadrupole splitting for pure dibutyltin dichloride (ΔE_Q = 3.45mms^{-1}) is typical of a six-co-ordinate tin compound with an associated structure, shown in figure 3.8(a). On dispersion in PVC at 1.2% by weight a reduction in the quadrupole splitting is observed to a value representative of a five-co-ordinate tin compound (ΔE_Q = 3.09mms^{-1}). Partial quadrupole splitting calculations confirm the suggestion of the five-co-ordinate dimer present in

PVC and shown in figure 3.8(b).

The relative concentration of the dimeric units in PVC is seen to decrease with increased concentration of the dibutyltin dichloride.

3.7 Other Organotin Stabilisers

3.7.1 Introduction

The results of the above investigation into the use of organotin compounds as stabilisers against thermal and U.V.- induced degradation of PVC confirmed the generalisation made by Wirth and Andreas (26) that compounds having sulphur-containing groups are the most efficient thermal stabilisers and that compounds having oxygen-containing groups derived from maleic acid, although weaker in their thermostabilising efficiency, are excellent U.V. stabilisers. As a further investigation of the validity of this generalisation a series of organotin(IV) compounds and two organotin(II) compounds were prepared with the aim of investigating their potential as thermal stabilisers and identifying their degradation products.

The organotin(IV) compounds were of the general formula R_2SnY_2 (where R = Me, Bu, Oct; and Y= $-SCH_2CH(NH_2)COOC_2H_5$, and $-OCOC_{11}H_{23}$ (laurate)). Dimethyl- and dibutyltin dilaurate are commercially used stabilisers although their degradation products have not been conclusively identified.

The two organotin(II) compounds prepared were stannous stearate, a commercially used stabiliser in clear PVC food packaging materials, and stannous cysteinate, a new compound, which has been found to be relatively air stable (71) and consequently considered to be a potential thermal stabiliser.

3.7.2 Results and Discussion

(a) Organotin(IV) Compounds

The Mössbauer results for the organotin(IV) compounds in PVC (at 1.6% w/w) and their thermal degradation products are given in Table 3.11; the results for the corresponding pure compounds are given in Table 3.12. The magnitudes of the quadrupole splittings for both of the dilaurate compounds (ΔE_Q= 3.43 mms^{-1} for R = Me and Bu) in the pure state are typical of six co-ordinate tin compounds and,on the basis of the previous interpretation of the results for dibutyltinbis-(isooctylmaleate), suggest both compounds to be associated. On dispersion in PVC the quadrupole splittings are seen to be reduced (ΔE_Q = 3.20 mms^{-1} and 3.24 mms^{-1} for R = Me and Bu respectively), as a result of the dilution effect (section 3.6). After prolonged thermal aging at 185°C further reduction in the quadrupole splittings is observed (ΔE_Q = 2.98 mms^{-1} and 2.86 mms^{-1} for R = Me and Bu respectively) suggesting the formation of a five co-ordinate tin species. On the basis of the results of the previous studies it is reasonable to suggest the degradation products to be the dialkylchlorotinlaurates although attempts to synthesise these two compounds were unsuccessful.

The Mössbauer data for the dialkyltinbis(ethylcysteinates) in the pure state are typical of four co-ordinate tin compounds (ΔE_Q = 2.32 mms^{-1} and 2.28 mms^{-1} for R = Bu and Oct respectively). Infrared data (Table 3.13) gives evidence of unco-ordinated carbonyl and primary amine groups in the two compounds and further support the suggestions from the Mössbauer data. On dispersion by hot milling in PVC (at 1.6% w/w) a yellow discolouration is observed which is accompanied by a small change in the quadrupole splitting (ΔE_Q = 2.12 mms^{-1} and 2.37 mms^{-1} for R = Bu and Oct respectively) for both compounds suggesting partial degradation occurring during the milling process. The discolouration increased with progressive aging and after 60 minutes of heating a significant change in the quadrupole splitting is observed which for the dioctyltinbis(ethylcysteinate)

Table 3.11 ^{119}Sn Mössbauer parameters for organotin compounds of the type R_2SnY_2 (R = Me, Bu, Oct; Y = $SCH_2CH(NH_2)COOC_2H_5$, or laurate) in PVC (at 1.6% w/w) at 80K.

Compound	Isomer Shift (mms^{-1})($\pm$0.05)	Quadrupole Splitting (mms^{-1})($\pm$0.05)	Full Width at Half-height (mms^{-1})
Dimethyltin dilaurate in PVC (unaged)	1.26	3.20	0.93
Dimethyltin dilaurate in PVC aged for 75 mins.	1.43	2.98	1.04
Dibutyltin dilaurate in PVC (unaged)	1.42	3.24	0.87
Dibutyltin dilaurate in PVC aged 120 mins.	1.49	2.86	1.30
Dibutyltinbis(ethylcysteinate) in PVC (unaged)	1.45	2.12	1.07
Dibutyltinbis(ethylcysteinate) in PVC aged 75 mins.	1.55	3.11	1.05
Dioctyltinbis(ethylcysteinate) in PVC (unaged)	1.42	2.37	1.07
Dioctyltinbis(ethylcysteinate) in PVC aged 60 mins.	1.58	2.98	1.02

Table 3.12 ^{119}Sn Mössbauer parameters for pure organotin(IV) compounds of the type R_2SnY_2 (R = Me,Bu, Oct; Y = $SCH_2CH(NH_2)COOC_2H_5$, or laurate) and for Stannous Stearate and Stannous Cysteinate at 80K

Compound		Isomer Shift (mms^{-1})($\pm$0.02)	Quadrupole Splitting (mms^{-1})($\pm$0.02)	Full Width at Half-Height (mms^{-1})
Dimethyltin dilaurate		1.30	3.43	1.04
Dibutyltin dilaurate		1.36	3.43	1.12
Dibutyltinbis(ethylcysteinate)		1.39	2.32	1.17
Dibutylchlorotinbis-(ethylcysteinate)		1.35	2.78	1.36
Dioctyltinbis(ethylcysteinate)		1.35	2.28	1.21
Dioctylchlorotinbis-(ethylcysteinate)		1.43	2.84	1.37
Stannous Stearate	(1)	3.50	1.77	1.14
	(2)	0.04	Unresolved	1.33
Stannous Cysteinate	(1)	3.15	1.84	1.04
	(3)	0.30	Unresolved	1.59

(1) Corresponds to parameters for the parent component.

(2) Corresponds to parameters for the SnO_2 component.

(3) Corresponds to parameters for the $SnOCl_2$ component.

Table 3.13 Infrared data for organotin(IV) compounds of the type R_2SnY_2 (R = Me, Bu, Oct; Y = $SCH_2CH(NH_2)COOC_2H_5$, or laurate).

Compound	c=o str (cm^{-1})	NH_2 str (cm^{-1})	n-H bend (cm^{-1})
Dimethyltin dilaurate	1581	-	-
Dibutyltin dilaurate	1600	-	-
Dibutyltinbis(ethylcysteinate)	1724	3333	1575
Dibutylchlorotinethylcysteinate	1724	3278	1550,1575
Dioctyltinbis(ethylcysteinate)	1725	3278	1575
Dioctylchlorotinethylcysteinate	1725	3280	1550,1575

(ΔE_Q = 2.95mms^{-1}) corresponds to the formation of the chlorotin ester.

The quadrupole splitting for the dibutyltinbis(ethylcysteinate) in aged PVC (ΔE_Q = 3.11mms^{-1}) does not correlate with the data for the dibutylchlorotinethylcysteinate but corresponds to the data previously observed for dibutyltin dichloride at low concentration in PVC (Table 3.10).

(b) Organotin(II) Compounds

Table 3.12 gives the Mössbauer parameters for the parent compounds stannous stearate and stannous cysteinate. The high value observed for the isomer shift for both compounds is typical of tin(II) compounds and allows for easy identification of any tin(IV) species present in the spectrum. The data shows that for both compounds an impurity is present which for stannous stearate has an isomer shift which corresponds to stannic oxide (δ = 0.04mms^{-1}), and for stannous cysteinate has parameters which correspond to those previously observed for stannic oxychloride (Table 3.9).

The stannic oxide impurity evidently arises from air oxidation of stannous stearate. The stannic oxychloride impurity, however, must be formed by a more complex mechanism involving the starting materials (stannous chloride and cysteine) and including the reported fact that stannous cysteinate is relatively air stable at room temperature having the 'cage' structure (71):

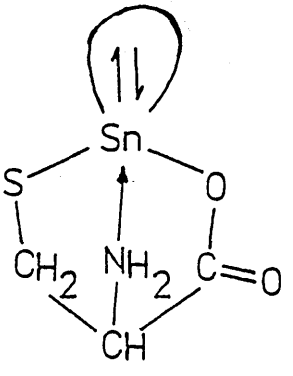

Table 3.14 shows the Mossbauer data for the two organotin(II) compounds incorporated in PVC and their thermal degradation products. For both compounds thermally aging the PVC increases the relative concentration of the impurity component until after 30 minutes all the stannous stearate is converted to stannic oxide, and after 45 minutes all the stannous cysteinate is converted to stannic oxychloride.

Tables 3.14 and 3.15 show the change in concentration of the impurity component with thermal aging time for stannous stearate and stannous cysteinate respectively. In each case the relative concentration was estimated by fitting the data as three lines comprising the quadrupole doublet of the stearate and a broad single line representing the impurity component and determining the proportionate area due to the impurity component.

Finally, it should be noted that during the milling of both compounds in the PVC all clarity is lost and opaque white sheets are produced.

3.7.3 Conclusions

For the organotin(IV) compounds studied, only the two dilaurate esters (which are commercially used stabilisers) efficiently retard colour developement in the PVC during progressive aging. The two ethyl-cysteinate compounds imparted a yellow colouration to the PVC after milling which was retained for up to 30 minutes of aging before further discolouration occurred. The Mössbauer data for the degradation products of each of the organotin(IV) stabilisers (with the exception of dibutyl-tinbis(ethylcysteinate)) indicated a change in co-ordiantion to the five-co-ordinate dialkylchlorotin ester (R_2SnClY). The quadrupole splitting for the degradation product of dibutyltinbis(ethylcysteinate), however, is comparable to that observed for dibutyltin dichloride in PVC at 1.2% w/w .

The organotin(II) compounds similarily showed little potential as thermal stabilisers. Different degradation products were identified for the two compounds. Stannous stearate was converted to stannic oxide

Table 3.14 ^{119}Sn Mössbauer parameters for organotin(II) compounds Stannous Stearate and Stannous Cysteinate in PVC (at 1.6% w/w) at 80K.

Compound		Isomer Shift (mms^{-1})($\pm$0.05)	Quadrupole Splitting (mms^{-1})($\pm$0.05)	Full Width at Half Maximum (mms^{-1})	Relative % SnO_2 / $SnOCl_2$ ($\pm$5%)
Stannous Stearate in PVC (solvent cast from dichloromethane)	(1)	3.14	1.96	1.11	
	(2)	0.08	Unresolved	1.33	70%
Stannous Stearate in PVC (milled)	(1)	3.42	1.56	1.12	
	(2)	0.06	Unresolved	1.30	96%
Stannous Stearate in PVC aged 30 mins		0.08	Unresolved	1.32	100%
Stannous Cysteinate in PVC (milled)	(1)	3.22	1.88	0.90	
	(3)	0.29	0.69	0.95	20%
Stannous Cysteinate		0.53	0.36	0.88	100%

(1) Corresponds to Stannous Stearate or Stannous Cysteinate.

(2) Corresponds to SnO_2

(3) Corresponds to stannic oxychloride.

Table 3.15 ^{119}Sn Mössbauer parameters for Stannous Cysteinate in PVC (at 1.6% w/w) at various aging times at 80K.

Time (mins)		Isomer Shift (±0.08)	Quadrupole Splitting ±0.08	Full Width at Half-Height	Relative Depth	Relative % $SnOCl_2$ (±5%)
0	(1)	3.22	1.88	0.90	4.2	
	(2)	0.29	0.69	0.95	1.0	20%
15mins	(1)	3.19	1.83	0.98	3.27	
	(2)	0.36	0.67	0.99	1.0	24%
30mins	(1)	3.32	1.27	1.10	1.15	
	(2)	0.46	0.72	0.92	1.0	40%
45mins		0.53	0.36	0.88	1.0	100%

(1) Corresponds to parameters for the Stannous cysteinate component.

(2) Corresponds to parameters for the Stannic Oxychloride component.

after milling in the PVC, whereas stannous cysteinate was found to be converted to stannic oxychloride. For both stabilisers all clarity was seen to be lost on incorporation into PVC.

3.8 Experimental

Table 3.16 lists the organotin compounds investigated as thermal and/or photochemical stabilisers in poly(vinyl chloride), their relative concentrations in the polymer, and the corresponding degradation products as identified from the Mössbauer studies. Samples of PVC containing the compounds listed were prepared by conventional hot milling techniques. Thermal degradation of the above samples was achieved by placing the PVC sheets in an oven in an air atmosphere 185°C for varying periods of time. Solvent cast samples were prepared by allowing a thin film of a solution of PVC and the appropriate stabiliser in an organic solvent (dichloromethane for the thioglycollate stabilisers and THF for the maleate stabilisers) to evaporate at room temperature.

The thioglycollate/maleate series of compounds and samples of PVC containing those compounds were supplied by Lankro Chemicals Ltd. The ethylcysteinate and laurate series and the organotin(II) compounds were prepared in collaboration with the International Tin Research Institute.

Dimethyl- and Dibutyl-tin dilaurates: a 1:2 mixture of the dialkyltin oxide and lauric acid in methylbenzene was heated under reflux for two hours in a Dean and Stark apparatus. On removal of the solvent a low-melting solid (dibutyltin dilaurate) or a white crystalline solid (dimethyltin dilaurate) was obtained.

Dibutyltinbis(ethylcysteinate): L - cysteine ethyl ester hydrochloride (4.89g, 0.026mol) in water (50cm^3) was added to sodium hydrogen carbonate (4.42g, 0.052 mol) in water (50cm^3). Dibutyltin dichloride (4g, 0.13 mol) in diethylether (100cm^3) was added slowly to the aqueous solution. The two solutions were then thoroughly mixed in a separating funnel and the

Table 3.16 Organotin compounds investigated as stabilisers in PVC, their respective concentrations during the investigation and their identified degradation products.

Compound (Pure)	Concentration in PVC (w/w)	Degradation Product
Dibutyltinbis(isooctylthioglycollate)	4%,1.2%	Dibutylchlorotinisooctylthioglycollate
Dioctyltinbis(isooctylthioglycollate)	4%	Dioctylchlorotinisooctylthioglycollate
Dibutyltinbis(isooctylmaleate)	4%,2%	Dibutylchlorotinisooctylmaleate
Dimethyltin dilaurate	1.6%	Dimethylchlorotin laurate
Dibutyltin dilaurate	1.6%	Dibutylchlorotin laurate
Dibutyltinbis(ethylcysteinate)	1.6%	Dibutyltin dichloride
Dioctyltinbis(ethylcysteinate)	1.6%	Dioctylchlorotin ethyl cysteinate
Stannous Stearate	1.6%	Stannic Oxide
Stannous Cysteinate	1.6%	Tin oxide chloride
Dibutyltin Dichloride	1.2%	
Dibutylchlordinisooctylthioglycollate		
Dioctylchlorotinisooctylthioglycollate		
Dibutylchlorotinisooctylmaleate		
Dioctylchlorotinethylcysteinate		
Dibutylchlorotinethylcysteinate		

ether layer collected and dried over anhydrous magnesium sulphate. On removal of the solvent, a clear oil dibutyltinbis(ethylcysteinate) was obtained. (Found: C,39.96; H, 7.07, N,5.00; S, 11.39. $C_{18}H_{38}N_2O_4S_2Sn$ requires C,40.83; H, 7.18; N, 5.29; S, 12.20 %.)

Dibutylchlorotinethylcysteinate: Dibutyltin oxide (6.69g, 0.026 mol) was added to L - cysteine ethyl ester hydrochloride (4.89g, 0.026 mol) in dry methanol (150cm^3), with stirring, over two hours. On removal of the solvent under vacuum a clear oil (dibutylchlorotinethylcysteinate) was obtained which slowly crystallised at room temperature. (Found: C,37.17; H, 6.50; N,3.27; Cl, 8.73; S,7.87. $C_{13}H_{28}ClNO_2SSn$ requires; C,37.50; H,6.72; N,3.36; Cl,8.41; S,7.68 %).

Dioctyltinbis(ethylcysteinate): was prepared by a similar method to the dibutyltin derivative giving a clear viscous oil. (Found: C,48.16; H,8.30; N,4.19; S,9.50. $C_{26}H_{54}N_2O_4S_2Sn$ requires: C,48.67; H,8.42; N,4.36; S,9.98 %).

Dioctylchlorotinethylcysteinate: was prepared by a similar method to the dibutylchlorotin derivative giving a dark viscous oil. (Found: C,47.45; H,8.35; N,2.59; Cl,6.06; S,6.33. $C_{21}H_{44}ClNO_2SSn$ requires: C,47.72; H,8.33; N,2.65; Cl,6.62; S,6.06 %).

Stannous Stearate: was prepared by the method described by Caldwell et al (72). M.pt. 59-62°c (lit. m.pt. 65.5°c). (Found: C,52.86; H,8.55. $C_{34}H_{70}O_4Sn$ requires: C,61.72; H,10.60 %).

Stannous Cysteinate: Anhydrous stannous chloride (10g,0.052 mol) in water (50cm^3) containing three drops of dilute hydrochloric acid as stabiliser was added to L - cysteine (6.40g, 0.052mol) in water (50cm^3), with constant stirring. The resulting solution was neutralised to pH 7.0 using sodium hydrogen carbonate resulting in the precipitation of a white solid (stannous cysteinate). The solid was filtered and successively washed with water, acetone and ether. M.pt. 190°c (decomp). (Found: C,14.17; H,2.02; N,5.14; S,12.58. $C_3H_5NO_2SSn$ requires: C,15.06; H,2.09; N,5.85; S,13.39 %).

CHAPTER 4. X-ray Crystallographic Structure of Dimethylchlorotin Acetate and room - temperature Mössbauer Studies

Contents:

4.1. Introduction

As an extension of the studies of the changes occurring to organotin stabilisers during thermal degradation of PVC, the structure, in the solid-state, of dimethylchlorotin acetate, a simple analogue to the chlorotin carboxylates encountered in the above studies, was investigated by Mössbauer spectroscopy and X-ray crystallography.

The structure, in the solid state, of these compounds has not previously been investigated and the Mössbauer quadrupole splitting parameter measured at 80K , which agrees with the previously published value (ΔE_Q= 3.56 mms^{-1}) (56), suggests that the tin atom is five - or six - co-ordinate. The Mössbauer spectrum has also been recorded at 300K , and this has previously been taken as evidence for a polymeric structure (73-75).However, this cannot be taken as conclusive, as a number of unassociated compounds have given absorption at room temperature (75). Consequently in order to determine the exact tin co-ordination, a single crystal X-ray analysis was undertaken.

4.2. Experimental

a) Preparative.

Dimethylchlorotin acetate was prepared by the addition of equivalent amounts (0.009 mol) of dimethyltin dichloride and triphenyltin acetate to 150cm^3 chloroform. Complete dissolution was achieved upon boiling and reduction of the volume of the solution to 75cm^3 led to the formation of colourless crystals upon cooling. Subsequent analysis confirmed the crystals to be dimethylchlorotin acetate. (found: C ,19.60; H,3.66; Cl ,14.43; $C_4H_9ClO_2Sn$ requires C,19.71; H,3.69; Cl,14.57; m.pt.179- 181°C lit.value 185°C(76)).

b) Data collection and reduction.

A crystal, approximate dimensions 0.16 x 0.40 x 0.48 mm was selected and mounted with the a - axis coincident with the rotation axis (ω) of a Stöe - Stadi - 2 two circle diffractometer. With monochromated Mo - K_α radiation and using the background - ω scan - background technique,

958 unique reflections were measured, of which 842 had $I \geq 3.0\sigma(I)$ and were considered to be observed. (The net intensity $I = T - B$, where T = scan count, B = mean background over the scan width; $\sigma(I) = (T + B.c^2/2t)^{\frac{1}{2}}$, where c = scan time, t = time for background measurement at end of scan). Corrections for Lorentz and polarisation effects were applied to the data, but no corrections for absorption were made.

Crystal Data

$C_4H_9ClO_2Sn$, M_r 243-3, orthorhombic, $Pna2_1$, a = 9.315(3), b = 11.061(3), c = 7.656(2) Å , U = 788.78 $Å^3$, Z = 4, D_c = 2.05, D_m = 2.07 mgm^{-3}, μ(Mo-Kα) = 3.247 mm^{-1}, F(000) = 464.

Structure Determination and Refinement

Systematic absences could not distinguish between space groups $Pna2_1$ and Pnma. Pnma would require the molecule to have mirror symmetry (Z = 4) and subsequent analysis confirmed the non-centrosymmetric space group as being correct, with occupation of the four general positions. The x and y co-ordinates of the tin atom were readily located using the Patterson function and the remaining atoms were located from successive electron density syntheses. The methyl hydrogens were located but given ideal geometry (C - H 1.08 Å) and a common isotropic temperature factor. Scattering factors were calculated using an analytical approximation (77) and the weighting scheme adopted was $\omega = 1.0000 / (\sigma(F_o) + 0.0075 (F_o)^2)$. Full matrix refinement with anisotropic temperature factors applied to all non-hydrogen atoms gave the final R = 0.040 and R' = 0.044.

4.3 Results and Discussion

Mössbauer parameters and R_{80} value (the ratio of the normalised areas at 300K and 80K) for dimethylchlorotin acetate are given in Table 4.1. (The R_{80} value has been used for suggesting a polymeric structure (for $R_{80} \geq$ 0.03 (74)) and is defined as the ratio of the normalised areas under the absorption peak at temperature 'T' and at 80K. The area under the absorption peak is defined by the expression (11):-

$$\text{Area} = \int_{-\infty} \eta\,(x)\,dx = \tfrac{1}{2}\,\pi\,\Gamma_H\,\sigma(\epsilon_o)\,n$$

where $\eta\,(x)$ is the probability of resonance absorption
Γ_H is the Full Width at Half Maximum
$\sigma(\epsilon_o)$ is the cross section at maximum absorption
n is the absorber thickness

The normalised area is thus: $\dfrac{\tfrac{1}{2}\,\pi\,\Gamma_H\,\sigma(\epsilon_o)\,n}{\text{Background counts}}$

Hence: $R_{80} = \dfrac{\text{Area under the absorption peak at temperature T}}{\text{Area under the absorption peak at 80K}}$)

The magnitude of the quadrupole splitting (ΔE_Q = 3.56 mms^{-1}) suggests the tin atom to be five or six co-ordinate, and the calaulated R_{80} value (= 0.032) is significant indicating a polymeric structure(74). Similar organotin carboxylates of known six co-ordinate structures have quadrupole splittings in the range (ΔE_Q= 3.6 — 3.9 mms^{-1})(69).

The crystal structure of dimethylchlorotin acetate is shown in figure 4.1 in which Me_2ClSn units are seen to be linked together via acetate bridges to give polymeric chains running along the a - direction.

Tables 4.2 and 4.3 give the final positional parameters and bond distances and bond angles respectively , and Table 4.4 gives the mean plane data. The thermal parameters and observed and calculated structure factors for dimethylchlorotin acetate are listed in Tables 4.5 and 4.6 respectively.

From the mean plane data the acetate ligands can be seen to be effectively planar and orientated such that the O(1), O(2), C(1), C(2), mean plane is almost coincident with the tin and chlorine atoms and bisects the C(3)-Sn-C(4) angle. (Sn, Cl, C(2), C(3), C(4), lie -0.56, -0.030, -1.982, 1.951 Å respectively out of the mean plane). The resulting co-ordination about the tin is best described as distorted trigonal bipyramidal with the chlorine and two methyl carbon atoms forming a trigonal arrangement about the metal. O(2) and O(1') occupy the axial positions such that the O(2)-Sn -O(1') bond angle is 170.1(2)° (Table 4.3), and the Sn-O(2), O(1') distances are 2.165(6) and 2.392(7) Å respectively. While these

FIG 4.1

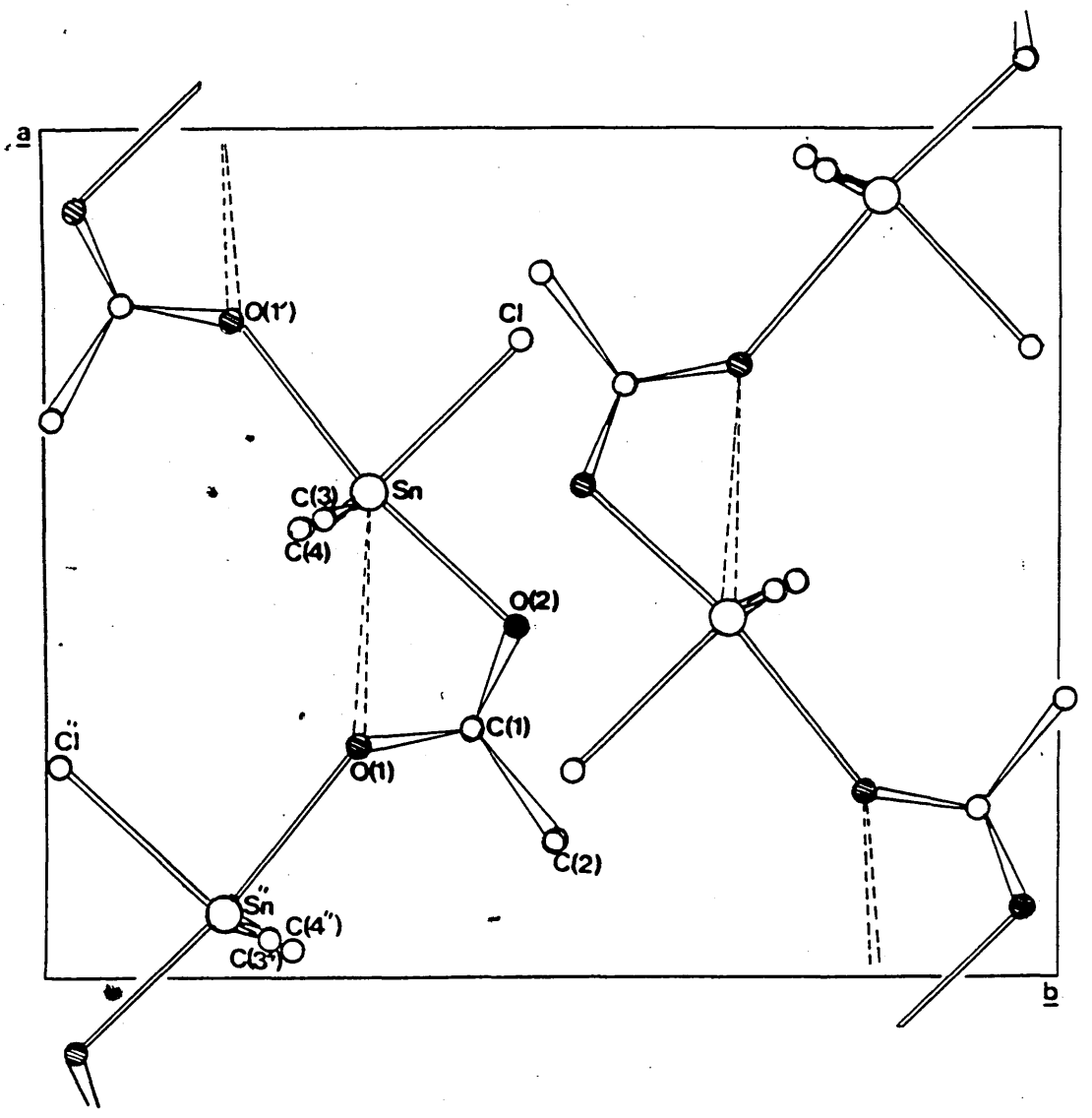

Projection down the c axis showing the polymeric nature of dimethylchlorotin acetate.

tin-oxygen distances fall within the range of reported values (78 - 81), they are significantly different and it is of note that the longer distance is associated with the oxygen atom involved in an additional tin - oxygen interaction. Although the Sn-O(1) distance of 2.782(7) Å is considerably larger than the sum of the covalent radii (2.13 Å) it is well within the sum of the van der Waals' radii (3.70 Å) and distortions about the tin can be attributed to a weak yet significant Sn-O(1) interaction. Thus the metal atom is found to be 0.173 A out of the C(1), C(3), C(4), plane and in a direction away from O(1') and toward O(1) and O(2). In addition the angular distortions about the tin viz C(3)-Sn-C(4) 140.9(6)°, O(1')-Sn-O(2) 170.1(2)°are such as to facilitate a Sn-O(1) interaction. Thus while O(2) is monodentate with respect to tin, O(1) interacts with both Sn and Sn" , thereby increasing the overall co-ordination number for tin to six.

4.4 Conclusions

X- ray crystallographic data confirm dimethylchlorotin acetate to have a distorted 6 - co-ordinate polymeric structure. The results of the crystallographic data in this instance lend weight to the use of the observation of a room temperature Mössbauer resonance to assign associated structures. It should be noted, however, that where the value for the quadrupole splitting suggests an uncertainty in assigning the co-ordination to the tin atom, such structural assignments cannot be made without the support of other data, such as crystallographic data.

TABLE 4.1

^{119m}Sn MÖSSBAUER DATA OF DIMETHYLCHLOROTIN ACETATE

Temperature (K)	Isomer Shift δ(mm s^{-1})a ±0.02 mm s^{-1}	Quadrupole Splitting ΔE_Q(mm s^{-1}) ±0.02 mm s^{-1}	Full Width at Half Height Γ(mm s^{-1})
80	1.38	3.56	1.12
300	1.34	3.70	0.87

R_{80} = 0.032 (Ratio of total normalised area at 300 K to total normalised area at 80 K)

a Relative to $BaSnO_3$

TABLE 4.2.

FRACTIONAL POSITIONAL PARAMETERS (x 10^5 for Sn; x 10^4 for remaining atoms) with e.s.d.'s for non-hydrogen atoms in parentheses

Atom	x	y	z
Sn	57335(5)	32330(4)	0
Cl	7536(3)	4750(2)	-89(14)
O(1)	2751(9)	3105(9)	-11(27)
O(2)	4179(6)	4687(5)	-65(38)
C(1)	2941(10)	4231(7)	-150(25)
C(2)	1666(11)	5072(9)	-54(53)
C(3)	5480(34)	2778(15)	1530(29)
C(4)	5316(31)	2553(17)	-2600(26)
H(21)	2047	5789	-197
H(22)	1149	4972	1200
H(23)	906	4873	-1080
H(31)	4610	2304	3163
H(32)	6148	2138	1841
H(33)	6115	3243	3501
H(41)	4421	2060	-3145
H(42)	5952	2933	-3644
H(43)	5972	1947	-1835

TABLE 4.3.

BOND DISTANCES (Å) AND ANGLES (°)

Symmetry Code

none x, y, z; (') 0.5 + x, 0.5 - y, z; ('') - 0.5 + x, 0.5 - y, z

Bond Distances (Å)

Sn-Cl	2.375(2)	Sn-C(4)	2.163(18)
Sn-O(1)	2.782(7)	O(1)-C(1)	1.262(10)
Sn-O(1')	2.392(7)	O(2)-C(1)	1.260(9)
Sn-O(2')	2.165(6)	C(1)-C(2)	1.511(12)
Sn-C(3)	2.015(21)		

Bond Angles (°)

Cl-Sn-O(1)	137.9(2)	O(2)-Sn-C(3)	97.4(11)
Cl-Sn-O(1')	83.2(2)	O(2)-Sn-C(4)	96.7(10)
Cl-Sn-O(2)	87.0(2)	C(3)-Sn-C(4)	140.9(6)
Cl-Sn-C(3)	106.7(7)	Sn-O(1)-Sn''	144.7(1)
Cl-Sn-C(4)	110.3(7)	Sn-O(1)-C(1)	79.0(7)
O(1)-Sn-O(1')	138.9(2)	Sn''-O(1)-C(1)	136.2(7)
O(1)-Sn-O(2)	50.9(2)	Sn-O(2)-C(1)	108.4(7)
O(1)-Sn-C(3)	82.7(10)	O(1)-C(1)-O(2)	121.3(6)
O(1)-Sn-C(4)	78.5(10)	O(1)-C(1)-C(2)	119.5(8)
O(1')-Sn-O(2)	170.1(2)	O(2)-C(1)-C(2)	118.0(8)
O(1')-Sn-C(3)	86.6(10)		
O(1')-Sn-C(4)	85.6(9)		

TABLE 4.4.

Equations of least squares planes referred to orthogonal axes with distances (Å) of relevent atoms from the planes in squares brackets and e.s.d.'s in parentheses

Plane A Cl, C(3), C(4)

$$-0.7569X + 0.6534Y - 0.0120Z + 1.8795 = 0.0000$$

(C , 0.000; C(3), 0.000; C(4), 0.000; Sn, 0.173;
O(2), 2.321; O(1), 2.184; O(1'), 2.216)

Plane B O(1), O(2), C(1), C(2)

$$-0.0082X - 0.0172Y - 0.9998Z + 0.0500 = 0.0000$$

(O(1), - 0.022; O(2), - 0.022; C(1), 0.062;
C(2), -0.018; Sn, - 0.056; C , - 0.030;
C(3), - 1.982; C(4), 1.951; Sn'', 0.011;
C '', 0.094; C(3''), - 1.933; C(4''), 1.99)

TABLE 4.5.

Dimethylchlorotin acetate

Final thermal parameters (x 10^4) with e.s.d.'s in parentheses

(a) Anisotropic temperature factors ($Å^2$) of the form:

$$\exp\left[-2\pi^2 (U_{11}h^2a^{*2} + U_{22}k^2b^{*2} + U_{33}l^2c^{*2} + 2U_{12}hka^*b^* + 2U_{13}hla^*c^* + 2U_{23}klb^*c^*)\right]$$

	U_{11}	U_{22}	U_{33}	U_{23}	U_{13}	U_{12}
Sn	346(4)	357(3)	403(3)	33(1)	-19(9)	27(6)
Cl	469(12)	500(9)	757(22)	145(8)	21(31)	-72(30)
O(1)	440(34)	416(24)	803(52)	-21(24)	378(67)	99(65)
O(2)	421(32)	375(23)	644(49)	-27(19)	-1(90)	18(88)
C(1)	359(33)	475(31)	277(61)	0(27)	-89(51)	6(43)
C(2)	518(51)	516(42)	894(77)	196(77)	162(153)	164(121)
C(3)	625(97)	480(81)	454(70)	83(69)	76(57)	-111(62)
C(4)	598(89)	401(52)	401(61)	73(62)	-80(59)	138(50)

(b) Final overall isotropic temperature factor ($Å^2$) for the hydrogen atoms of the form:

$$\exp\left[-U\sin^2\theta / \lambda^2\right]$$

U = 0.304(72)

TABLE 4.6 Observed and Calculated Structure Factors for Dimethylchlorotin Acetate

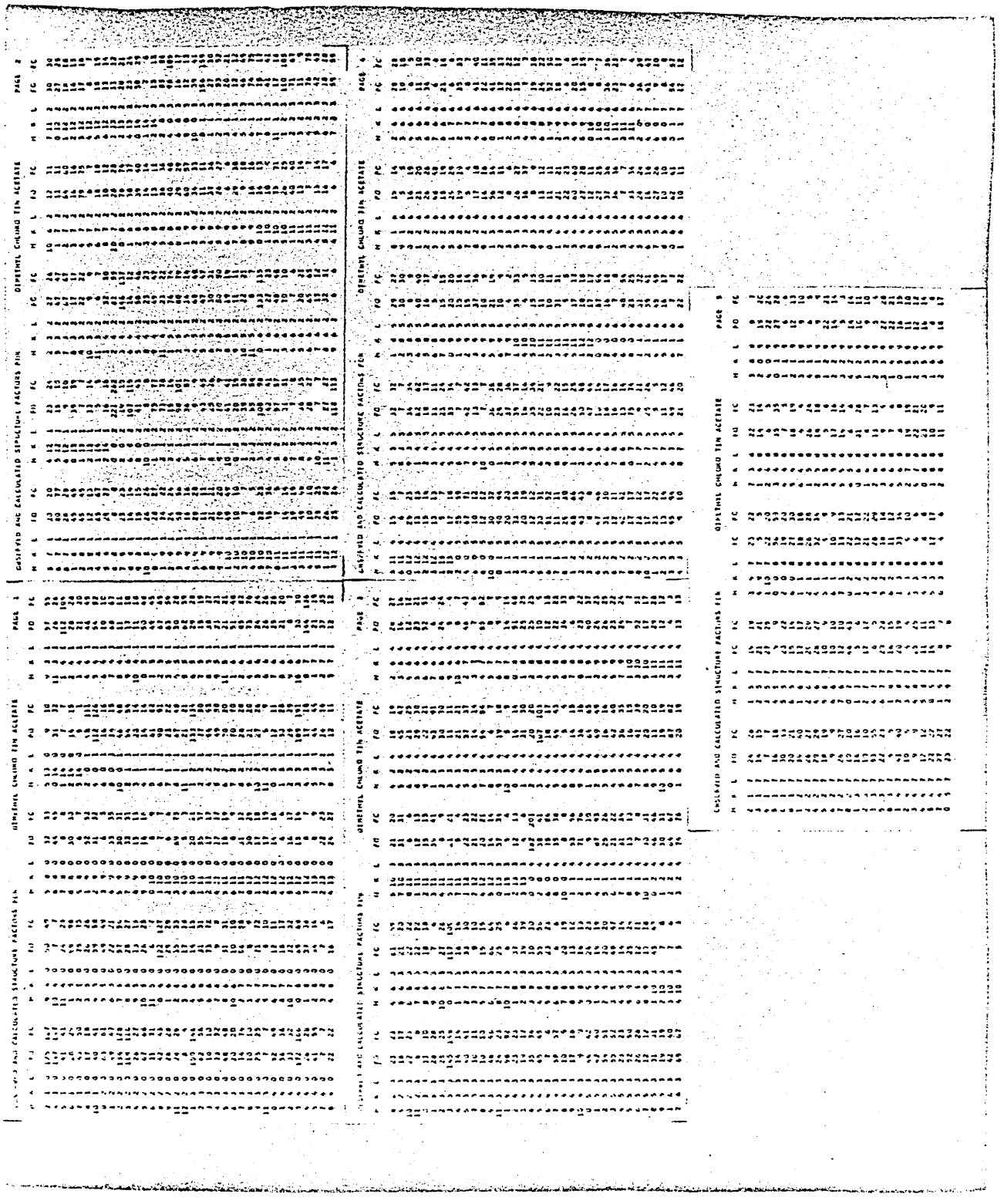

OF CYSTEINE AND HOMOCYSTEINE FROM ^{119}Sn MÖSSBAUER STUDIES.

Contents:

5.1 Introduction

Triorganotin compounds R_3SnX are reported to be biologically active due to the interaction of the R_3Sn moiety with certain proteins (82-86). Both sulphur (as in a thiol) and nitrogen (as in a histidine residue) atoms have been identified as important active binding sites to the R_3Sn moiety(87-89). Davies and Smith (1),in a review of organotin chemistry, report triphenyltin compounds to have a high fungicidal activity, trineophyl- and tricyclohexyltin compounds to be active against mites, and tributyltin compounds to inhibit oxidative phosphorylation. It is also suggested that the biological activity is dependent on the effectiveness of the interaction at the active site which involves co-ordination to an amino-acid. To investigate this interaction and determine the co-ordination about the tin atom a series of novel triorganotin derivatives of the sulph-hydryl- containing amino-acids, cysteine and homocysteine, $R_3SnS(CH_2)_nCH(NH_2)COOH$ (where n=1 or 2, and R= butyl, phenyl, neophyl, or cyclohexyl) have been prepared and studied by Mössbauer spectroscopy.

5.2. Results and Discussion

The Mössbauer data for the organotin derivatives of the type R_3Snx (where R = butyl, phenyl, neophyl, cyclohexyl, and X = cysteine, homocysteine) are given in Table 5.1. The quadrupole splittings for the compounds (ΔE_Q = 1.34 - 1.77 mms^{-1}) are typical of 4 - co-ordinate tin compounds containing tin-sulphur bonds.

A further indication of the co-ordination number of the tin atom is given by the value of the ratio (ρ) of the quadrupole splitting (ΔE_Q) to the isomer shift (δ). This ratio was defined by Herber (90) who suggested that for values of ρ in the range 0 — 1.9 the tin atom can be considered to be 4 - co-ordinate whereas for values greater than 2.1 the tin atom can be considered to be 5 - or 6 - co-ordinate. The values of ρ given in Table 5.1 are seen to be no greater than 1.4 and all the compounds can therefore be considered to be 4 - co-ordinate.

as broad guidelines to structure. On considering the structure of the cysteine and homocysteine ligands further co-ordination from either the amino- or carboxylic acid group is possible although steric crowding from the R-groups is likely to inhibit further association. Several 5-co-ordinate structures have been suggested, on the basis of infrared, N.M.R. and mass spectroscopic studies, for some organotin derivatives of L- cysteine and L- cysteine ethyl ester (85). Infrared data of the compounds listed in Table 5.1, however, give carbonyl stretching frequencies of 1630 cm^{-1} which have been reported (for trimethyltin glycinate (91)) as being indicative of non-co-ordinating carbonyl groups.

Further Maddock and Platt (92) used quadrupole splitting data empirically to discuss intermolecular association in organotin compounds. It was suggested that compounds of the type Ph_3SnX (ΔE_Q - 2.25 - 2.56 mms^{-1}) and $Neophyl_3SnX$ (ΔE_Q = 2.24 - 2.65 mms^{-1}) (X = CI, Br, I) are isostructural having tetrahedral geometry and that $(neophyl)_3Sn(OCOCH_3)$(ΔE_Q = 2.45 mms^{-1}) and $Ph_3Sn(OCOCH(CH_2\ CH_3)C_4H_9)$($\Delta E_Q$ = 2.26 mms^{-1}) are also tetrahedral. It was also suggested that the tetrahedral structures found for the trineophyl- and tripenyltin halides and carboxylates were due to possible steric crowding from the bulky phenyl and neophyl groups and thereby preventing intermolecular association via halid or carboxylate bridges.

The quadrupole splittings values given in Table 5.1 also suggest a steric interaction of the R group with cysteine and homocysteine ligands which result in changes in geometry around the tin nucleus. In general as the size of the R-group increases so the quadrupole splitting increases.

The isomer shift data in Table 5.1 reflects a typical trend for the electron- withdrawing effects of the R group on the tin nucleus. Since the isomer shift is a direct measure of the '<u>s</u>' - electron density around the tin nucleus then any observed changes in the isomer shift values must be a result of electron - releasing effects from the attached ligands. Table 5.2 gives the trend observed in the isomer shift for the

Table 5.1 Mössbauer data for triorganotin compounds R_3SnY at 80K.

Compound	Isomer Shift (mms^{-1})($\pm$0.02)	Quadrupole Splitting (mms^{-1})($\pm$0.02)	Full Width at Half Height (mms^{-1})	ρ values ($= \frac{\Delta E_Q}{\delta}$)
Triphenyltincysteinate	1.24	1.34	0.90	1.08
Tricylohexyltincysteinate	1.44	1.68	0.90	1.16
Trineophyltincysteinate	1.37	1.77	1.02	1.31
Tributyltinhomocysteinate	1.35	1.54	1.04	1.14
Triphenyltinhomocysteinate	1.28	1.48	1.22	1.15
Tricyclohexyltinhomocysteinate	1.45	1.63	1.05	1.12
Trineophyltinhomocysteinate	1.35	1.70	1.03	1.25

Table 5.2 Some trends in the Isomer Shift (mms^{-1}) for compounds of the type R_3SnY

R \ Y=	$-SCH_2CH_2CH(NH_2)COOH$	- Cl	- OH	-NCS	$-OCOCH_2CH_3$	$-OCO(CH_2)_{11}CH_3$
Phenyl	1.28	1.34	1.18	1.35	1.33	1.30
Neophyl	1.35	1.39	1.13	--	--	--
Butyl	1.35	1.46	1.36	1.60	1.46	1.40
Cyclohexyl	1.44	1.64	1.46	1.68	1.69	--

compounds $R_3Sn(SCH_2CH_2CH(NH_2)COOH)$ (where R= butyl, phenyl, neophyl, and cyclohexyl) and compares this trend with other values reported for compounds of the general formula R_3SnY (5). The isomer shift values for the compounds of general formula R_3SnY support the trend observed in Table 5.1 and are found to correlate with the expected electron-withdrawing properties of the R-groups in the order:

Phenyl > Neophyl ≥ Butyl > Cyclohexyl.

5.3 Conclusions

The organotin derivatives of cysteine and homocysteine are found to be 4- co-ordinate involving tin-sulphur bonds on the basis of Mössbauer and infrared data. The effects of the R-groups on the structures of the organotin compounds studied by Maddock and Platt support the suggestion that the size of the R group sterically influences the positioning of the ligands around the nucleus and prevents intermolecular association occurring.

The formation of the tin-sulphur linkage supports the suggestions (88) that sulphur acts as an important active site for binding the R_3Sn moiety. That no further association occurs via the amino- or carboxylic acid groups also suggests the sulphur to be a specific binding site in biological systems.

Finally, the trend observed in the isomer shift values is found to correlate with the electron- withdrawing properties of the R groups:

i.e. Phenyl > Neophyl ≥ Butyl > Cyclohexyl.

TEMPERATURE MÖSSBAUER DATA OF TWO BIS(TRIALKYLTIN) DERIVATIVES.

Contents:

The Mössbauer spectra of two trialkyltin compounds (3 - mercaptopropionato)bis(tributyltin) ($Bu_3SnSCH_2CH_2COOSnBu_3$) (1) and (3 - mercaptopropionato)bis(triphenyltin) ($Ph_3SnSCH_2CH_2COOSnPh_3$) (2) were recorded at 80K and for both compounds showed two resolved quadrupole doublets (figures 6.1 and 6.2). The inner and outer doublets are representative of the two tin atoms in (1) and (2) being in different electronic environments. In addition the spectra show the outer doublet to have a greater area under the absorption peak relative to the inner doublet implying that the tin atoms have different recoilless fractions.

Several workers(74,93-102) have reported a relationship between the recoilless fraction and the effective vibrating mass of the molecule using the Debye model of solids. On the basis of the initial Mössbauer observations at 80K which showed two distinct tin sites in both compounds it was decided to investigate the co-ordination at both sites and to relate the interpretation to the recoilless fraction at both sites using the model developed by Herber and Leahy. Mössbauer data were recorded over the ranges 20 - 140K (for R = butyl) and 80 - 200K (for R = phenyl).

6.2 Results and Discussion

Figure 6.1 (a - g) shows the variable temperature Mössbauer spectra over range 20 - 140K for the tributyltin compound (1). At a temperature of 20K the inner and outer doublets are seen to have approximately equal areas under the absorption peaks indicating the recoilless fractions to be the same for both tin sites. At higher temperatures up to 140K the area under the absorption peaks of the inner doublets are seen to diminish relative to those of the outer doublet. At 140K no appreciable absorption is observed due to the inner doublet suggesting that the recoilles fraction of the tin species giving rise to that absorption is reduced to a value approaching zero. The observation of an absorption curve at 140K which has a quadrupole splitting corresponding to the outer doublet suggests that one of the tin species still has

Figure 3.4 Sn Mössbauer spectrum of $Bu_3SnSCH_2CH_2COOSnBu_3$

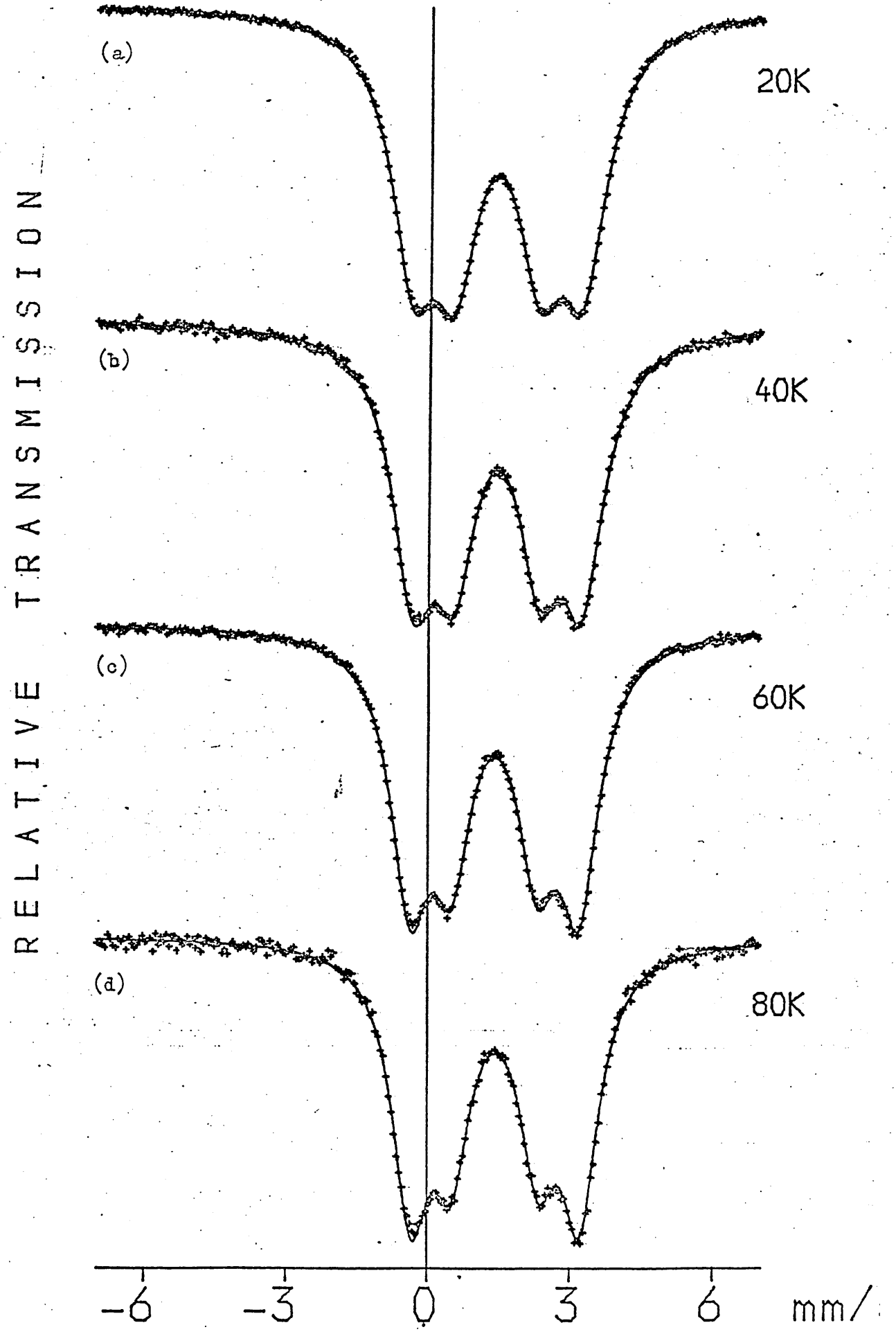

Figure 6.1 (e): T = 100K

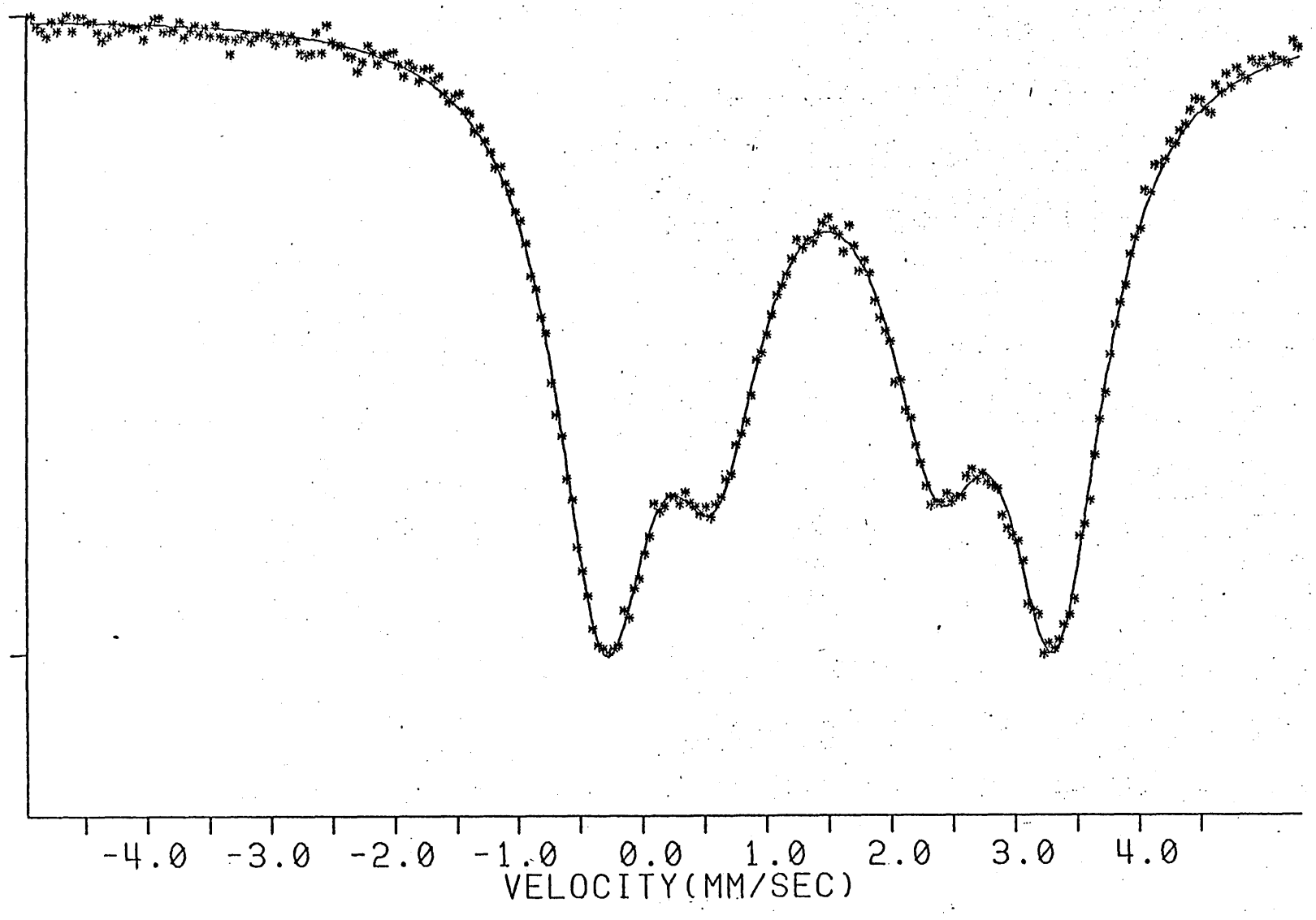

Figure 6.1 (f): T = 120K

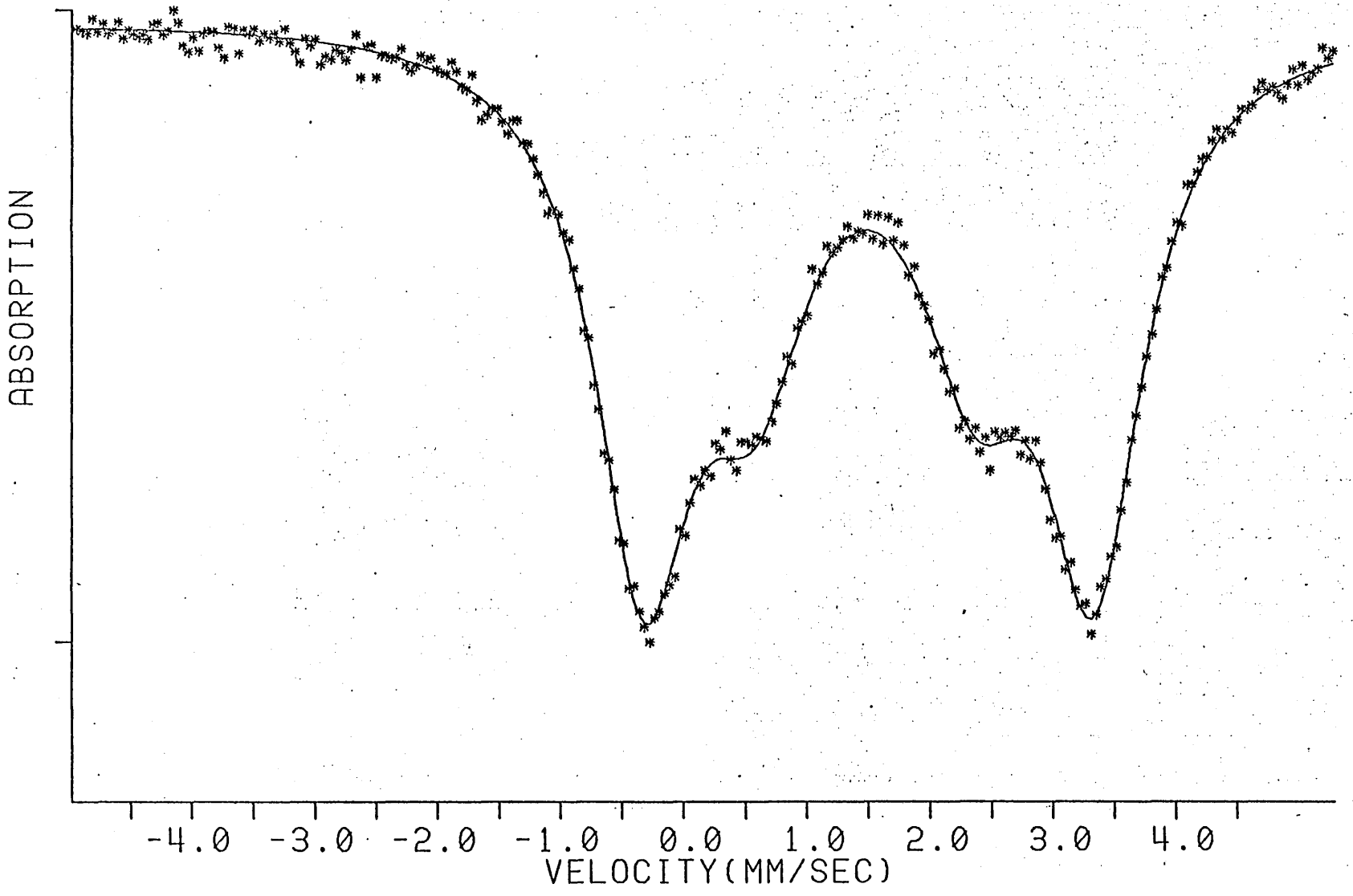

Figure 6.1 (g): T = 140K

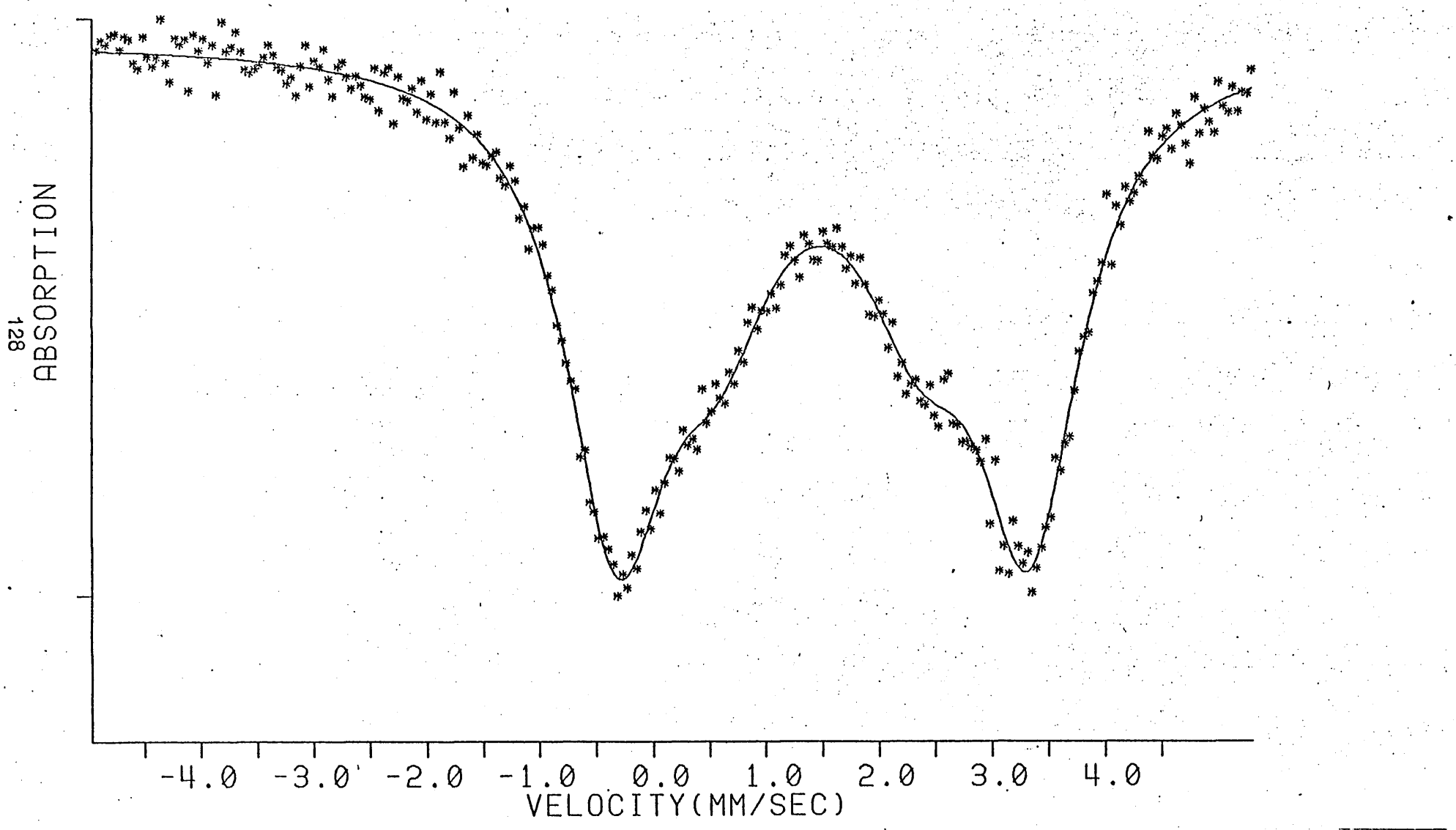

Table 6.1 ^{119}Sn variable temperature Mössbauer data for (3 - mercaptopropionato)bis(tributyltin) recorded over the range 20 - 140 K

Temperature (K)		Isomer Shift (±0.05)mms^{-1}	Quadrupole Splitting (±0.05)mms^{-1}	Intensity Ratio	Total Area	Ln Area	Individual Areas (A')	Ln A'
20	(1)	1.41	1.78	0.48	71.4	4.27	34.3	3.53
	(2)	1.42	3.59	0.52			37.1	3.61
40	(1)	1.44	1.80	0.47	59.1	4.08	27.7	3.32
	(2)	1.45	3.58	0.53			31.4	3.45
60	(1)	1.41	1.81	0.45	47.4	3.86	21.4	3.06
	(2)	1.42	3.58	0.55			26.0	3.26
80	(1)	1.43	1.82	0.43	35.8	3.58	15.5	2.74
	(2)	1.44	3.57	0.57			20.3	3.01
100	(1)	1.43	1.82	0.39	29.4	3.38	11.4	2.44
	(2)	1.46	3.63	0.61			17.9	2.89
120	(1)	1.43	1.68	0.34	24.0	3.18	8.18	2.10
	(2)	1.47	3.66	0.66			15.9	2.76
140	(1)	1.40	1.70	0.29	17.1	2.84	4.96	1.60
	(2)	1.47	3.66	0.71			12.1	2.50

(1) Corresponds to parameters for the tin - thiolate species.

(2) Corresponds to parameters for the tin - carboxylate species.

a significant recoilless fraction and therefore a higher co-ordination number.

Table 6.1 gives the Mössbauer data and the calculated areas under the absorption peaks over the temperature range 20 - 140 K for the tributyltin compound (1). The Mössbauer spectra were fitted to Lorentzian line shapes using Option 4 (section 2.3.2). The values for the individual areas were obtained by evaluating the expression:

$$\text{Area} = \Gamma_H \times \left(\frac{\text{Background counts - Counts at absorption peak}}{\text{Background Counts}} \right)_{\times 100}$$

for each absorption peak.

(Γ_H = Experimental full width of the absorption line at half height)

The quadrupole splitting for the outer doublet ($\Delta E_Q = 3.58 mms^{-1}$) is typical of a 5 co-ordinate tin species and compares with the Mössbauer data obtained by other workers for organotin carboxylates (56). The quadrupole splitting for the inner doublet ($\Delta E_Q = 1.80 mms^{-1}$) is typical of a 4 co-ordinate tin species and agrees with parameters reported for tetrahedral trialkyltin thiolates(87).

The Mössbauer results for the triphenyltin compound (2) obtained over a temperature range of 80 - 200 K show the same trend observed for the tributyltin compound. The results are given in Table 6.2 and the Mössbauer spectra recorded over the temperature range are shown in Figure 6.2 (a -f).

The observations from the Mössbauer data are further supported by the work of Barbieri et al (98) who report variable temperature Mössbauer data on the trimethyltin analog of compounds (1) and (2). A structure is also suggested on the basis of their results in which 4 co-ordinate tin-thiolate and intermolecularly associated 5 co-ordinate tin-carboxylate species are shown.

Figure 6.2 (a) ^{119}Sn Mössbauer Spectrum of $Ph_3SnSCH_2CH_2COOSnPh_3$

T = 80K

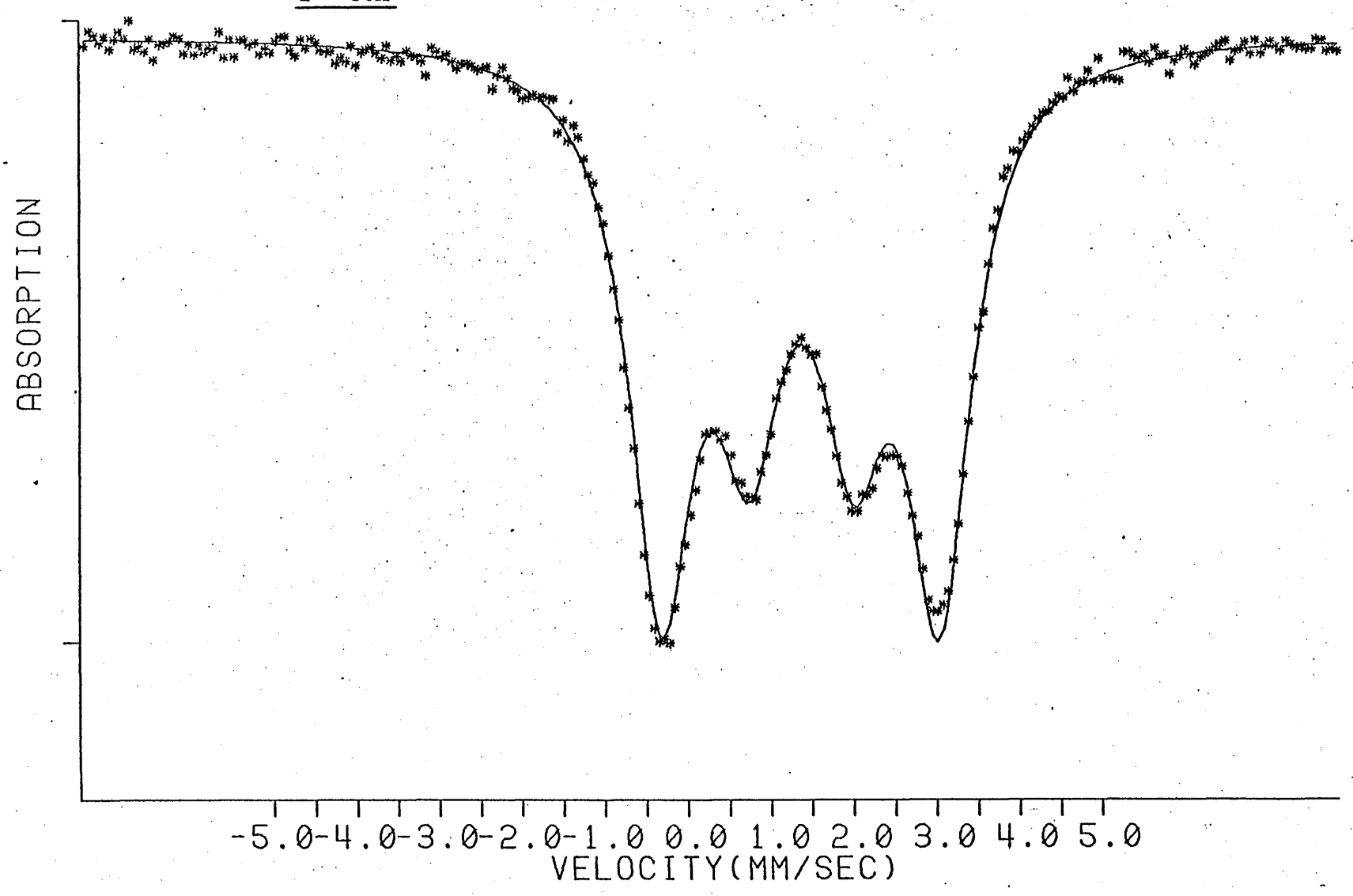

Figure 6.2 (b): T = 100K

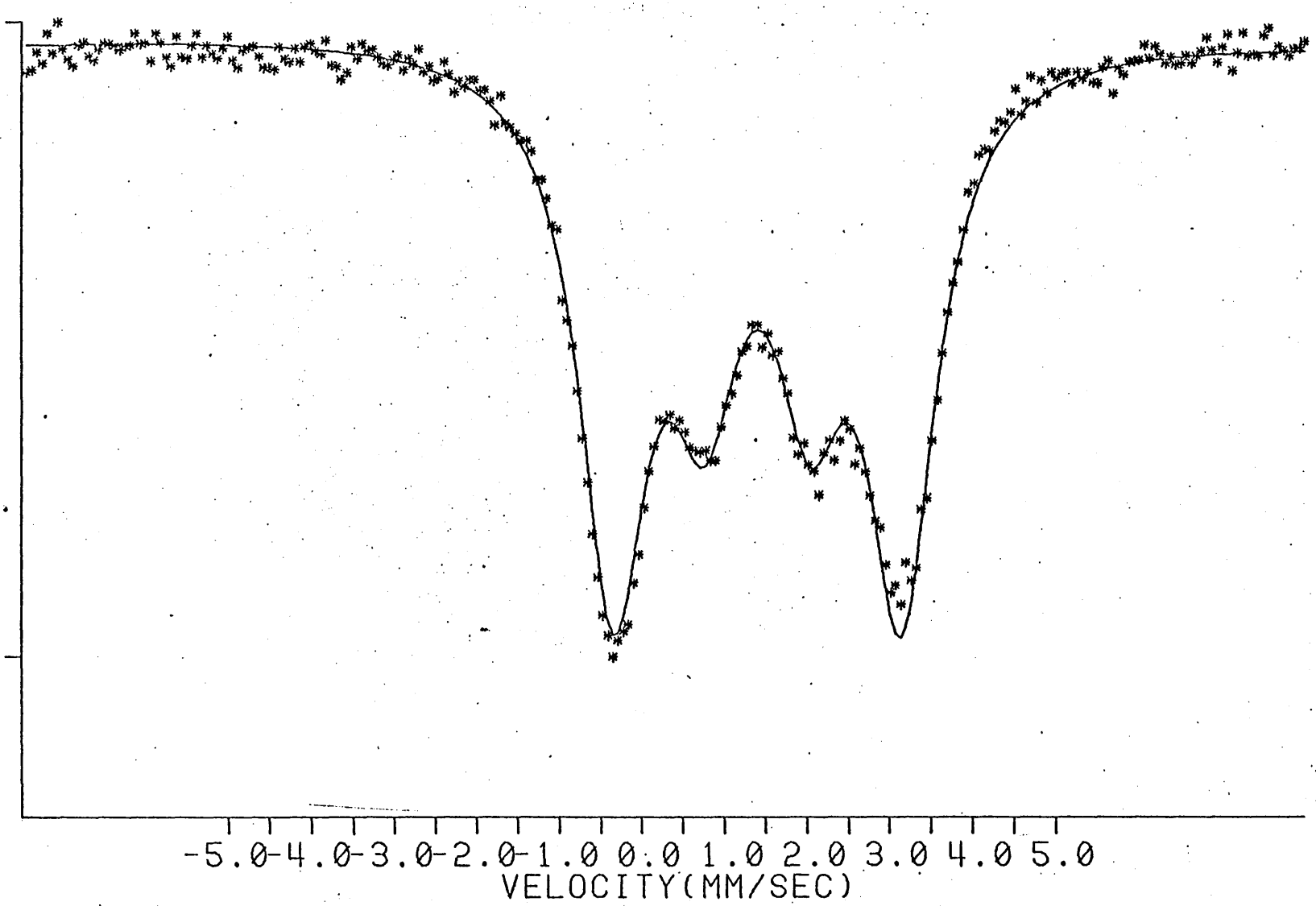

Figure 6.2 (c): T = 120K

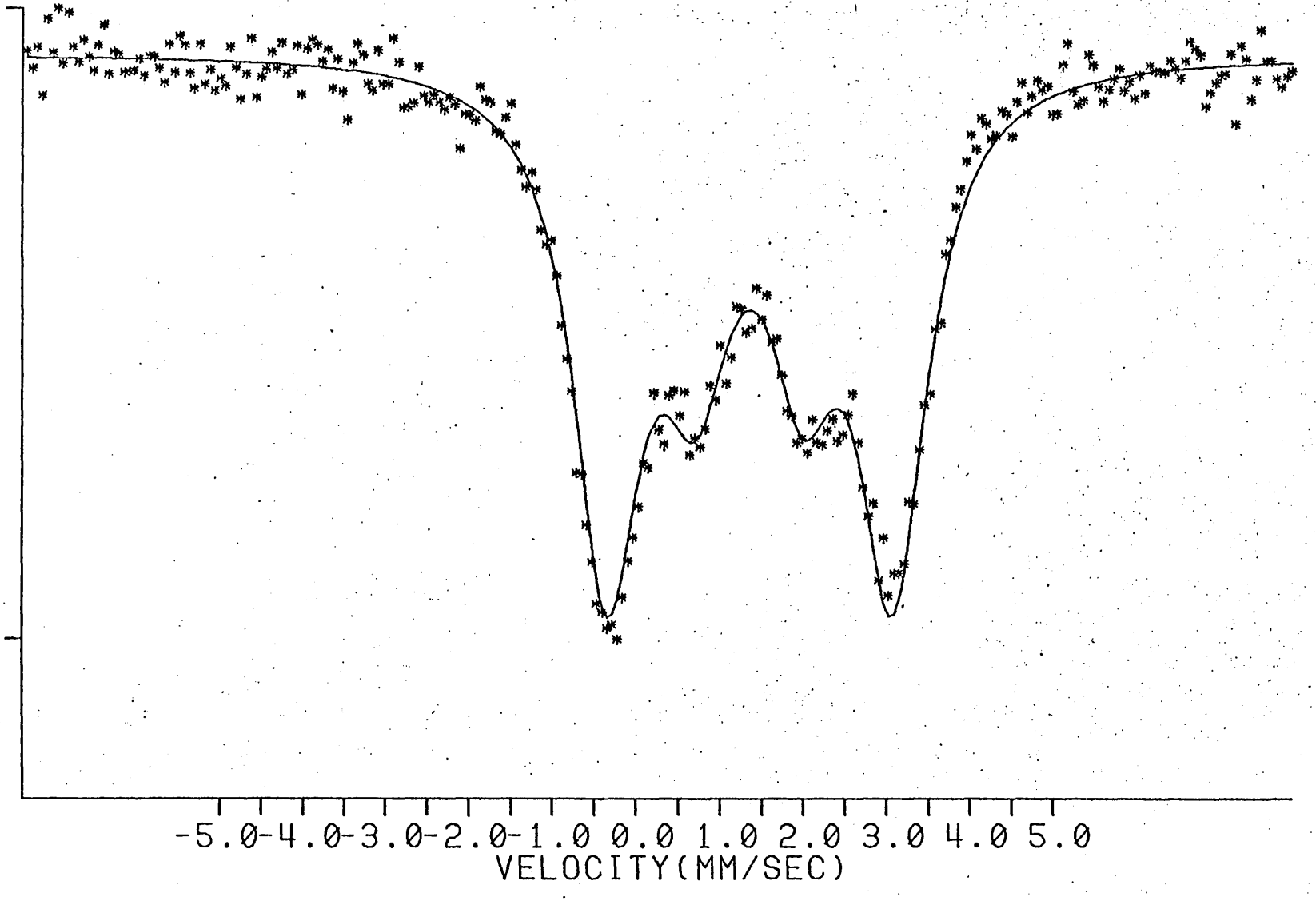

Figure 6.2 (d): T = 14.0K

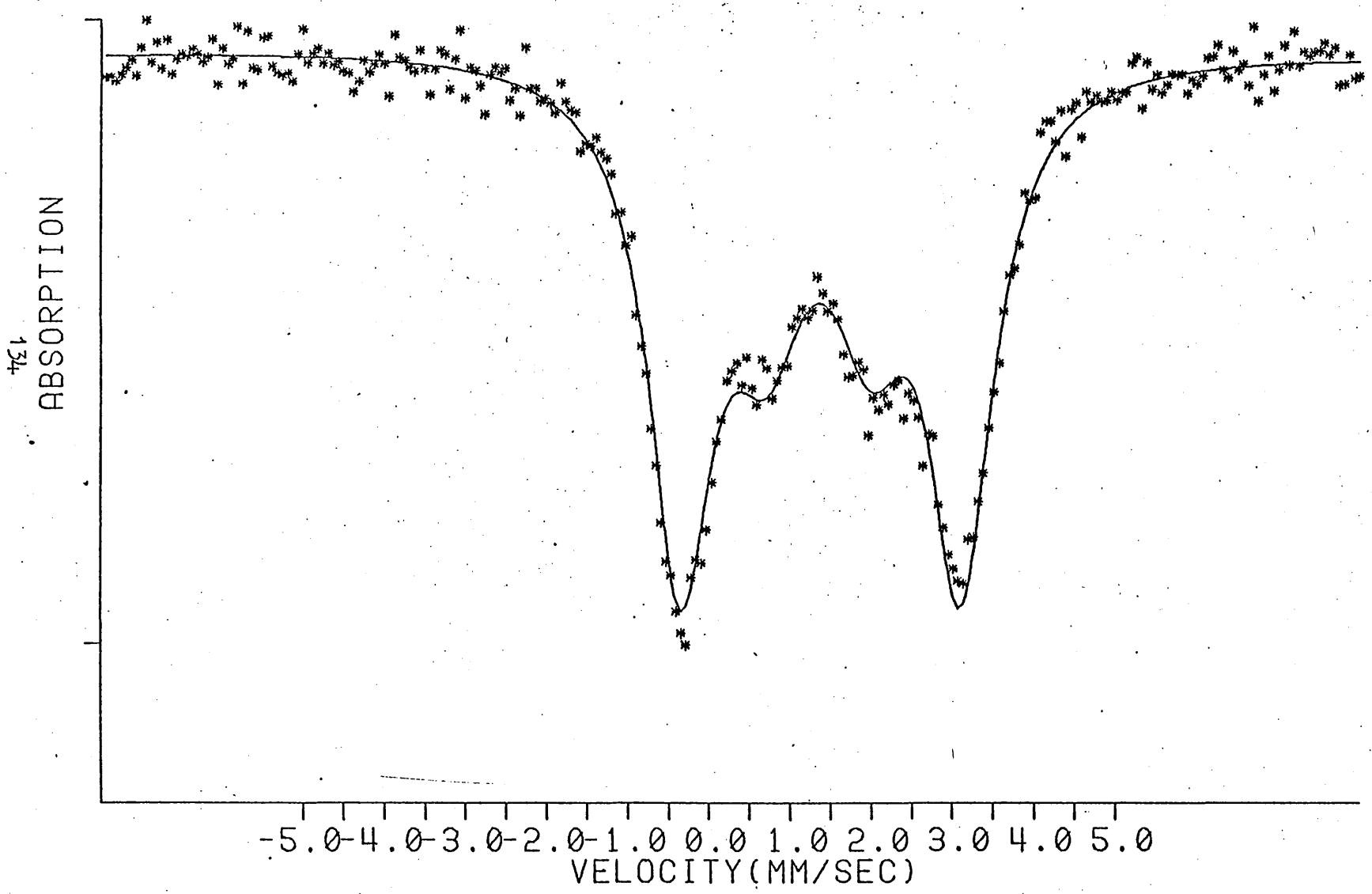

Figure 6.2 (e): T = 160K

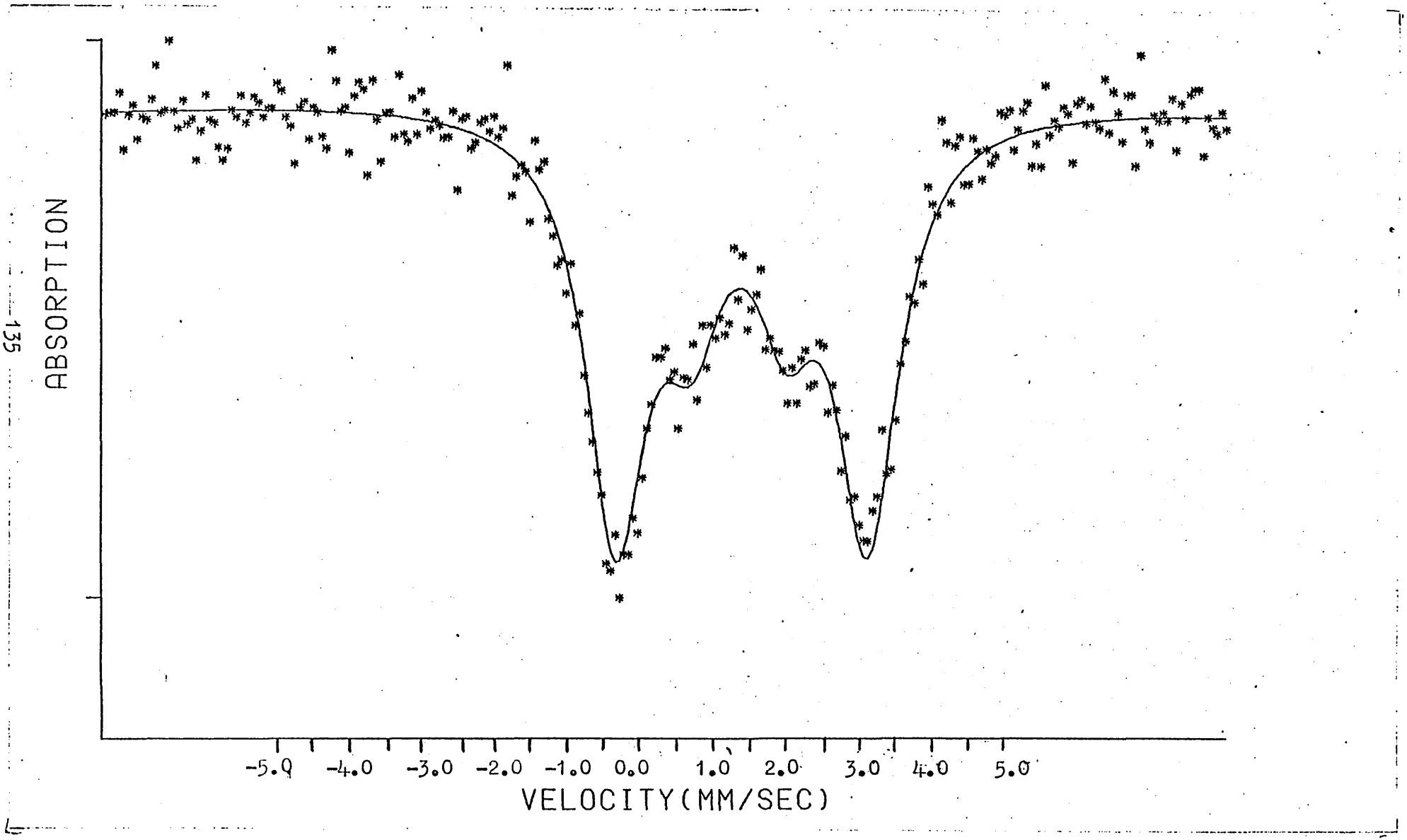

Figure 6.2 (f): T = 200K

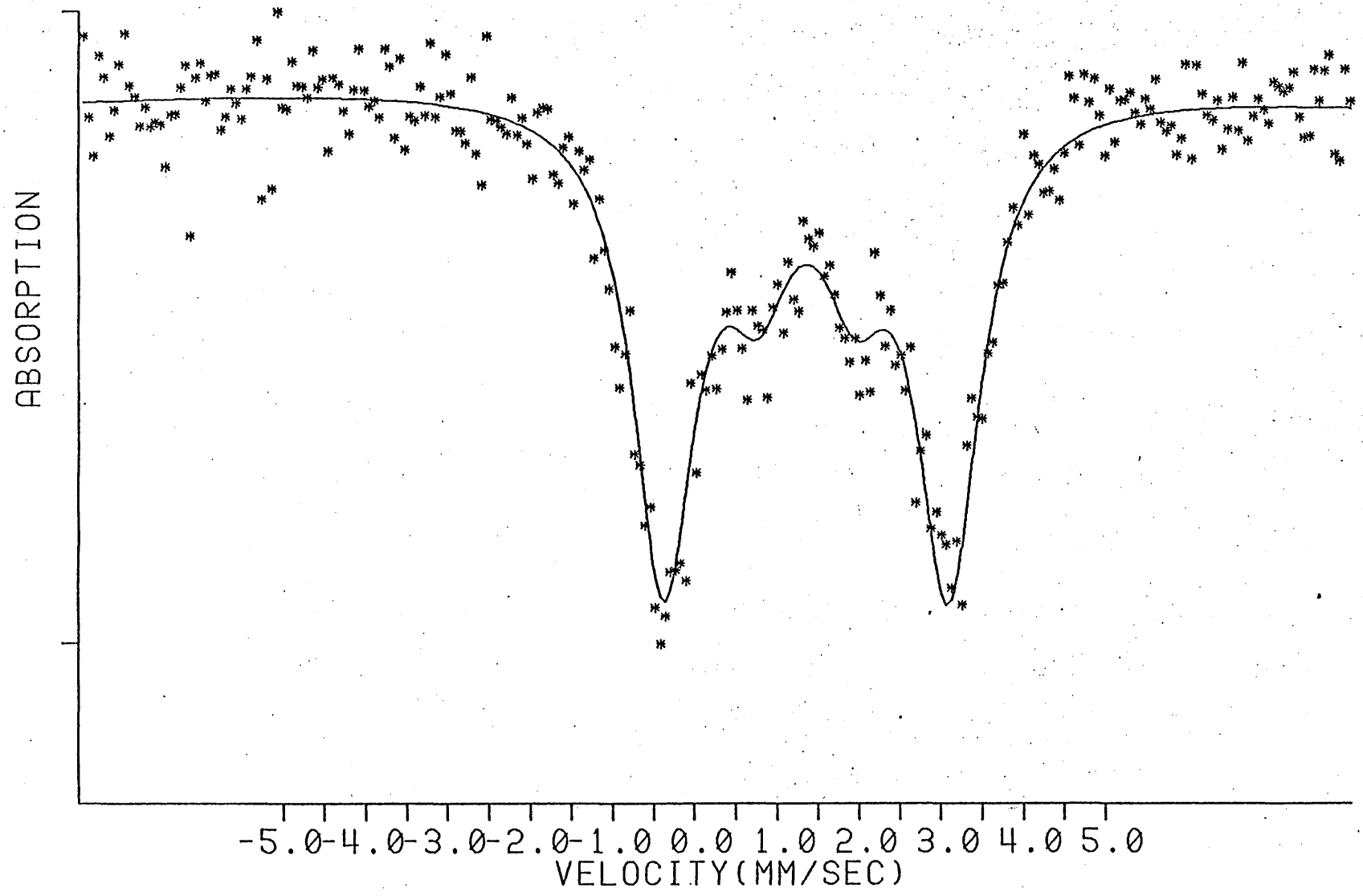

Table 6.2 ^{119}Sn variable temperature Mössbauer data for (3 - mercaptopropionato)bis(triphenyltin) recorded over the range 80 - 200 K

Temperature (K)		Isomer Shift $(\pm 0.05)mms^{-1}$	Quadrupole Splitting $(\pm 0.05)mms^{-1}$	Intensity Ratio	Total Area	Ln Area	Individual Areas (A')	Ln A'
80	(1)	1.35	1.32	0.39	277.1	5.62	111.6	4.71
	(2)	1.34	3.49	0.61			165.5	5.11
100	(1)	1.	1.29	0.36	169.7	5.13	63.6	4.15
	(2)	1.32	3.45	0.64			106.1	4.66
120	(1)	1.32	1.24	0.33	101.5	4.62	33.7	3.52
	(2)	1.32	3.45	0.67			67.8	4.22
140	(1)	1.30	1.29	0.33	77.0	4.34	27.8	3.32
	(2)	1.32	3.46	0.67			49.2	3.90
160	(1)	1.25	1.31	0.28	43.5	3.77	13.6	2.61
	(2)	1.31	3.45	0.72			29.9	3.40
180	(1)	1.28	1.25	0.25	25.9	3.25	7.6	2.03
	(2)	1.31	3.45	0.75			18.3	2.91
200	(1)	1.28	1.18	0.24	16.3	2.79	3.71	1.31
	(2)	1.30	3.48	0.76			12.6	2.53

(1) Corresponds to parameters for the tin - thiolate species.

(2) Corresponds to parameters for the tin - carboxylate species.

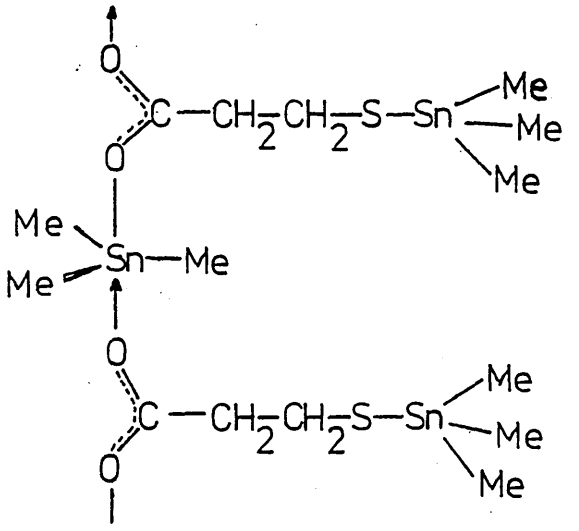

In the above structure two types of molecular association involving the tin atoms are evident. Hazony and Herber (103) report that acoustical and optical modes of vibration can be identified in the model of a molecular solid made up of monomeric molecular units in which the intermolecular bonding forces are weaker than the intramolecular bonding forces.

The mean displacement after the passage of a standing wave is dependent upon the effective vibrating mass and the magnitude of the inter - and intra - molecular force constants. It is not possible, however, to accurately identify the effective vibrating mass at the two tin sites, although on considering the above structure and the implications from the Mössbauer data it is reasonable to suggest that the two masses may be different. Consequently the optical and acoustical modes of vibration will also have different frequencies of vibration (104). Further it is evident that since the effective vibrating masses and the force constants at the two tin sites are different then the recoilless fractions ' f ' of the tin atoms will also be different.

6.2.1. The Effective Vibrating Mass Model

Herber and Leahy have reported a model which relates the temperature dependence of the recoilless fraction 'f' to the structure and bonding in organotin compounds (102). The recoilless fraction has been defined by the equation:

$$f = \exp\left[\frac{-4\pi^2 \cdot \langle \chi \rangle^2}{\lambda^2}\right]$$

However, since the lattice vibrations arise from thermal excitations in the solid, then application of the simple Debye model of the solid defines the temperature dependence of the recoilless fraction of the absorber, f_a, in the Debye - Waller relationship :

$$f_a = \exp\left\{-\frac{3}{2}\frac{E_R}{K\theta}\left[1 + 4\left(\frac{T}{\theta}\right)^2 \int_0^{\theta/T} \frac{x}{e^x - 1} \cdot dx\right]\right\} \qquad (6.1)$$

where: $E_R = \frac{E_\gamma^2}{2 M_{eff}}$ (M_{eff} is the effective recoilling mass)

and: $X = \frac{h\omega}{2\pi KT}$

At the high temperature limit i.e. $T \geq \theta/2$:

$$f_a = \exp\left\{-\frac{3}{2}\frac{E_R}{K\theta_m} + \frac{6E_R}{K\theta_m} \cdot T\right\} \qquad (6.2)$$

and hence $$\frac{df_a}{dT} = -\frac{6E_R}{K\theta_m^2} \qquad (6.3)$$

Since the area (A) under the absorption peaks is proportional to the recoilless fraction then it is more convenient to follow the temperature dependence of the area (A_T) under the resonance curve.

Since for small absorber thicknesses $A \propto t$ (11)

and $t = n \cdot f_a \cdot \sigma_o$ (section 2.2)

then $A_{(T)} \propto f_{a(T)}$

Therefore evaluating $\frac{d\ln A}{dT}$ will give a linear relationship with a gradient $= \frac{-6E_R}{K\theta_m^2}$ which, from (6.3), becomes:

$$\frac{d\ln A}{dT} = \frac{-3 \cdot E_\gamma}{M_{eff} \cdot C^2 \cdot K\theta_m^2} \qquad (6.4)$$

θ_m is a characteristic temperature which, for an ideal monatomic isotropic cubic solid, is equivalent to the Debye temperature, θ_D . Hence (6.4) becomes:

$$\frac{d\ln A}{dT} = \frac{-3 \cdot E}{M_{eff} \cdot C^2 \gamma \cdot K \cdot \theta_D^2} \qquad (6.5)$$

Hazony and Herber (103) further suggest that where there is a distinct separation between the inter - and intra - molecular vibrational modes, the dominant contribution to lnf (and hence lnA) is from the inter-molecular or acoustical vibrations since, in general, these will be excited at the lowest thermal excitation energies. However in most cases the distinction between the inter- and intra- molecular vibrations is not clear and it is not obvious which value to assign M_{eff} in (6.5). Consequently in applying the Debye approximation, which considers only the acoustical branches in a monatomic, isotropic solid, the value for M_{eff} is taken to be the relative molecular mass of the molecule, and will yield different Debye temperatures for the two tin sites.

Figures 6.3 and 6.4 show a linear change in lnA with temperature for both organotin compounds (1) and (2) respectively. The two slopes labelled (a) and (b) on the graphs represent the variation of the individual areas arising from the Mössbauer resonances of the two tin sites with temperature. Substituting for the gradients of the two lines in (6.5) produces a value for θ_D for the two tin sites. In addition, equation (6.5) also yields a more significant value for the term $M_{eff}\theta_D^2$, which is a measure of the intermolecular bonding strengthsat the two tin sites. Table 6.3 summarises the data from the two graphs and gives values for θ_D and $M_{eff}\theta_D^2$ obtained for the two tin sites in the tributyl- and triphenyl- tin compounds.

6.2.2 Evaluation of θ_D for (3-mercaptopropionato)bis(tributyltin).

From figure 6.3: $G_1 = -0.9 \times 10^{-2}$

$G_2 = -1.3 \times 10^{-2}$

where G_1 and G_2 are the gradients of the slopes representing the areas

Figure 6.3 Temperature Dependence of the Areas under the Inner and Outer pair of Resonance Maxima of $Bu_3SnSCH_2CH_2COOSnBu_3$

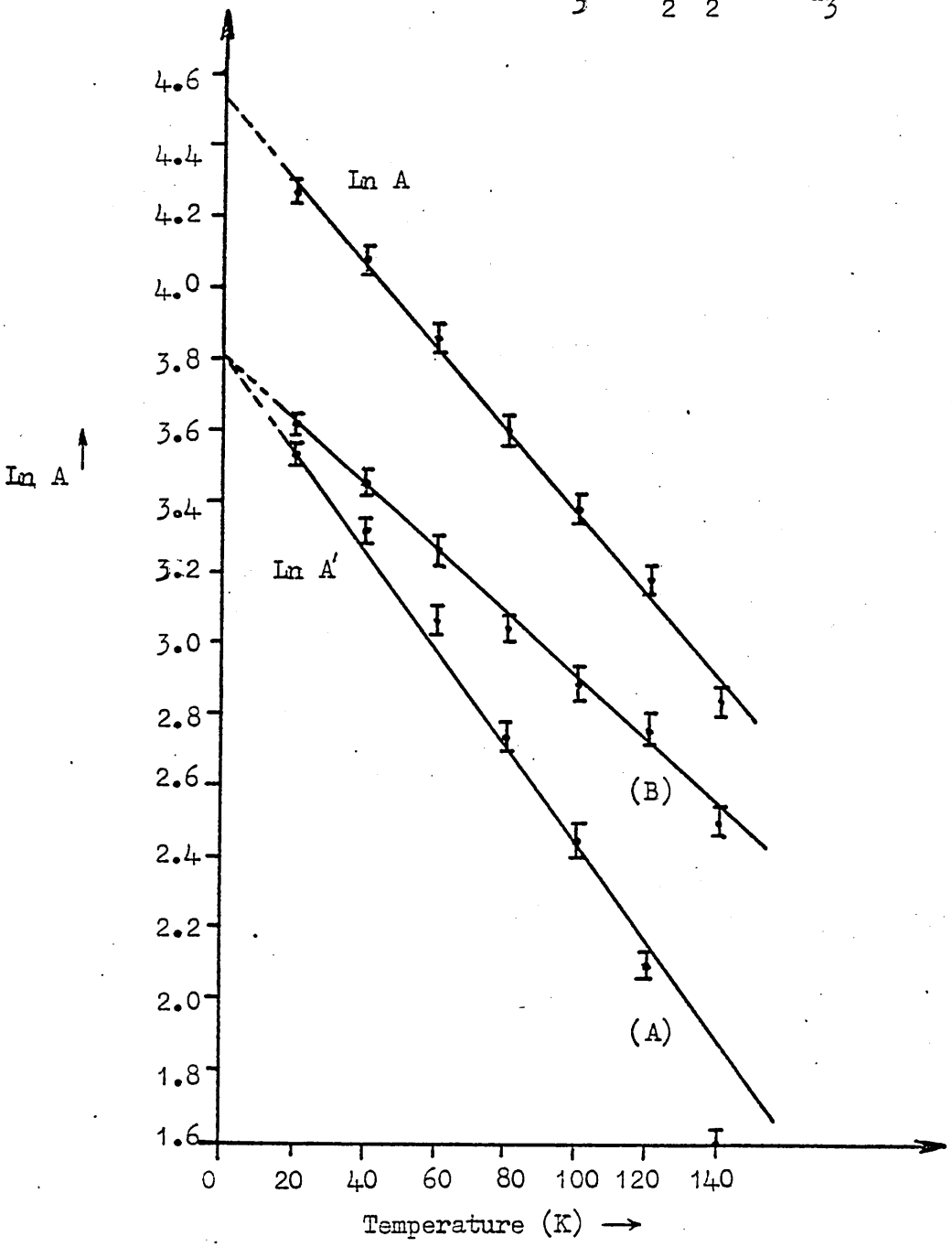

Ln A is the TOTAL Lorentzian area under the resonance peaks.

Ln A' represents the temperature dependence of the individual areas due to the Inner (A) and Outer (B) resonance peaks.

Figure 6.4 Temperature Dependence of the Areas under the Inner and Outer pair of Resonance Maxima of $Ph_3SnSCH_2CH_2COOSnPh_3$

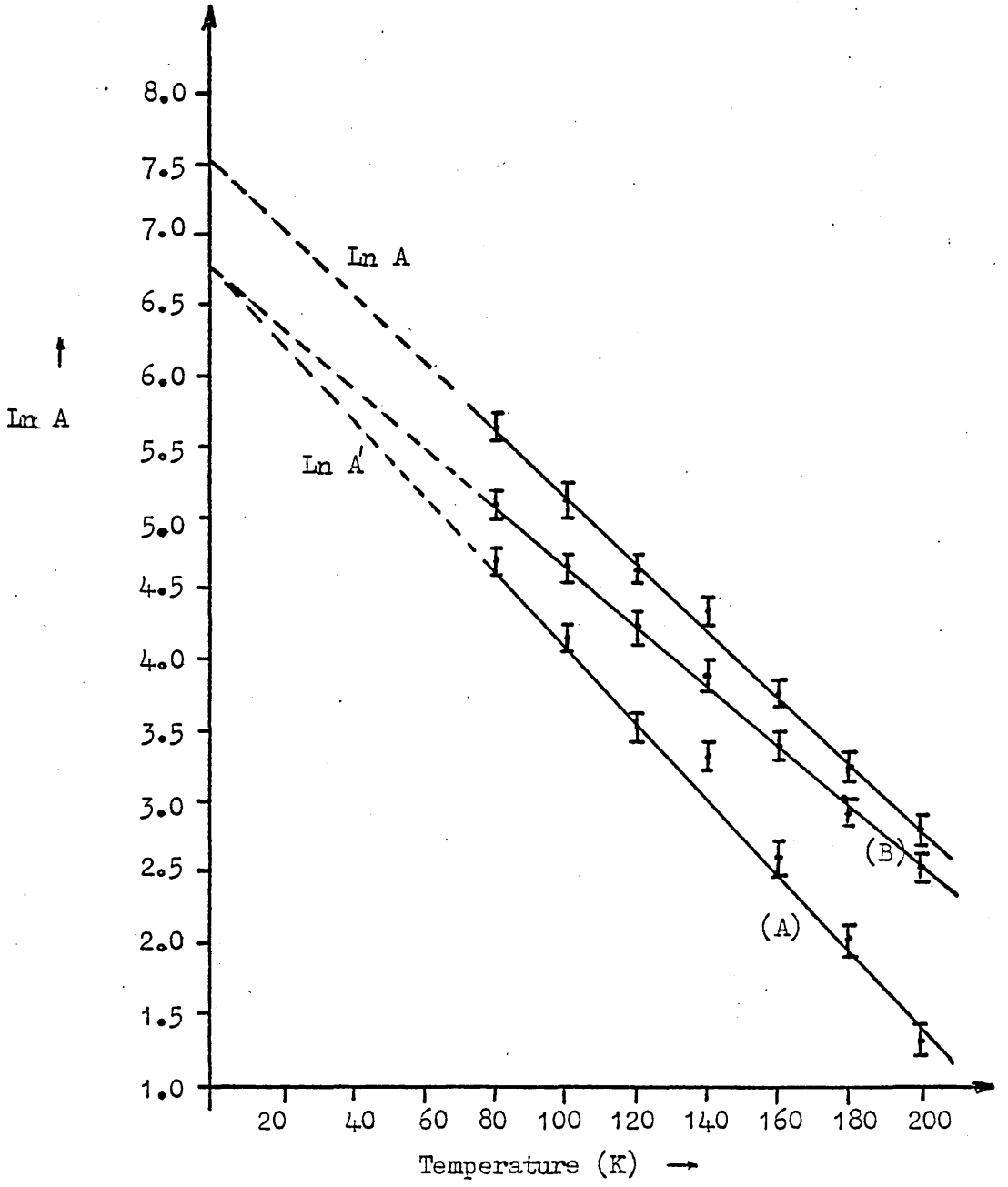

Ln A is the TOTAL Lorentzian area under the resonance peaks.

Ln A' represents the temperature dependence of the individual areas due to the Inner (A) and Outer (B) resonance peaks.

Table 6.3 Mössbauer and Lattice Dynamics parameters for (3 - mercaptopropionato)bis(tributyl - and triphenyltin)

Compound	$\frac{d \ln A}{dT}$	$M_{eff}\theta_D^2$ amu.deg^2	θ_D (K)
(3- mercaptopropionato)-bis(tributyltin)	(1) - 0.9×10^{-2}	2.388×10^6	59.1
	(2) - 1.3×10^{-2}	1.653×10^6	49.1
(3- mercaptopropionato)-bis(triphenyltin)	(1) - 2.125×10^{-2}	1.011×10^6	35.5
	(2) - 2.653×10^{-2}	0.810×10^6	31.7

(1) Corresponds to the data for the inner quadrupole doublet.

(2) Corresponds to the data for the outer quadrupole doublet.

under the Mössbauer resonances for the tin-carboxylate and tin-thiolate sites respectively.

M_{eff} for (3-mercaptopropionato)bis(tributyltin) = 684

$K = 1.381 \times 10^{-23}\ JK^{-1}$

Substituting in (6.5) gives:

$$\text{for } G_1: \quad -0.9 \times 10^{-2} = \frac{-3 \times (24 \times 10^3) \times 1.6 \times 10^{-19}}{931.5 \times 10^6 \times 1.381 \times 10^{-23} \times 684 \times \theta_D^2}$$

Rearranging gives:

$$\theta_D^2 = \frac{-2.76 \times 10^{-10}}{-7.92 \times 10^{-14}}$$

$$\underline{\theta_D = 59.1\ K}$$

$$\text{Similarily for } G_2: \quad -1.3 \times 10^{-2} = \frac{-3 \times (24 \times 10^3) \times 1.6 \times 10^{-19}}{931.5 \times 10^6 \times 1.381 \times 10^{-23} \times 684 \times \theta_D^2}$$

Rearranging gives: $\underline{\theta_D = 49.1\ K}$

The calculated Debye temperatures of the two tin sites in both compounds given in Table 6.3 show similar behaviour. In both cases the tin-carboxylate species are seen to have the larger θ_D values which further supports the suggestion that these tin atoms have the higher co-ordination.

Further since the term $M_{eff}\theta_D^2$ represents the intermolecular force constant parameter, then the larger values obtained for the tin-thiolate units imply stronger bonding forces between the atoms.

It should be noted, however, that the above implications can only be taken as approximations for the following reasons:

(i) in applying the Debye model the value used for M_{eff} was the total molecular mass since the effective vibrating mass of the two tin sites cannot be accurately defined.

(ii) the Debye model is also limited in its application since only acoustical modes of vibration are considered.

6.3 Conclusions

Variable temperature Mössbauer data have identified two tin sites having different co-ordination numbers in both the trialkyltin compounds studied. In both cases a 4 co-ordinate tin-thiolate species and a 5 co-ordinate tin-carboxylate species are identified. On the basis of a recently reported study (98) it is suggested that the tin-carboxylate species forms an intermolecularly associated chain with other tin-carboxylate units.

Application of a simple Debye model of the solid to the variable temperature Mössbauer data confirms a linear temperature dependence of the recoilless fraction over the ranges 20 - 140 K (for R = butyl) and 80 - 200 K (for R = phenyl). Two different Debye temperatures are obtained for both compounds suggesting two different modes of vibration and further supports the suggestion that the two tin sites have different co-ordination numbers and different recoilless fractions.

REFERENCES

1. A.G. Davies and P.J. Smith, Adv. Inorg and Radiochem., (1980), 23 , 1.

2. P.B. Moon, Proc. Phys. Rev., (1951), 105, 124.

3. R.L. Mössbauer, Z. Physik., (1958), 151, 124.

4. G. Breit and E. Wigner, Phys. Rev., (1936), 49, 519.

5. N.N. Greenwood and T.C. Gibb, 'Mössbauer Spectroscopy' (1971), Chapman and Hall.

6. A.J. Boyle and H.E. Hall, Rep. Proc. Phys., (1962), 25, 141.

7. C. Hohenemser, Phys. Rev., (1965), A-185, 139.

8. G.M. Bancroft, Mössbauer Spectroscopy, (1973), McGraw-Hill.

9. G.K. Shenoy and F.E. Wagner, Mössbauer Isomer Shifts, (1978), North-Holland.

10. J.G. Stevens and V.E. Stevens, Mössbauer Effect Data Index, (1975).

11. J.M. Williams and J.S. Brooks, Nucl. Instr. Meth., (1975), 128, 363.

12. W.J. Price, Nuclear Radiation Detection, 1972, McGraw-Hill.

13. G. Lang and B.W. Dale, Nucl. Instr. Meth., (1974), 116, 567.

14. R. Formstone, M. Phil./Ph.D. Transfer Report, (1976), Sheffield City Polytechnic.

15. V.I. Goldanskii and L.A. Korytko, Applications of Mössbauer Spectroscopy, ed. R.L. Cohen, (1980), 1, 287.

16. Polymer Science and Technology, (1964-72), 12, 725.

17. A.H. Frye, R.W. Horst and M.A. Paliobagis, J. Polym. Sci., (1964), A-2, 1765.

18. J. Stepek and C. Jirkal, Chem. Listy., (1965), 59, 1, 1201.

19. C.H. Fuschman, Stabilisation of Polymers and Stabilisation Processes, (1967), 20.

20. G. Ayrey, R.C. Poller and I.H. Siddiqui, J. Polym. Sci., A-1, (1972), 10, 725.

21. S.Z. Abbas and R.C. Poller, Polym. Lett., (1974), 15, 543.

22. G. Geuskens, Degradation and Stabilisation of Polymers, (1975), 1, 1,(App. Science Ltd.)

23. G. Scott, Developments in Polymer Stabilisation, (1980), 2, 1,(App. Science Ltd.)

24. J. Wypych, Die Angew. Makromol. Chemie., (1975), 48, 1.

25. C.I. Balcombe, Elwood E.C. McMullin and M.E. Peach, J. Inorg. Nucl. Chem., (1975), 37, 1353.

26. H.O. Wirth and H. Andreas, Pure and Appl. Chem., (1977), 49, 627.

27. D. Lanigan and E.L. Weinberg, Adv. Chem. Ser., (1976), 157, 134.

28. D. Lanigan, Proc. Int. Conf. PVC Processing, (1978), 4, 1.

29. G. Scott, M. Tahan and J. Vyvoda, Eur. Polym. J., (1978), 14, 377.

30. W.H. Starnes, Adv. Chem. Ser., (1978), 169, 309.

31. N.D. Ghatge, Kautsch. Gummi Kunstst., (1979), 32, 254.

32. B.B. Cooray and G. Scott, Polym. Deg. and Stab., (1980), 2, 35.

33. B.B. Cooray and G. Scott, Eur. Polym. J., (1972), 16, 169.

34. F. Alavi-Moghadam, G. Ayrey and R.C. Poller, Polymer, (1975), 16, 833.

35. V. Bellinger, J. Verdu and L.B. Caurette, Polym. Deg. and Stab., (1980), 3, 3.

36. M. Lequan, Y. Besace and R.C. Poller, Eur. Polym. J., (1980, 47, 141.

37. A.A. Caraculacu, E.C. Bezdadea and G. Istrate, J. Polym. Sci. A-1, (1970), 8, 1246.

38. K. Figge and W. Findeis, Angew. Makromol. Chemie., (1975), 47, 141.

39. J.W. Burley, R.E. Hutton and V. Oakes, J. Organometal Chem., (1978), 156, 369.

40. J.W. Burley, P. Hope, R.E. Hutton and C. Groenenboom, J. Organometal Chem., (1979), 170, 21.

41. P. Klemchuk, Adv. Chem. Ser., (1968), 85, 1.

42. G. Ayrey, R.C. Poller and I.H. Siddiqui, Polym. Lett., (1970), 8, 1.

43. C.H. Stapfer and J.D. Grannick, J. Polym. Sci., A-1, (1971), 9, 2625.

44. R.C. Poller, Adv. Chem. Ser., (1976), 157, 177.

45. R.C. Poller, J. Macromol Sci. - Chem., A12(3), (1978), 373.

46. G. Ayrey, F.P. Man, and R.C. Poller, J. Organometal Chem., (1979), 173, 171.

47. P.G. Harrison, T.J. King and M.A. Healy, J. Organometal Chem., (1979), 182, 17.

48. M. Mellor, Private Communication.

49. R.G. Parker and C.J. Carman, Adv. Chem. Ser., (1978), 169, 363.

50. B.B. Troitskii, L.S. Troitskaya, V.N. Denisova, M.A. Novikova and Z. Bluzinov, Eur. Polym. J., (1977), 13, 1033.

51. G.A. Rasuvaev, L.S. Troitskaya and B.B. Troitskii, J. Polym. Sci. A-1, (1971), 9, 2673.

52. C.H. Stapfer and R.H. Herber, J. Organometal. Chem., (1974), 66, 425.

53. R.E. Hutton and J.W. Burley, J. Organometal. Chem., (1976), 105, 61.

54. G.M. Bancroft and T.K. Sham, Can. J. Chem., (1972), 54, 1361.

55. B.W. Fitzsimmons, N.J. Seeley and A.W. Smith, J. Chem. Soc. (A), (1969), 143.

56. W.D. Honnick and J.J. Zuckerman, J. Organometal. Chem., (1979), 178, 133.

57. A.D. Cohen and C.R. Dillard, J. Organometal. Chem., (1970), 25, 421.

58. G. Geuskens, Degradation and Stabilisation of Polymers, (1975), 1, 23, App. Sci. Ltd.

59. G. Scott, Developments in Polymer Stabilisation, (1979), 1, 261, App. Sci. Ltd.

60. J.F. Rabek and B. Ranby, Photodegradation, Photo-oxidation and Photostabilisation of Polymers, (1975), J. Wiley & Sons Ltd.

61. J.F. Rabek, G. Canback and B. Ranby, J. App. Polym. Sci., (1977), 21, 2211.

62. W.H. Gibb and J.R. MacCallum, Eur. Polym. J., (1971), 7, 1231.

63. W.H. Gibb and J.R. MacCallum, Eur. Polym. J., (1974), 10, 529.

64. R.B. Fox, Pure Appl. Chem., (1972), 30, 81.

65. I. Lukac, P. Hrdlovic, Z. Manasek, D. Bellus, J. Polym. Sci. A-1, (1971), 9, 69.

66. H.S. Cheng, and R.H. Herber, Inorg. Chem., (1971), 10, 1315

67. A.G. Davies, H.J. Milledge, D.C. Puxley and P.J. Smith, J. Chem. Soc. (A), (1970), 2862.

68. N.W. Alcock and J.R. Sawyer, J. Chem. Doc. Dalton Trans., (1977) 1040.

69. G.M. Bancroft, V.G. Kumar Das, T.K. Sham and M.G. Clark, J. Chem. Soc. Dalton Trans., (1976), 643.

70. G.M. Bancroft and R.H. Platt, Adv. Inorg. Radiochem., (1972), 15, 59.

71. J. Donaldson, P.J. Smith and P.A. Cusack, Inorg. Chim. Acta., (1980), 46, L73.

72. S. Sylvester, S. Caldwell, G.J. Chertoff and G.B. Curtis, U.S. Patent, 2,629,700 (1953).

73. H.A. Stockler, H. Sano, and R.H. Herber, J. Chem. Phys., (1967), 47, 1561.

74. R.C. Poller, J.N.R. Ruddick, B. Taylor and D.L.B. Toley, J. Organometal. Chem., (1970), 24, 341.

75. G.M. Bancroft, K.D. Butler, and T.K. Sham, J. Chem. Soc. Dalton Trans., (1975), 1483.

76. R. Okawara, D.E. Webster, and E.G. Roechow, J. Amer. Chem. Soc., (1960), 82, 3289.

77. International Tables for X-ray Crystallography, Vol IV, (1974), Table 2.2B, Kynoch Press, Birmingham.

78. H. Chim and B.R. Penfold, J. Cryst. Mol. Struct., (1973), 3, 285.

79. W.W. Alcock and V.L. Tracey, Acta. Cryst. B., (1979), 35, 80.

80. R. Faggioni, J.P. Johnson, L.D. Brown and T. Birchall Acta. Cryst. B., (1978), 34, 3742.

81. G.A. Miller and E.O. Schlemper, Inorg. Chem., (1973), 12, 677.

82. L. Smith and P.J. Smith, Chem. Brit., (1975), 11, 208.

83. W.T. Hall and J.J. Zuckerman, Inorg. Chem., (1977), 16, 1239.

84. G. Domazetis, R.J. Magee and B.D. James, Inorg. Chim. Acta., (1979), 32, L48.

85. G. Domazetis, R.J. Magee and B.D. James, J. Organo-metal. Chem., (1978), 162, 329.

86. G. Domazetis, R.J. Magee, B.D. James and J.D. Cashion, J. Inorg. Nucl. Chem., (1981), 43, 1351.

87. R.C. Poller and J.N.R. Ruddick, J. Chem. Soc. (Dalton Trans.), (1973), 60, 87.

88. B.G. Farrow, and A.P. Dawson, Eur. J. Biochem., (1978), 86, 85.

89. B.M. Elliot and W.N. Aldridge, Biochem. J., (1977), 163, 583.

90. R.H. Herber, H.A. Stockler, and W.T. Reichle, J. Chem. Phys., (1965), 42, 2447.

91. B.Y.K. Ho and J.J. Zuckerman, Inorg. Chem., (1973), 12, 1552.

92. A.G. Maddock and R.H. Platt, J. Chem. Soc. (A), (1971), 1191.

93. H.A. Stockler, H. Sano and R.H. Herber, J. Chem. Phys., (1967), 47, 1567.

94. R.H. Herber, S. Chandra and Y. Hazony, J. Chem. Phys., (1970), 53, 3330.

95. C-D Hager, F. Huber, A. Silvestri, and R. Barbieri, Inorg. Chem. Acta., (1981), 49, 31.

96. A. Silvestri, E. Rivarola and R. Barbieri, Inorg. Chem. Acta., (1977), 23, 144.

97. A. Silvestri, E. Rivarola and R. Barbieri, Inorg. Chem. Acta., (1978), 28, 223.

98. R. Barbieri, A. Silvestri, L Pellerito, A. Gerviaro, M. Petrera, and N. Burriesci, J. Chem. Soc. Dalton Trans., (1980), 1983.

99. K.C. Molloy, J.J. Zuckerman, H. Schuman and G. Rodewald, Inorg. Chem., (1980), 19, 1089.

100. P.G. Harrison, M.G. Begley and K.C. Molloy, J. Organometal. Chem., (1980), 186, 213.

101. B.Y.K. Ho, K.C. Molloy, J.J. Zuckerman, F. Reidinger and J.A. Rubieta, J. Organometal. Chem. (1980), 187, 213.

102. R.H. Herber and M.F. Leaky, Adv. Chem. Ser., (1976), 157, 134.

103. Y. Hazony and R.H. Herber, J. Chem. Phys., (1972), 107.

104. C. Kittel, Introduction to Solid State Physics, (1966), J. Wiley & Sons Ltd.

Acknowledgements

The author has pleasure in extending his appreciation and sincere gratitude to his two supervisors Dr. J.S.Brooks and Dr. D.W.Allen for their interest, encouragement, patience, and practical help while working on the topics included in this thesis.

Further, the author would like to acknowledge the two collaborating establishments: the International Tin Research Institute, and in particular his external supervisor, Dr. P.J.Smith, for allowing the author to spend a period of 10 weeks at the Institute to develop the practical aspects of his research, and for the many helpful discussions with the author; and Lankro Chemicals Ltd., in particular Mr. A.G. Williamson and Dr. M.T.J.Mellor for their initial interest, supply of chemicals, and many helpful discussions concerning polymer chemistry.

The author also has pleasure in expressing his thanks to Dr. I.W.Nowell of the Chemistry Department at Sheffield City Polytechnic for his help, expertise, and patience during the Crystallographic determination in this thesis.

Finally, the author wishes to extend his gratitude to all those who have shown an interest and given help during the author's research, in particular: the Chemistry Department at the International Tin Research Institute; Dr. G.C.Corfield; Dr. D.Clegg; Dr. M.Goldstein; technician R.Smith; and typist Miss Ann Hughes.

Appendix 1: Courses Attended

1. Introduction to Mössbauer Spectroscopy, 6 x 1 hour Lectures, October, 1978.
2. BASIC and Further BASIC Computing, 14 x 2 hours Lectures, April, 1979.
3. FORTRAN Computing, 7 x 2 hours Lectures, February, 1980.
4. Introduction to X - ray Crystallography, 6 x 1 hour Lectures, January, 1980.
5. Mössbauer Spectroscopy, 15 x 1 hour Lectures, January, 1980.

ode of action of organotin stabilisers in PVC : a study by ₁n Mössbauer spectroscopy

id W Allen, John S Brooks, Richard W Clarkson
ield City Polytechnic, Pond Street, Sheffield
Malcolm T J Mellor and Alfred G Williamson
o Chemicals, Eccles, Manchester

tyltin *bis*-isooctylthioglycollate [$Bu_2Sn(SCH_2CO_2C_8$-$_2$] is widely used for the thermal stabilisation of PVC. ever, the mechanism of stabilisation is not yet fully rstood. Poller[1] has suggested that the stabiliser performs roles: (i) during an induction period, the stabiliser ions in a preventative way by exchanging allylic chlorine s present in the polymer with the thioglycollate groups ii) during the main degradation process, it serves to ve liberated hydrogen chloride, forming Bu_2SnCl_2 and a which then adds to the double bonds in the degrading er. However, Parker and Carman[2] have shown recently dialkyltin dimercaptides of the above type readily go a ligand exchange reaction with dialkyltin dichlorides rm the mixed halomercapto derivatives $R_2SnClSR'$. eaction serves to remove the dialkyltin dichloride which lso act as a Lewis acid catalyst for the degradation of although there is some disagreement over this latter [1-3]

an extension of work on the application of high dilution bauer spectroscopy to the study of chemical applications ganotin compounds,[4] the authors have studied the es which occur in the organotin stabiliser present in the atrix during thermal degradation of the polymer.

ples of PVC containing dibutyltin *bis*-isooctyl-ycollate (4 per cent by weight of the polymer) were red by conventional hot-milling techniques and then ted to thermal degradation at 185°C for 1h. The es were cooled to 80K using a continuous flow cryostat elium exchange gas and then analysed on a constant ration Mössbauer spectrometer, with a room tempera-^{5m}Ci ^{119m}Sn calcium stannate source. The parameters btained from least-squares fits to the spectra using tzian line shapes. Owing to the low concentration of ^{119}Sn in the samples, long run times were necessary (~ 48h), resulting in increased errors owing to instrumental instability. The Mössbauer parameters of the samples, together with those of the pure stabilisers and other organotin compounds are given in the Table. Typical spectra obtained for the unaged stabilised polymer and the thermally-aged samples are shown in Fig 1.

These results are of considerable interest from several viewpoints. In the case of the above stabiliser, there is no evidence of any co-ordinative interactions between the chlorine atoms of the polymer and the tin atom, as has been suggested by other workers.[5] From the Mössbauer parameters, the tin atom in dibutyltin *bis*-isooctylthioglycollate remains four co-ordinate in the PVC matrix. Furthermore, it is clear that the main reaction product from this stabiliser in the thermally aged polymer is the mixed halomercaptide $Bu_2SnCl(SCH_2CO_2C_8H_{17})$. It was not possible to detect Bu_2SnCl_2 in the polymer matrix. This result, therefore, supports the recent work of Parker and Carman.[2] (In a separate experiment, it was shown that the pure stabiliser is itself unchanged on heating to 185°C for one hour.) How-

Table
^{119m}Sn Mössbauer parameters of organotin compounds (all parameters accurate to ± 0.02mm s^{-1})

Sample	Isomer shift* (δmm s^{-1})	Quadrupole splitting (ΔE_Qmm s^{-1})
$Bu_2Sn(SCH_2CO_2C_8H_{17})_2$	1.39	2.20
$Bu_2Sn(SCH_2CO_2C_8H_{17})_2$ present at 4% w/w in unaged PVC	1.43	2.26
Thermally aged stabilised PVC	1.45	2.83
Bu_2SnCl_2	1.62	3.45
$Bu_2SnCl(SCH_2CO_2C_8H_{17})$	1.44	2.88
$Bu_2SnCl(SCH_2CO_2C_8H_{17})$ present in PVC matrix	1.45	2.85

* Relative to $CaSnO_3$

rption

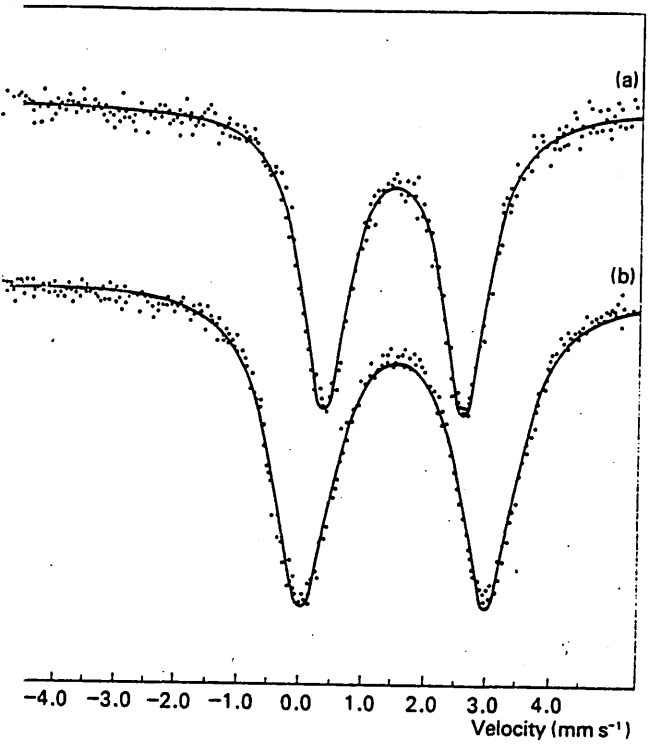

Mössbauer absorption spectra of (a) $Bu_2Sn(SCH_2CO_2C_8H_{17})_2$ r cent w/w) in unaged PVC and (b) $Bu_2Sn(Cl)SCH_2CO_2C_8H_{17}$ rmally aged PVC

ever, the amount of any dibutyltin dichloride formed will fall as the level of the stabiliser is increased.[3] As the level of the stabiliser in the present work is higher than is used in practice, any general conclusions remain doubtful, and work is now in progress to repeat this work at lower levels of the organotin stabiliser.

These results again illustrate the usefulness of the Mössbauer effect for the chemical analysis of low concentrations of organotin compounds *in situ* in industrial formulations. The investigation of the mode of action of other organotin compounds used for the stabilisation of PVC is being continued.

Dr P. J. Smith of the International Tin Research Institute is thanked for valuable discussion.

Received 25 June 1979

References

1 Poller, R. C., *J. Macromol. Sci. Chem. A.*, 1978, **12**, 373
2 Parker, R. G. & Carman, C. J., *Am. Chem. Soc. Adv. Chem. Ser.*, 1978, **169**, 363
3 Wirth, H. O. & Andreas, H., *Pure and Applied Chemistry*, 1977, **49**, 627
4 Smith, P. J., Crowe, A. J., Allen, D. W., Brooks, J. S. & Formstone, R., *Chem. Ind. (London)*, 1977, 874
5 Frye, A. H., Horst, R. W. & Paliobagis, M. A., *J. Polymer Sci. A.*, 1964, **2**, 1765

Journal of Organometallic Chemistry, 171 (1979) C29–C33

Preliminary communication

SYNTHESIS OF AIR STABLE TRIORGANOTIN DERIVATIVES OF AMINO ACIDS

PETER J. SMITH AND ROBERT L. HYAMS*
International Tin Research Institute, Fraser Road, Perivale, Greenford, Middlesex, UB6 7AQ (Great Britain)

JOHN S. BROOKS AND RICHARD W. CLARKSON
Department of Applied Physics, Sheffield City Polytechnic, Pond Street, Sheffield, S1 1WB (Great Britain)

(Received February 26th, 1979)

SUMMARY

A series of air stable S-triorganostannyl derivatives of L-cysteine and DL-homocysteine has been prepared by reacting the appropriate triorganotin hydroxide or bis(triorganotin) oxide with the sulphydryl-containing amino acids in methanol/water at room temperature.

Triorganotin compounds, R_3SnX, where R = ^nBu, Ph, cyclo-C_6H_{11} (Cy) and Neophyl (Np), are widely used in industry as biocides [1] and their biological activity is due to an interaction of the triorganotin moiety with certain proteins [2]. It has been suggested that both thiol [3] and histidine [4] residues are involved in binding the organotin compound and the recent interest [5,6,7] in organotin derivatives of the former type has prompted us to report our own preliminary results in this area. At physiological pH, the triorganotin derivative, R_3SnX, is likely to be present in the cell essentially as [8] the hydroxide, R_3SnOH, or the bis(oxide), $R_3SnOSnR_3$, and we have therefore studied the reactions of these compounds with the sulphydryl-containing amino acids, L-cysteine and DL-homocysteine, in polar media at room temperature.

*Formerly at the University of Warwick.

TABLE 1

Physical, Analytical and Mössbauer Data for S-Triorganostannyl Derivatives

		Analysis Calculated (Observed)				^{119m}Sn Mössbauer data	
	M Pt (°C)	C	H	N	S	δ [a] ($mm.s^{-1}$)	ΔE_Q ($mm.s^{-1}$)
$Bu_3SnSCH_2CH_2CHNH_2COOH$	210 (d)	45.28(44.59)	8.25(8.34)	3.30(3.60)	7.55(6.93)	1.35	1.54
$Ph_3SnSCH_2CHNH_2COOH$	152 (d)	53.61(53.10)	4.47(4.40)	2.98(3.05)	6.81(6.98)	1.24	1.34
$Ph_3SnSCH_2CH_2CHNH_2COOH$	159-164	54.54(54.57)	4.75(4.66)	2.89(2.20)	6.61(5.72)	1.28	1.48
$Cy_3SnSCH_2CHNH_2COOH$	185-187	51.64(50.87)	7.99(8.05)	2.87(2.62)	6.56(6.25)	1.44	1.68
$Cy_3SnSCH_2CH_2CHNH_2COOH$	198-201	52.59(52.40)	8.17(8.06)	2.79(2.14)	6.37(5.66)	1.45	1.63
$Np_3SnSCH_2CHNH_2COOH$	200-203	62.07(61.55)	7.05(7.00)	2.19(2.08)	5.02(4.54)	1.36	1.79
$Np_3SnSCH_2CH_2CHNH_2COOH$, H_2O	154-220	60.89(60.99)	7.31(7.20)	2.09(1.84)	4.78(4.39)	1.35	1.70
$Ph_3Sn-SCH_2CHOH$ $Ph_3Sn-SCH_2CHOH$	113-114	55.82(56.34)	4.46(4.63)	-	7.51(6.88)	b	b

[a] Relative to $CaSnO_3$. [b] Not determined.

On adding a methanol or methanol/ether solution of the bis(triorganotin) oxide (0.5 mol) or the triorganotin hydroxide (1 mol) to a solution of the amino acid (1 mol) in water at room temperature, a voluminous white precipitate of the S-triorganostannyl derivative is formed immediately (equations 1 and 2):

$$(R_3Sn)_2O + 2\ HS(CH_2)_nCHNH_2COOH \rightarrow 2R_3SnS(CH_2)_nCHNH_2COOH + H_2O \quad (1)$$

(n=1, R=Np; n=2, R= Bu or Np)

$$R_3SnOH + HS(CH_2)_nCHNH_2COOH \longrightarrow R_3SnS(CH_2)_nCHNH_2COOH + H_2O \quad (2)$$

(n= 1 or 2, R= Ph or Cy)

A slight warming of the solutions was found to be necessary to form the two trineophyltin derivatives. After filtration and drying at room temperature, the products were obtained analytically pure as air stable white powders, which could be recrystallised from aqueous methanol. Under the same conditions, however, we were unable to isolate pure derivatives using trimethyl- or triethyltin hydroxides and, in line with this, it has recently been found [6] that the ethyl ester of S-trimethylstannyl-cysteine is rather unstable on standing. The analytical and Mössbauer data for the new compounds are shown in Table 1. Mössbauer spectra were recorded at 80°K using a constant acceleration spectrometer which has been described previously [9].

All the compounds showed a strong band in their far infrared spectra at 327-338 cm^{-1}, confirming the presence of an Sn-S bond. The low values of the Mössbauer quadrupole splitting parameter, ΔE_Q (≤ 1.79 mm. s^{-1}) are characteristic [9] of a tetrahedral R_3SnX tin atom geometry, as found in the corresponding bis(triorganostannyl) sulphides, e.g. $Ph_3SnSSnPh_3$, which shows [10] $\delta = 1.20$ mm. s^{-1}, $\Delta E_Q = 1.46$ mm. s^{-1}, and is known [11] by X-ray crystallography to contain four-coordinate tin. The ν(CO) values found in the infrared spectra of the compounds (ca. 1630 cm^{-1}) are indicative of non-coordinating carbonyl groups, as in trimethyltin glycinate, where $\nu(CO) = 1630\ cm^{-1}$ [12].

Although trialkylstannyl esters of amino acids, which are relatively sensitive to hydrolysis, have been known for some time [2,12], there are very few examples of stable organotin-amino acid derivatives [5,6,7] and these all contain the organometallic moiety bond via sulphur. An interesting comparison may be drawn

here with mercaptoacetic acid, $HSCH_2COOH$, where reaction with 0.5 moles of a bis(triorganotin) oxide leads to substitution at the carboxyl group and not at sulphur [13].

We have also found that, under identical conditions, triphenyltin hydroxide (2 mol.) will react rapidly with dithiothreitol (1 mol.) to form the bis(S-triphenylstannyl) derivative (Table 1). This dithiol has recently been shown by Gould [14] to be capable of reversing the inhibition of the ATP synthases in chloroplasts by triphenyltin chloride. A similar derivative of 1,2-ethanedithiol has been reported by Poller [15].

Our work indicates that a facile reaction occurs between certain triorganotin hydroxides or oxides and biologically important mono- and di-thiols in polar media at room temperature. Reactions of this type are likely to be of considerable importance in understanding the mode of action of the triorganotin compounds. Further studies are under way to prepare stable triorganotin derivatives of histidine and these will be reported at a later date.

ACKNOWLEDGEMENTS

The International Tin Research Council, London, is thanked for permission to publish this paper. The authors are also grateful to Mr. R. Jones, Shell Chemical Company and Dr. B. Sugavanam, ICI Plant Protection Division, for providing generous gifts of bis(trineophyltin) oxide and tricyclohexyltin hydroxide, respectively, and to Dr. D.E. Griffiths, University of Warwick, for helpful discussions.

REFERENCES

1. L.Smith and P.J.Smith, Chem. Brit., 11 (1975) 208.
2. W.T. Hall and J.J. Zuckerman, Inorg. Chem., 16 (1977) 1239.
3. B.G. Farrow and A.P. Dawson, Eur. J. Biochem., 86 (1978) 85.
4. B.M. Elliott and W.N. Aldridge, Biochem. J., 163 (1977) 583.
5. H.O. Wirth, H.J. Lorenz and H-H. Friedrich, U.S. Pat., 3,933, 877 (1976).

6. G. Domazetis, R.J. Magee and B.D. James, Inorg. Chim. Acta., 32 (1979) L 48.

7. G. Domazetis, R.J. Magee and B.D. James, J. Organometal Chem., 162 (1978) 329.

8. R.S. Tobias in F.E. Brinckman and J.M. Bellama (Eds.), "Organometals and Organometalloids : Occurrence and Fate in the Environment", ACS Symposium Ser., 82 (1978) 130.

9. D.W. Allen, J.S. Brooks, R. Formstone, A.J. Crowe and P.J. Smith, J. Organometal Chem., 156 (1978) 359.

10. R.C. Poller and J.N.R. Ruddick, J. Organometal. Chem., 39 (1972) 121.

11. O.A. D'yachenko, A.B. Zolotoi, L.O. Atovmyan, R.G. Mirskov and M.G. Voronkov, Dokl. Akad. Nauk. SSSR., 237 (1977) 863.

12. B.Y.K. Ho and J.J. Zuckerman, Inorg. Chem., 12 (1973) 1552.

13. C.H. Stapfer and R.H. Herber, J. Organometal. Chem., 56 (1973) 175.

14. J.M. Gould, FEBS Letters, 94 (1978) 90.

15. R.C. Poller and J.N.R. Ruddick, J. Chem. Soc. Dalton, (1972) 555.

Journal of Organometallic Chemistry, 199 (1980) 299—310
Elsevier Sequoia S.A. Lausanne — Printed in The Netherlands

A ^{119}Sn MÖSSBAUER STUDY OF THE THERMAL DEGRADATION OF ORGANOTIN STABILISERS IN PVC

David W. Allen*, John S. Brooks†, Richard W. Clarkson†
Departments of Chemistry* and Applied Physics†
Sheffield City Polytechnic, Pond Street, Sheffield S1 1WB

Malcolm T. J. Mellor and Alfred G. Williamson,
Research Department, Lankro Chemicals Ltd,
Boardman Street, Eccles, Manchester, M30 0BH

(Received June 25th, 1980)

Summary

^{119m}Sn Mössbauer studies of the thermal degradation of PVC containing the stabilisers dibutyltinbis(isooctylthioglycollate) (1.2% by weight of the polymer), dioctyltinbis(isooctylthioglycollate) (4% by weight of the polymer) and dibutyltinbis(isooctylmaleate) (2% by weight of the polymer) indicate that in each case the stabiliser is converted into the dialkylmonochlorotin ester $R_2SnCl(X)$ ($X = SCH_2CO_2C_8H_{17}$ or $O_2C.CH = CHCO_2C_8H_{17}$), and not into the dialkyltin dichloride, R_2SnCl_2, as recently suggested by other workers. Comparison of the Mössbauer data for organotin-stabilised PVC samples prepared by both hot-milling and room temperature solvent casting processes indicates that there is little degradation of the polymer (and stabiliser) during the initial hot-milling process.

Introduction

Recently, we reported ^{119}Sn Mössbauer studies of the thermal degradation of samples of PVC containing the organotin stabiliser, dibutyltinbis(isooctylthioglycollate) ($Bu_2Sn(IOTG)_2$), present at 4% w/w of the polymer [1]. Our results indicated the formation of dibutyl(monochloro)tin (isooctylthioglycollate) after degradation of the polymer at 185° C for 1 hour. Harrison et al [2] have recently reported their findings in a similar study of PVC samples containing 1 - 2% of the above organotin stabiliser, and concluded that partial exchange of IOTG for chlorine occurred during the milling stage but following thermal degradation, the stabiliser was completely converted into dibutyltin dichloride.

Using a new 15 mCi ^{119}Sn ($BaSnO_3$) source, we have repeated our original experiments at the commercially-used level of 1.2% w/w of the $Bu_2Sn(IOTG)_2$ stabiliser in the polymer, and now report a detailed study of the progressive changes in the stabiliser during thermal degradation of the polymer. Also reported are related studies on other organotin stabilisers.

Experimental

Samples of PVC containing dibutyltinbis(isooctylthioglycollate) (1.2% by weight of the polymer) were prepared by conventional hot-milling techniques and then subjected to thermal degradation at 185°C for varying periods of time. The samples were then cooled to 80 K using a continuous flow cryostat with helium exchange gas and then analysed on a constant acceleration Mössbauer spectrometer, with a room temperature 15 mCi ^{119}Sn barium stannate source. The parameters were obtained from least-squares fits to the spectra using Lorentzian line shapes.

Dibutyl(monochloro)tin(isooctylthioglycollate) was prepared as described by Hutton et al [3], and incorporated into a PVC sample by the hot-milling process, also at a level of 1.2% by weight of the polymer.

In a similar manner, samples of PVC containing dioctyltinbis(isooctylthioglycollate) (4% by weight of the polymer) and dibutyltinbis(isooctylmaleate) (2% by weight of the polymer) respectively, were prepared.

The related dialkyltin(chloro) esters were prepared by the general procedures described by Hutton et al [3] and incorporated into PVC samples by the hot-milling process.

Analytical data for the previously unknown monochloro esters:

Monochloro(dioctyl)tin(isooctylthioglycollate) (a viscous oil which decomposed on attempted distillation)
(Found : C, 52.95; H, 8.9; Cl, 5.6; S, 5.5; Sn, 20.7; $C_{26}H_{53}ClO_2SSn$ requires C, 53.5; H, 9.1; Cl, 6.1; S, 5.5; Sn, 20.4%)

Dibutyl(monochloro)tin(isooctylmaleate) (a viscous oil which decomposed on attempted distillation)
(Found : C, 48.75; H, 7.55; Cl, 6.95: Sn, 24.6; $C_{20}H_{37}ClO_4Sn$ requires C, 48.5; H, 7.5; Cl, 7.2; Sn, 24.0%)

Solvent-cast samples were prepared by allowing a thin film of a solution of PVC and the appropriate stabiliser in an organic solvent (CH_2Cl_2 for thioglycollate stabilisers and THF for the maleate stabiliser) to evaporate at room temperature.

Results and Discussion

The Mössbauer parameters of samples of PVC stabilised by $Bu_2Sn(IOTG)_2$, together with those of the pure stabiliser and dibutyltin dichloride are given in Table 1. A typical spectrum obtained for the thermally aged samples is shown

TABLE 1

^{119m}Sn Mössbauer Parameters of Dibutyltinbis(isooctylthioglycollate)

Sample	*Isomer Shift mm/sec	Quadrupole Splitting mm/sec	Full Width at Half Height mm/sec
$Bu_2Sn(IOTG)_2$ (Pure)	1.39	2.20	0.88
Bu_2SnCl_2 (Pure)	1.64	3.47	0.97
$Bu_2SnCl(IOTG)$ (Pure)	1.44	2.88	1.14
$Bu_2SnCl(IOTG)$ in PVC	1.43	2.85	0.95
$Bu_2Sn(IOTG)_2$ in PVC at 1.2% (freshly milled)	1.45	2.29	1.07
$Bu_2Sn(IOTG)_2$ in PVC at 4.0% (solvent cast)	1.48	2.32	0.90
$Bu_2Sn(IOTG)_2$ in PVC at 1.2% Thermally aged for 85 mins	1.47	2.86	1.08

in Figure 1. The computer fit is the sum of two components corresponding to the unaged stabiliser and the monochlorotin ester.

Comparison of the data for the freshly-milled sample with that for the pure stabiliser indicates a small change, which is probably due to a small degree of degradation during the initial hot-milling process, as concluded by Harrison et al [2]. However, the similarity of the data clearly indicates that there is no significant structural change in the stabiliser which might have arisen as a result of co-ordination between the chlorine atoms of the polymer and the tin atoms of the stabiliser, as has been suggested by other workers, (Frye et al [4]).

After prolonged thermal degradation at 185°C, when the sample had become completely blackened, the Mössbauer

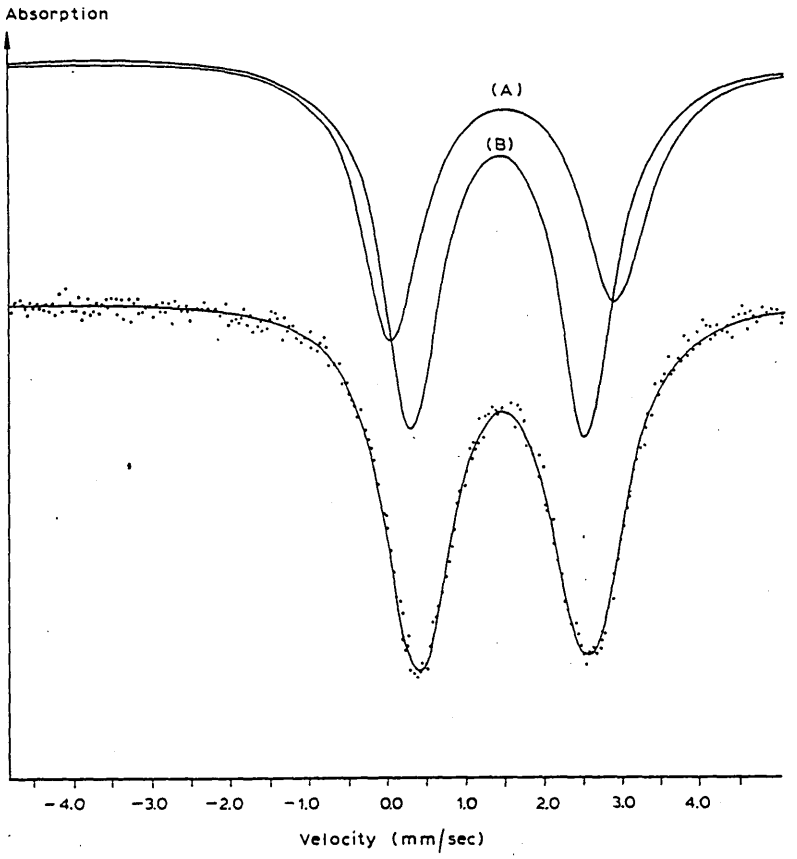

Fig. 1. Mössbauer spectra of thermally degraded PVC-containing $Bu_2Sn(IOTG)_2$ stabiliser at 1.2% after heating at 185°C for 30 min. The two components of the computer fit are shown corresponding to (A) $Bu_2SnCl(IOTG)$ and (B) $Bu_2Sn(IOTG)_2$.

parameters compare exactly with those of the sample of the monochlorotin ester dispersed in the polymer.

Further studies of progressive aging for short periods in the range 5 - 85 minutes indicate a gradual increase in the apparent quadrupole splitting from that of the pure stabiliser to that of the monochloro ester (Table 2). This trend is shown in Figure 2. It is apparent that during the course of thermal degradation, the presence of both the monochloro ester and unchanged stabiliser would

TABLE 2

^{119m}Sn Mössbauer Parameters of thermally aged Dibutyltinbis(isooctyl-thioglycollate)

Sample	*Isomer Shift mm/sec	Apparent Quadrupole Splitting mm/sec	Full Width at Half Height mm/sec
$Bu_2Sn(IOTG)_2$ in PVC at 1.2% Thermally aged for:			
5 mins	1.48	2.38	1.13
10 mins	1.45	2.42	1.14
15 mins	1.46	2.41	1.11
30 mins	1.47	2.56	1.27
50 mins	1.48	2.90	1.00
70 mins	1.47	2.84	0.99
85 mins	1.47	2.86	1.08

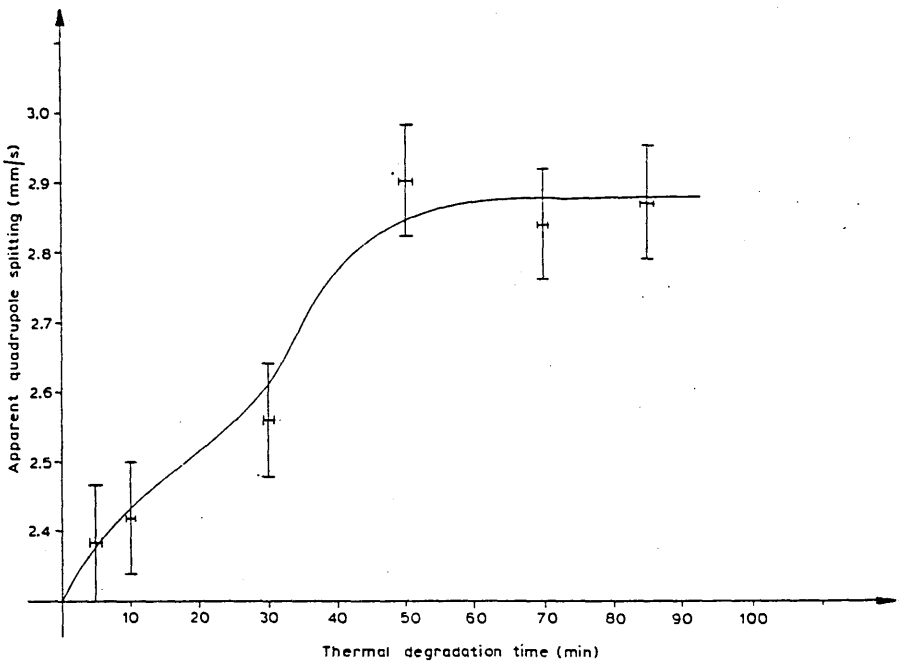

Fig. 2. Apparent quadrupole splitting as a function of thermal degradation time.

result in unresolved Mössbauer quadrupole doublets. However, a gradual increase in the apparent quadrupole splitting and a broadening of the line-width would be expected for such a mixture, and our data is consistent with this.

The trend shown in Figure 2 indicates the gradual change in 'apparent quadrupole splitting parameter' corresponding to the change to the monochloro ester as degradation occurs. There is no indication that further degradation occurs at 185°C to form Bu_2SnCl_2. We have computer fitted the data at 10, 30 and 50 mins using two doublets with parameters corresponding to the unchanged stabiliser and the monochlorotin ester and a significant reduction in the χ^2 term was obtained. The line width parameters were also comparable to those expected for the absorber thickness used. From the relative areas of the two contributions, the percentage of Bu_2SnCl(IOTG) was calculated and this is shown in Figure 3. From these results, it is not clear how rapidly the conversion to Bu_2SnCl(IOTG) occurs as the technique is

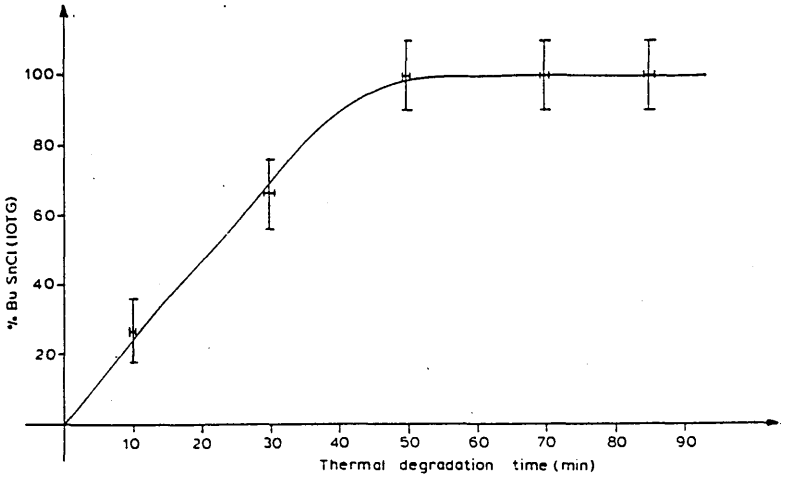

Fig. 3. Percentage of Bu_2SnCl(IOTG) as a function of thermal degradation time.

relatively insensitive to small contributions in unresolved mixed quadrupole spectra. However, complete conversion to $Bu_2SnCl(IOTG)$ has taken place after 50 mins heating, and this corresponds to the rapid darkening observed in the PVC as degradation occurs. The optical density of thermally degraded PVC samples was measured using a radiological densitometer. Figure 4 shows the change in optical density (arbitrary units) as a function of heating time, and a rapid increase is seen after 50 minutes when the stabiliser has been completely converted to $Bu_2SnCl(IOTG)$.

From these results, it is quite clear that the final product is the monochlorotin ester, and not dibutyltin dichloride as concluded by Harrison et al [2]. The discrepancy between our results and those of Harrison et al may arise due to the

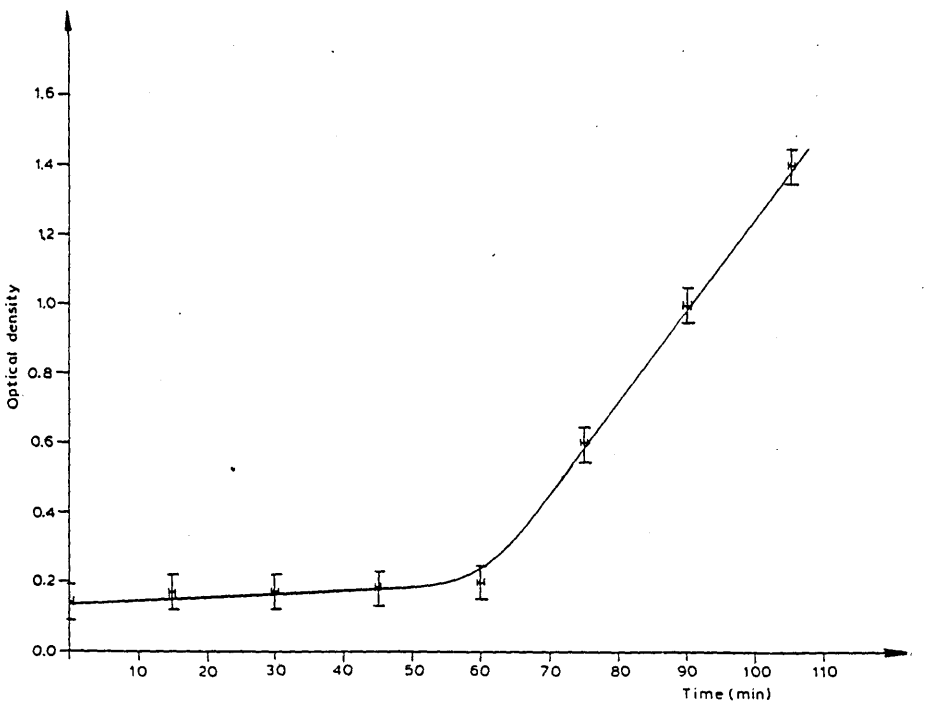

Fig. 4. Optical density of PVC as a function of thermal degradation time.

low value of the quadrupole splitting parameter of dibutyltin dichloride quoted by those workers [5] and also possibly larger experimental errors resulting from long run times due to the weakness of their source and low levels of tin in the absorber.

We have also carried out similar studies of the degradation of PVC stabilised with dioctyltinbis(isooctylthioglycollate) ($Oct_2Sn(IOTG)_2$)(Table 3) and dibutyltinbis(isooctylmaleate) ($Bu_2Sn(IOM)_2$) (Table 4) respectively.

TABLE 3

^{119m}Sn Mössbauer Parameters of Dioctyltinbis(isooctylthioglycollate)

Sample	*Isomer Shift mm/sec	Quadrupole Splitting mm/sec	Full Width at Half Height mm/sec
$Oct_2Sn(IOTG)_2$ (Pure)	1.49	2.36	0.96
Oct_2SnCl_2 (Pure)	1.75	3.73	1.03
$Oct_2SnCl(IOTG)$ (Pure)	1.47	2.94	1.03
$Oct_2SnCl(IOTG)$ in PVC at 1.2%	1.46	2.97	1.02
$Oct_2Sn(IOTG)_2$ in PVC at 4% (freshly milled)	1.50	2.27	0.97
$Oct_2Sn(IOTG)_2$ in PVC at 4% Thermally aged for 60 mins	1.46	2.62	1.03

In the case of the $Oct_2Sn(IOTG)_2$ stabiliser, the data in Table 3 shows quite clearly that on thermal degradation, the stabiliser is, as for the dibutyltin analogue, converted into the monochlorotin ester.

Similarly, the maleate stabiliser, $Bu_2Sn(IOM)_2$ is also seen to be converted into the monochlorotin ester. In the case

TABLE 4

^{119m}Sn Mössbauer Parameters of Dibutyltinbis(isooctylmaleate)

Sample	*Isomer Shift mm/sec	Quadrupole Splitting mm/sec	Full Width at Half Height mm/sec
$Bu_2Sn(IOM)_2$ (Pure)	1.44	3.62	1.04
$Bu_2Sn(IOM)_2$ in PVC at 2% (freshly milled)	1.42	3.36	0.94
$Bu_2Sn(IOM)_2$ in PVC at 2% (solvent cast)	1.36	3.34	0.98
$Bu_2SnCl(IOM)$ (Pure)	1.49	3.54	1.02
$Bu_2SnCl(IOM)$in PVC at 2%	1.40	3.16	0.97
$Bu_2Sn(IOM)_2$ in PVC at 2% Thermally aged for 60 mins	1.39	3.18	0.98

* All isomer shifts measured at 80 K relative to $BaSnO_3$

All parameters accurate to ± 0.02 mm s^{-1}

of this stabiliser, it is of interest that distinct differences in the quadrupole splitting are observed for the stabiliser in the pure state and when incorporated by hot-milling or by solvent-casting into the polymer. From the magnitude of the quadrupole splitting in the pure state, it would appear that the tin atom is probably six-co-ordinate with a trans-octahedral structure. The observed reduction in ΔE_{QS} on incorporation into the polymer may indicate a disruption of intra or inter-molecular co-ordination by ester carbonyl groups or possible co-ordination by chlorine atoms of the polymer.

It is also noteworthy that for dibutyl(monochloro)tiniso-octylmaleate, there is a significant difference in the magnitude of the quadrupole splitting between the pure

compound (Δ = 3.54 mm s^{-1}) and that of the compound dispersed in the PVC matrix (Δ = 3.16 mm s^{-1}), indicating that the structure has changed. Honnick and Zuckerman [6] have recently discussed the structures of the diorganotin-halide carboxylates and suggested that the origin of certain changes in infrared spectroscopic properties, in passing from the pure compound to a solution in an inert solvent, might be a change from a polymeric pentaco-ordinated structure (A) to a monomeric pentaco-ordinated structure (B).

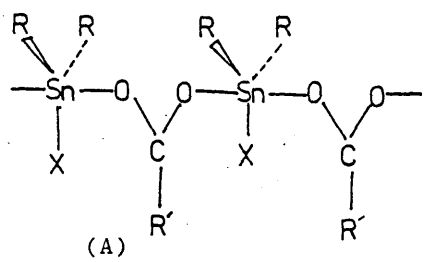

(A)

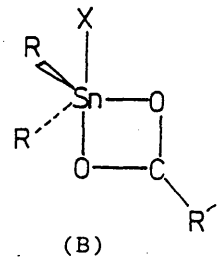

(B)

The change in quadrupole splitting between the pure dibutyl(monochloro)tin(isooctylmaleate) and the compound dispersed in the PVC matrix at the 2% level might be explained by a similar structural change.

In conclusion, it is also of interest that comparison of the Mössbauer parameters for hot-milled and solvent-cast samples containing respectively the $Bu_2Sn(IOTG)_2$ and $Bu_2Sn(IOM)_2$ stabilisers, indicates that the extent of thermal degradation of the stabiliser during the hot-milling process is very small.

We thank the SRC for an equipment grant.

References

1. D W Allen, J S Brooks, R W Clarkson, M T J Mellor and A G Williamson, Chem and Ind (London) (1979) 663

2. P G Harrison, T J King and M A Healy, J Organometal Chem, 182 (1979) 17.

3. R E Hutton and J W Burley, J Organometal Chem, 105 (1976) 61.

4. A H Frye, R W Horst and M A Paliobagis, J Polymer Sci A, 2 (1964) 1765.

5. A Ju Aleksandrov, Ya G Dofman, O L Lependina, K P Mitafanov, M V Plotnikov, L S Polak, A Y Jemkin and V S Shpinel, Russ J Phys Chem, 38 (1964) 1185

6. W D Honnick and J J Zuckerman, J Organometal Chem, 178 (1979) 133

Journal of Organometallic Chemistry, 219 (1981) 29—34
Elsevier Sequoia S.A., Lausanne — Printed in The Netherlands

MÖSSBAUER AND SINGLE CRYSTAL X-RAY STUDIES OF POLYMERIC DIMETHYLCHLOROTIN ACETATE

D.W. ALLEN, I.W. NOWELL *,

Department of Chemistry, Sheffield City Polytechnic, Pond Street, Sheffield S1 1WB (England)

J.S. BROOKS * and R.W. CLARKSON

Department of Physics, Sheffield City Polytechnic, Pond Street, Sheffield S1 1WB (England)

(Received March 30th, 1981)

Summary

The solid state structure of dimethylchlorotin acetate has been investigated by Mössbauer spectroscopy and single crystal X-ray analysis. Tin-119 Mössbauer spectra have been recorded at 80 K and 300 K, and the measured isomer shift and quadrupole splitting parameters have been correlated with the crystallographic data. The crystal structure has been determined using heavy-atom methods in conjunction with least-squares refinement of data measured on a two-circle X-ray diffractometer. Crystals are orthorhombic, space group $Pna2_1$, with four formula weights in a cell having the dimensions a = 9.315(3), b = 11.061(3), c = 7.656(2) Å and U = 788.78 Å^3. The observed and calculated densities are 2.07 and 2.05 mg m^{-3}, respectively. The structure was refined using 842 observed reflections to give conventional discrepancy factors of R = 0.040 and R' = 0.044. The crystal structure is composed of Me_2ClSn units bridged by acetate ligands giving rise to polymeric chains which run along the a direction. The tin atom is in a distorted trigonal bipyramidal environment consisting of two axial oxygen atoms distanced 2.165(6) and 2.392(7) Å from the metal, and equatorial positions occupied by two methyl groups and a chlorine atom. Distortions within the coordination polyhedron may be attributed to a further weak but apparently significant tin—oxygen interaction (Sn—O 2.782(7) Å), resulting in the tin atom becoming six-coordinate.

Introduction

Dimethylchlorotin acetate is a simple analogue of the chlorotin carboxylates observed in our recent studies of the changes occurring to organotin stabilisers

0022-328X/81/0000—0000/$02.75

during the thermal degradation of PVC [1]. The Mössbauer quadrupole splitting parameter measured at 80 K agrees with the previously published value (ΔE_Q = 3.56 mm s^{-1} [2]) and suggests that the tin atom is five or six coordinate. The Mössbauer spectrum has also been recorded at 300 K, and this has been taken as evidence for a polymeric structure [3—5]. However, this cannot be taken as conclusive as a number of unassociated compounds have given absorption at room temperature [5]. Therefore, in order to determine the exact tin coordination a single crystal X-ray analysis has been undertaken.

Experimental

Dimethylchlorotin acetate was prepared by the addition of equivalent amounts (0.009 mol) of dimethyltin dichloride and triphenyltin acetate to 150 cm^3 chloroform. Complete dissolution was achieved upon boiling, and reduction of the volume of the solution to 75 cm^3 led to the formation of colourless crystals upon cooling. Subsequent analysis confirmed the crystals to be dimethylchlorotin acetate (found: C, 19.60; H, 3.66; Cl, 14.43; $C_4H_9ClO_2Sn$ calcd.: C, 19.71; H, 3.69; Cl, 14.57%; M.pt. 179—181°C, lit. value 185°C [6].

Mössbauer data

The Mössbauer spectra were recorded at 80 K and 300 K using a constant acceleration Mössbauer spectrometer [7] with a room temperature 10 mCi ^{119m}Sn barium stannate source. A continuous flow cryostat with helium exchange gas was used to cool the sample to 80 K. The measured Mössbauer parameters (Table 1) were determined by computer fitting the data using Lorentzian line shapes [8].

Crystal data

$C_4H_9ClO_2Sn$, M_r 243.3, orthorhombic, $Pna2_1$, a = 9.315(3), b = 11.061(3), c = 7.656(2) Å, U = 788.78 Å, Z = 4, D_c = 2.05, D_m = 2.07 mg m^{-3}, μ(Mo-K_α) = 3.247 mm^{-1}, $F(000)$ = 464.

Data collection and reduction

A crystal, approximate dimensions 0.16 × 0.40 × 0.48 mm was selected and mounted with the a axis coincident with the rotation (ω) axis of a Stoë Stadi-2 two circle diffractometer. With monochromated Mo-K_α radiation and using the

TABLE 1

^{119m}Sn MÖSSBAUER DATA OF DIMETHYLCHLOROTIN ACETATE

Temperature (K)	Isomer shift δ (mm s^{-1}) [a] ±0.02 mm s^{-1}	Quadrupole splitting ΔE_Q (mm s^{-1}) ±0.02 mm s^{-1}	Full width at half weight Γ (mm s^{-1})
80	1.38	3.56	1.12
300	1.34	3.70	0.87

R_{80} = 0.032 (ratio of total normalised area at 300 K to total normalised area at 80 K).
[a] Relative to $BaSnO_3$.

TABLE 2

FRACTIONAL POSITIONAL PARAMETERS ($\times 10^5$ FOR Sn; $\times 10^4$ FOR REMAINING ATOMS) WITH e.s.d.'s FOR NON-HYDROGEN ATOMS IN PARENTHESES

Atom	*x*	*y*	*z*
Sn	57335(5)	32330(4)	0
Cl	7536(3)	4750(2)	−89(14)
O(1)	2751(9)	3105(9)	−11(27)
O(2)	4179(6)	4687(5)	−65(38)
C(1)	2941(10)	4231(7)	−150(25)
C(2)	1666(11)	5072(9)	−54(53)
C(3)	5480(34)	2777(15)	1530(29)
C(4)	5316(31)	2553(17)	−2600(26)
H(21)	2047	5789	−197
H(22)	1149	4972	1200
H(23)	906	4873	−1080
H(31)	4610	2304	3163
H(32)	6148	2138	1841
H(33)	6115	3243	3501
H(41)	4421	2060	−3145
H(42)	5952	2933	−3644
H(43)	5972	1947	−1835

background-ω scan-background technique, 958 unique reflections were measured, of which 842 had $I \geqslant 3.0\sigma(I)$ and were considered to be observed. [The net intensity $I = T - B$, where T = scan count, B = mean background count over the scan width; $\sigma(I) = (T + Bc/2t)^{1/2}$ where c = scan time, t = time for background measurement at each end of the scan.] Corrections for Lorentz and polarisation effects were applied to the data, but no corrections for absorption were made.

TABLE 3

BOND DISTANCES (Å) AND ANGLES (°)

Symmetry code.
none *x*, *y*, *z*; (′) 0.5 + *x*, 0.5 − *y*, *z*; (″) − 0.5 + *x*, 0.5 − *y*, *z*

Bond distances			
Sn—Cl	2.375(2)	Sn—C(4)	2.163(18)
Sn—O(1)	2.782(7)	O(1)—C(1)	1.262(10)
Sn—O(1′)	2.392(7)	O(2)—C(1)	1.260(9)
Sn—O(2′)	2.165(6)	C(1)—C(2)	1.511(12)
Sn—C(3)	2.015(21)		
Bond angles			
Cl—Sn—O(1)	137.9(2)	O(2)—Sn—C(3)	97.4(11)
Cl—Sn—O(1′)	83.2(2)	O(2)—Sn—C(4)	96.7(10)
Cl—Sn—O(2)	87.0(2)	C(3)—Sn—C(4)	140.9(6)
Cl—Sn—C(3)	106.7(7)	Sn—O(1)—Sn″	144.7(1)
Cl—Sn—C(4)	110.3(7)	Sn—O(1)—C(1)	79.0(7)
O(1)—Sn—O(1′)	138.9(2)	Sn″—O(1)—C(1)	136.2(7)
O(1)—Sn—O(2)	50.9(2)	Sn—O(2)—C(1)	108.4(7)
O(1)—Sn—C(3)	82.7(10)	O(1)—C(1)—O(2)	121.3(6)
O(1)—Sn—C(4)	78.5(10)	O(1)—C(1)—C(2)	119.5(8)
O(1′)—Sn—O(2)	170.1(2)	O(2)—C(1)—C(2)	118.0(8)
O(1′)—Sn—C(3)	86.6(10)		
O(1′)—Sn—C(4)	85.6(9)		

Structure determination and refinement

Systematic absences do not distinguish between space groups $Pna2_1$ and *Pnma*. *Pnma* would require the molecule to have mirror symmetry ($Z = 4$) and subsequent analysis has confirmed the non-centrosymmetric space group as being correct, with occupation of the four general positions. The x and y coordinates of the tin atom were readily located using the Patterson function and the remaining atoms were located from successive electron density syntheses. The methyl hydrogens were located but given ideal geometry (C—H 1.08 Å) and a common isotropic temperature factor. Scattering factors were calculated using an analytical approximation [9] and the weighting scheme adopted was $w = 1.000/(\sigma^2(F_o) + 0.0075\ (F_o)^2)$. Full matrix refinement with anisotropic temperature factors applied to all non-hydrogen atoms gave the final $R = 0.040$ and $R' = 0.044$. The final positional parameters are given in Table 2, bond distances and angles in Table 3. Lists of structure factors, thermal parameters and mean planes data are available on request from the authors (I.W.N.).

Discussion

The Mössbauer parameters for dimethylchlorotin acetate are given in Table 1. The R_{80} value of 0.032 is significant, indicating a polymeric structure [4], and the quadrupole splitting ($\Delta E_Q = 3.56$ mm s^{-1}) suggests that the tin atom is five or six coordinate. Similar organotin carboxylates of known six coordinate structures have quadrupole splittings in the range $\Delta E_Q = 3.6$—3.9 mm s^{-1} [10].

The X-ray analysis confirms the polymeric nature of dimethylchlorotin acetate (Fig. 1) and Me_2ClSn units are found to be linked together via acetate bridges to give chains running along the *a* direction. The acetate ligands are effectively planar and orientated such that the O(1), O(2), C(1), C(2) mean plane is almost coincident with the tin and chlorine atoms, and bisects the C(3)—Sn—C(4) angle. (Sn, Cl, C(3), C(4)) lie —0.56, —0.030, —1.982, 1.951 Å, respectively, out of the mean plane). The resulting coordination about tin is best described as distorted trigonal bipyramidal with the chlorine and two methyl carbon atoms forming a trigonal arrangement about the metal. O(2) and O(1′) occupy the axial positions such that the O(2)—Sn—O(1′) bond angle is 170.1(2)° and the Sn—O(2), O(1′) distances are 2.165(6) and 2.392(7) Å, respectively. While these tin—oxygen distances fall within the range of reported values [11—14], they are significantly different and it is of note that the longer distance is associated with the oxygen atom involved in an additional tin—oxygen interaction. Although the Sn—O(1) distance of 2.782(7) Å is considerably larger than the sum of the covalent radii (2.13 Å), it is well within the sum of the Van der Waals' radii (3.70 Å) and distortions about the tin can be attributed to a weak yet significant Sn—O(1) interaction. Thus the metal atom is found to be 0.173 Å out of the Cl, C(3), C(4) plane and in a direction away from O(1′) and toward O(1) and O(2). In addition, the angular distortions about tin, viz. C(3)—Sn—C(4) 140.9(6)°, O(1′)—Sn—O(2) 170.1(2)°, are such as to facilitate a Sn—O(1) interaction. Thus, while O(2) is monodentate with respect to tin, O(1) interacts with both Sn and Sn″, thereby increasing the overall coordination number for tin to six.

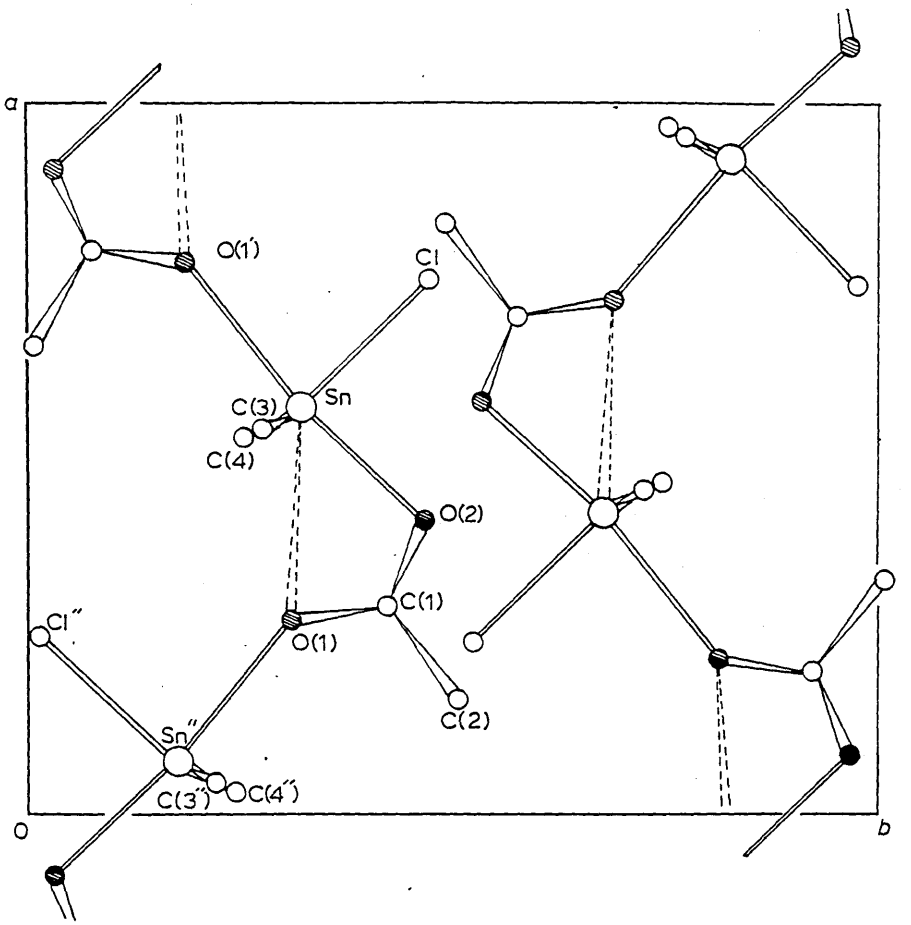

Fig. 1. Projection down the *c* axis showing the polymeric nature of dimethylchlorotin acetate.

The crystallographic results are in accord with the Mössbauer data and in this instance lend weight to the use of a room temperature Mössbauer resonance as evidence for a polymeric structure.

Acknowledgements

We thank the S.R.C. for computing facilities and equipment grants (to I.W.N. and J.S.B.) and the International Tin Research Institute for the supply of starting materials.

References

1 D.W. Allen, J.S. Brooks, R.W. Clarkson, M.T.J. Mellor and A.G. Williamson, J. Organometal. Chem., 199 (1980) 299.
2 W.D. Honnick and J.J. Zuckerman, J. Organometal. Chem., 178 (1979) 133.
3 H.A. Stockler, H. Sano and R.H. Herber, J. Chem. Phys., 47 (1967) 1567.
4 R.C. Poller, J.N.R. Ruddick, B. Taylor and D.L.B. Toley, J. Organometal. Chem., 24 (1970) 341.
5 G.M. Bancroft, K.D. Butler and T.K. Sham, J. Chem. Soc. Dalton Trans., (1975) 1483.

6 R. Okawara, D.E. Webster and E.G. Roechow, J. Amer. Chem. Soc., 82 (1960) 3287.
7 P.J. Smith, A. Crowe, D.W. Allen, J.S. Brooks and R. Formstone, Chem. and Ind. (London), (1977) 874.
8 G. Lang and W. Dale, Nucl. Instr. Meth., 116 (1974) 567.
9 International Tables for X-Ray Crystallography, Vol. IV, (1974), Table 2.2B, Kynoch Press, Birmingham.
10 G.M. Bancroft, V.G. Kumar Das and T.K. Sham, J. Chem. Soc. Dalton Trans., (1976) 643.
11 H. Chim and B.R. Penfold, J. Cryst. Mol. Struct., 3 (1973) 285.
12 N.W. Alcock and V.L. Tracy, Acta. Cryst. B, 35 (1979) 80.
13 R. Faggiani, J.P. Johnson, I.D. Brown and T. Birchall, Acta Cryst. B, 34 (1978) 3742.
14 G.A. Miller and E.O. Schlemper, Inorg. Chem., 12 (1973) 677.